YILDIZ TECHNICAL UNIVERSITY
FACULTY OF MECHANICAL ENGINEERING

GROUNDED UPPER LIMB EXOSKELETAL REHABILITATION ROBOT

Özgür Ege AYDOĞAN / 1706A602

Fatih KARADENİZ / 16067008

Emin Abdullah KAZANCI / 17067602

PREPARED IN MECHATRONICS ENGINEERING DEPARTMENT

SENIOR PROJECT REPORT

Academic Member: Assoc. Prof. Dr. Erhan AKDOĞAN

İSTANBUL, 2019

CONTENTS

SYMBOL LIST

θ_i	joint angle [°*degree*]
d_i	link offset [*mm*]
a_i	link length [*mm*]
α_i	twist angle [°*degree*]
η_{3x3}	perspective vector [*0*]
δ	Scaler Vector [*1*]
$\dot{\theta}$	Velocity []
$\ddot{\theta}$	Acceleration [rad/s^2]
τ	Torque [*kg.cm & N.m*]
F	Force
r	distance
m	mass [*gr*]
V	Voltage
μs	microsecond
mA	miliampere
mAh	miliampere-hour
x,y,z	Coordinate Axes
Π	Multiplication Symbol
Σ	Summation Symbol [*Sigma*]
c_i	cosine *[°degree]*
s_i	sine *[°degree*]
c_{ij}	addition of cosines *[°degree*]
s_{ij}	addition of sines *[°degree*]
P_x	Translational Transform
T_i^{i-1}	Transformation Matrix
D_i^{i-1}	Rotation Matrix
ω	Angular Velocity
v	Linear Velocity
${K_E}^{(R)}$	Rotational Kinetic Energy
$K_{E_1}^{(T)}$	Translational Kinetic Energy
P_E	Potential Energy
$\mathcal{L}$	Lagrangian Function
J	Moment of Inertia [$kg \cdot m^2$]
b	Motor viscous friction constant [$N \cdot m \cdot s$]
K_b	Electromotive Force Constant [$V/rad/s$]
K_t	Motor Torque Constant [$N \cdot m/Amp$]
R	Electrical Resistane [Ω]
L	Electrical Inductance [H]
K_p	Proportional Controller Gain
K_i	Integral Controller Gain
K_d	Derivative Controller Gain

ABBREVIATION LIST

EMG	electromyography
EEG	electroencephalography
FPS	frames per second
RGB	Red Green Blue
DH	Denavit - Hartenberg
FDM	Fused Deposition Modeling
DOF	Degrees of Freedom
SDK	Software Development Kit
TTL	Transistor to Transistor Logic
URDF	Unified Robot Description Format
PID	Proportional-Integrator-Derivative
CAD	Computer Aided Design
et. al.	et alia
mm	Millimeter
cm	Centimeter
rad	Radian
kg	kilogram
s	Second
gr	Gram

FIGURE LIST

TABLE LIST

ACKNOWLEDGEMENTS

We would like to extend our sincere thanks to our respectable advisor ***Asst. Prof. Erhan AKDOĞAN*** *who shared her valuable information so sincerely with us during this work and to* ***Yildiz Technopark Prototpe Workshop*** *employees who helped us in production of the prototype during the project.*

This work was supported by the ***Scientific and Technological Research Council of Turkey (TUBITAK)*** *under grant number 1139B411900912.*

ABSTRACT

The number of cerebrovascular and neuromuscular diseases is increasing in parallel with the rising average age of the world’s population. Since the shoulder anatomy is complex, the number of rehabilitation robots for shoulder movements is limited. This paper presents the mechanical design, control, and testing of 4 degrees of freedom (DOF) grounded upper limb exoskeletal robot. It is capable of four different therapeutic exercises (passive, active assistive, isotonic and isometric). Also, a low-cost electromyograph device was developed and integrated into the system to measure muscular activation for feedback and instantaneously muscle activation control for the physiotherapist during the therapy. The system can be used for rehabilitation on the shoulder and elbow. A PID controller and position-force based impedance controller with EMG signals were developed. The test results were presented in terms of simulation and the real system exercises. According to test results, the developed system can perform passive, active-assistive, isotonic and isometric exercises and can be used for other therapeutic exercises.

1. INTRODUCTION

Rehabilitation is a general treatment process that covers all the necessary stages that enable people who have lost some of their physical abilities or limbs as a result of an illness or accident, to re-adapt to life, to improve their life quality and to live seamlessly with their families and society [1].

The number of cerebrovascular and neuromuscular diseases is increasing in parallel with the rising average age of the world's population. For example, as reported by the Council for Economic Planning and Development in Taiwan [2], the percentage of the aged community is predicted to reach 39.4% in 2060 in Taiwan. Because of that, usage of the rehabilitation robots for physiotherapy of patients who have lost their limb motor functions gains importance.

The World Health Organization's (WHO) estimation about the number of individuals which would be affected by chronic diseases by 2030 is 23.3 [3]. The number of rehabilitation robots developed especially after the 2000s is increasing day by day. This growth have been continuing steadily. Since the shoulder anatomy is complex, the number of rehabilitation robots for shoulder movements is limited. In this study, a grounded type rehabilitation robot was developed. The literature has been researched in accordance with this type of robot. One of the world-wide studies in this field is the robot MIME [4]. This robot has 6 degrees of freedom and is used for wrist and shoulder rehabilitation. With the help of a PUMA manipulator, the system applies the same movements as the intact arm to the rehabilitated. A 5 DOF haptic arm is designed for training and rehabilitation by Gupta and O'Malley [5]. The system works with kinesthetic feedback equipped for the joints of the lower arm and wrist of the operator. Vertechy et al. [6] introduced an upper limb exoskeleton design with a modular custom-designed architecture for upper limb rehabilitation. The system meets the requirements for patient safety and high performance application flexibility. Ren et al. [7] designed a user-friendly robot with single motor named IntelliArm which is able to controlling the whole arm consisting hand opening and closing mechanism separately and synchronically by using 8+2 DOF. Ganesan et al. [8] used EMG and IMU in the upper limb exoskeleton design. The system uses the data from the good hand as a feedback and controls the rehabilitation process. Lenzi et al. [9] worked on 10 healthy person's proportional EMG reaction applied by an elbow drived exoskeleton. There are many other examples of upper limb rehabilitation [10 – 11].

Some of the rehabilitation robots for upper limb which are grounded and works on the shoulder region. Hsieh et al. [12] has produced a parallel actuated shoulder mechanism which has two spherical mechanisms, two slider crank mechanisms and a gravity balancing mechanism. As a conclusion of the design the robot has superior inertia properties and is compact and light. Also it has an adaptive mechanism that can resolve the misalignment problems. Hunt et al. [13] introduced a five degree of freedom shoulder exoskeleton. One of the main properties of the system is low inertia. The system consists of three parallel linear actuators coupled to the shoulder joint with a three DOF tie-rod joint. With the help of a passive slip interface the shoulder joint and upper arm are connected together. Oguntosin et al. [14] demonstrated an exoskeleton actuated with the soft modules which consists 3D-printed parts. With the light weight of 3D parts the aim was to compensate gravity and with active joints to rotate the shoulder and elbow joints. The system contains soft materials and pneumatic actuation systems. Shao et al. [15] designed a three DOF cable-driven upper-arm exoskeleton. For an optimal design two sufficient systems are proposed according to analysis. The optimum design provided with projected force indices. Wu et al. [16] developed a gravity balanced rehabilitation robot for upper limb. The kinematic structure is obtained in a way which interaction is available. As a hybrid combination, auxiliary links are used to balance the effect of gravity with zero-free length springs. Accogli et al. [17] provided an exoskeleton with a cooperative human-machine interface. Also EMG based advanced machine learning algorithms are used for motion detection and decoding movement direction.

In addition to these studies, there are also rehabilitation robots used as commercial products. Some of grounded models are compared with the robot prototype in the table. As can be seen from Tab.1 designed robot is able to make 4 different type of exercises and is more cost efficient.

Table 1: Commercial upper limb rehabilitation robot's comparison

Name of System		**MIT-MANUS**	**NeReBot**	**ArmeoPower**	**Designed Robot**
Year		2010	2017	2017	2019 - 2020
DOF		2+(3+1)	3	6+(1)	3+1
The Supported Movements and Areas	**Shoulder**	X	X	X	X
	Elbow	X	X	X	X
	Wrist	X		X	
Exercise Modes	**Passive**	X	X	X	X
	Active - Assistive	X	X	X	X
	Active				X
	Resistive				X
Robot Type and System Form	**Grounded**	X	X	X	X
	End - Effector Type	X	X	X	
	Exoskeleton Type			X	X
Cost		110.000 $	50.000 $	190.000 $	~ 4.000 $

Existing grounded upper limb exoskeleton rehabilitation robots have some problems which are listed below;

• The glenohumerial joint in the shoulder is inside the body. Because of that, it is very hard to set the rotation axis of the robot and rotation axis parallel.

• When the robots in the market are analyzed it can be seen that a lot of the robots are bulky and big.

• Some robots have a solid structure which is not adjustable. Because of that patient with different body sizes have difficulties.

In this study, design, producing and control of a 4 DOF grounded upper limb exoskeletal rehabilitation robot for the shoulder area which can be used by elderly, stroke or Parkinson patients was performed. The mechanical design will include three active shoulder movements and one passive elbow movement. These movements are; shoulder vertical flexion-extension, shoulder horizontal flexion-extension, shoulder abduction/adduction and elbow flexion-extension. The robot will be able to do these exercises in passive, active-assistive, isotonic and isometric modes. The mechanical design, dynamic model and test results in terms of simulations and real time results for the passive exercises are presented.

2. THEORETICAL BACKGROUND

2.1. Rehabilitation Robots

Rehabilitation robots can be classified under 4 groups. As can be seen from Tab. 2 these are aimed therapy region, mechanical specifications and design, control strategies of exercises and treatment application area.

Table 2: Classification of rehabilitation robots [18]

Classification	Sub -Groups
Aimed therapy region	Upper Limb robots
	Lower Limb robots
	One sided or both sided robots
	The joint movements (shoulder, hand, elbow) robots
Mechanical specifications and designs	End-effector
	Exoskeletal
Control strategies of exercises	Passive
	Active-Assistive
	Active
	Resistive
	Bimanual
Treatment application area	**Daily life support robots (assistive)**
	1) Manipulation Help
	2) Mobility Help
	2.1.) Robotic system wheelchair
	2.2.) Exoskeletal robotic manipulator
	3) Social Help
	Motion System Support Robots
	1) Prosthesis
	2) Exoskeletal Robots
	Therapeutic Exercise Robots
	1) Upper Limb Robots
	2) Lower Limb Robots

Aimed therapy region: There are 4 different types for aimed therapy region. These are upper limb robots, lower limb robots, one or both sided robots and the name of the joint which the movement happens. Especially for upper limb these are named for shoulder, elbow wrist or hand movements.

Mechanical specifications and designs: End-effector type robotic devices works by applying force to the end point of the limb. These devices doesn’t have parallel axis with the human body so sometimes there are difficulties and problems with these robots. Exoskeleton type robots have parallel axis with the patient’s body so it can control the joints directly without problems. It can be connected to the body or it can be wearable.

<u>*Control strategies of exercises:*</u> There are 5 types of exercises which are done with different control strategies. The rehabilitation robot developed in this study can perform passive, active-assistive, isometric and isotonic exercises for shoulder rehabilitation. The definitions of these are given below.

Passive exercise: The robot moves the extremity of the patient all by itself. The purpose is to achieve range of motion. This method can be used in unconscious or paralyzed patients.

Active – assistive exercise: The patient tries to make the movement and the robot will help the patient when he/she needs. Assistance by the physiotherapist while the patient is making movements and the effect of gravity is eliminated. These exercises will improve the patient's muscle strength and strengthens coordination.

Isometric exercise: The length of the muscle stays unchanged while muscle activity rises. Isometric exercises are performed against a fixed resistance. The joint angle does not change. It is an effective method at the bottom of the muscle strengthening process. It is used in the early stages of orthopedic and sports rehabilitation. However, it is not preferred during all exercise movements. In isometric exercises, a joint movement may not occur. Only an increase in the size of the muscle body appears.

Isotonic exercise: The limb works against a constant force which can be changed according to improvements and needs of the patient. It increases the force more than the isometric movements. Isotonic exercise is done against gravity. Isotonic exercises resist constant resistance across the range of motion. It is performed with dynamic muscle contractions.

2.2. Theory of Shoulder Rehabilitation

The dominant joint which connects upper limb to trunk is the glenohumeral joint (shoulder joint). Rehabilitation robot is able to perform vertical flexion-extension, horizontal flexion-extension and abduction-adduction for shoulder which can be seen in Fig.1 [19]. Also vertical flexion-extension for elbow. The definitions of these movements are explained below.

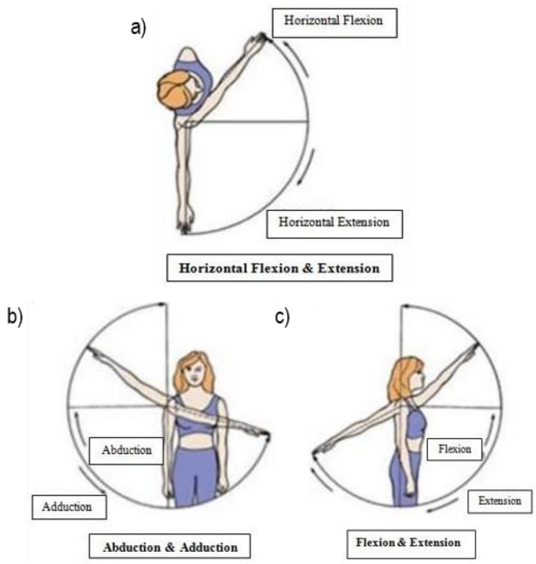

Figure 1: Shoulder exercises: a) horizontal abduction-adduction, b) vertical flexion-extension, c) horizontal flexion-extension [19]

Horizontal flexion – extension: lifting the arm is called extension and lowering the flexion movement. The arm is straight and parallel to ground at start and perpendicular to ground at the end or vice versa.

Vertical flexion – extension: lifting the arm is called extension and lowering the flexion movement. The arm is straight and parallel to ground at start and perpendicular to ground at the end or vice versa.

Abduction-adduction: lifting the arm is called abduction and lowering the adduction movement. The arm is straight and parallel to the body at start and perpendicular to ground at the end or vice versa.

The agonist and antagonist muscles used for each movement are represented on the Tab.3. *Antagonist* is the name of the muscle which is straitening and *antagonist* is the name of the muscle which is expanding. The surface electrodes are placed on these muscle pairs to measure the muscle activation level by EMG circuit.

Table 3: Movement – muscle groups

Movement	Agonist Muscle	Antagonist Muscle
Shoulder Flexion	Anterior Deltoid	Posterior Deltoid
Shoulder Extension	Posterior Deltoid	Anterior Deltoid
Shoulder Abduction	Medial Deltoid	Latissimus Dorsi
Shoulder Adduction	Latissimus Dorsi	Medial Deltoid
Elbow Flexion	Biceps	Triceps
Elbow Extension	Triceps	Biceps

The muscle groups named in table 3 working on shoulder area are shown in Fig.2.

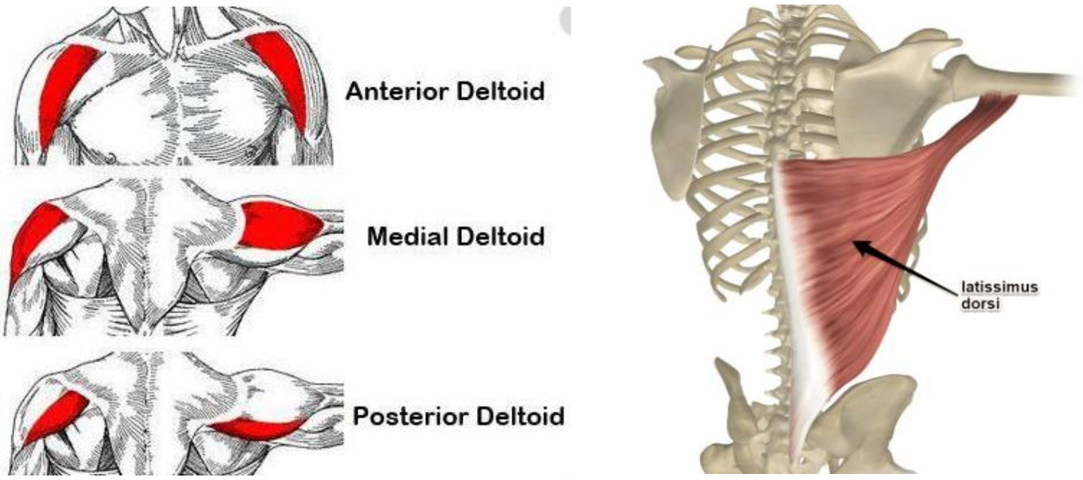

(a) (b)

Figure 2: Muscles on shoulder area [20]

3. MATERIALS AND METHODS

3.1. Functional Requirements and Design Parameters

The Functional requirements of the developed exoskeletal robot are as follows:

- Capable of shoulder and elbow movement.
- The length should be adjustable related to limb length.
- To protect the patient against problems, the system should be protected with mechanical, electrical and software precautions.
- The robot should be able to make passive, active, isometric and isotonic exercises.
- It can be used easily.

The design parameters that meet the functional requirements are as follows:

- A robot manipulator with 4 DOF should be designed.
- A mechanism that can adjust the length depending on the limb length should be designed.
- Mechanical safety with mechanical limits, electrical safety with emergency stop button and software safety with emergency code has to be provided for the system.
- A motor, reducer, encoder, force and EMG should be used in the system to feedback and control. Force and position control algorithm should be developed to perform related exercises.
- An interface that can the user use comfortably should be designed.

3.2. Mechanical Design and Structure

The mechanical design was made by looking at the design parameters. The robot is developed for home-based robotic rehabilitation for disabled and aged patients in any circumstances. Therefore, the system must be simple, easy to transfer and can be used by any patient not required much effort for adjustments. According to these needs it is designed basically and can be moved on a platform to anywhere it is needed. Also it has an adjustable mechanism which can be changed easily.

The ranges for the movements are given in Tab.4. In the design the ranges are considered and the robot is designed in a way which it will work in the ranges. If a failure happens and the robot is going out of range, the mechanical precautions are there for stop the system. The range limitations are very important for safety. For smooth movement, bearings are used on the rotating parts according to calculations. Because of weight, cost and rust protection aluminum material is used. Besides, aluminum is one of the most suitable materials that can be used in the robot since it is a light and durable material. Feeders and other enhancer parts are used to make the system reliable and stronger. The last form of the design can be seen in Fig. 3 and Fig.4 and the produced prototype is illustrated in Fig. 5.

Table 4: Movement ranges

Motion	Range
Shoulder (horizontal) flexion (Flex.) / ex-tension (Ext.)	135°/ 50°
Shoulder adduction (Add.) / abduction (Abd.)	108°/0°
Shoulder (vertical) flexion (Flex.) / extension (Ext.)	135°/ 50°

Figure 3: Isometric view of the system

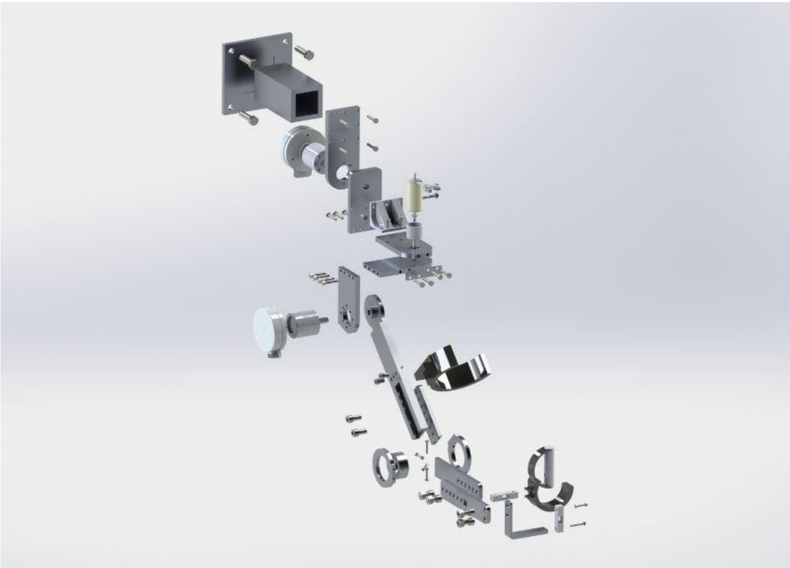

Figure 4: Explosion view of the mechanical design

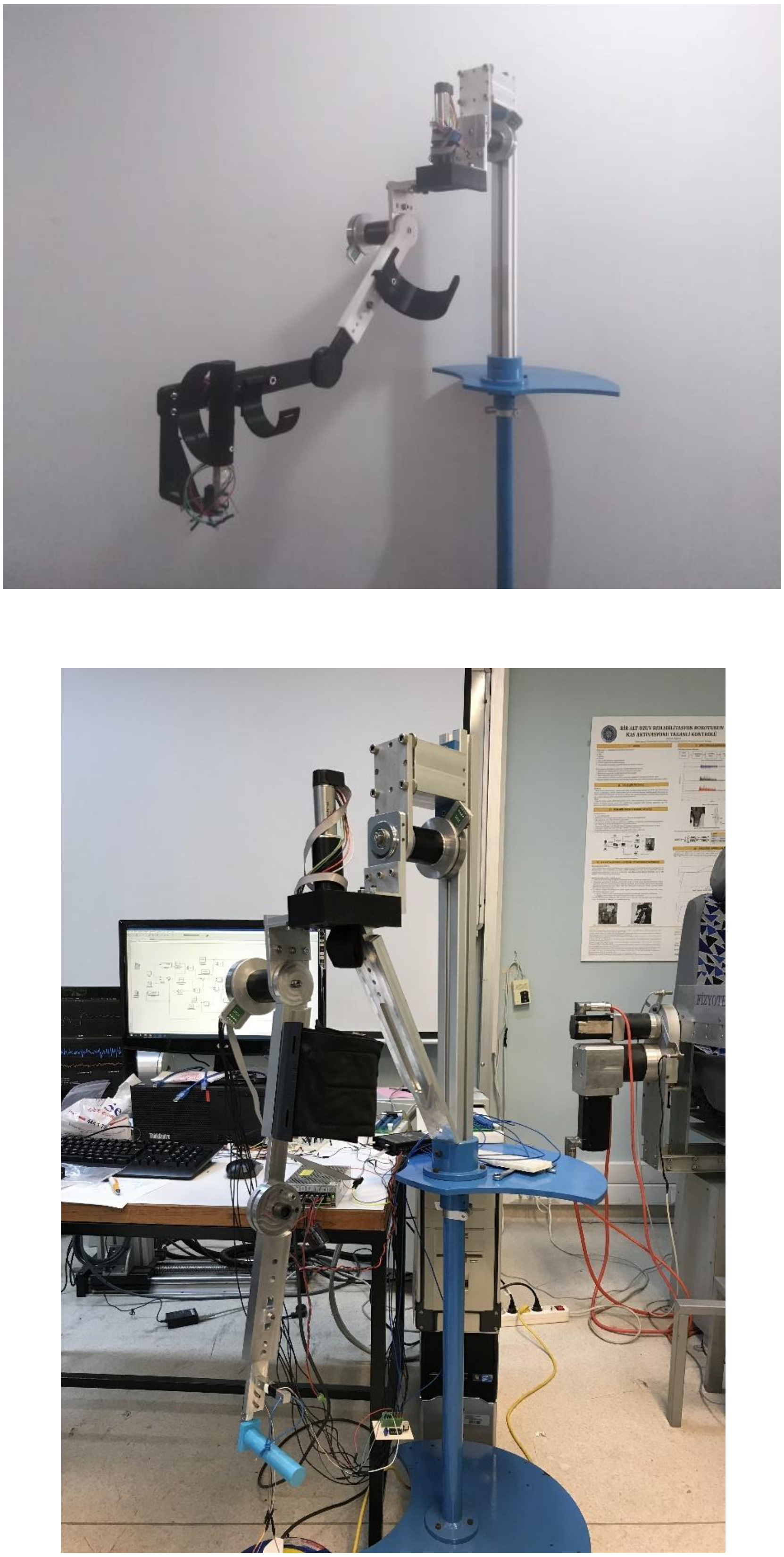

(a)

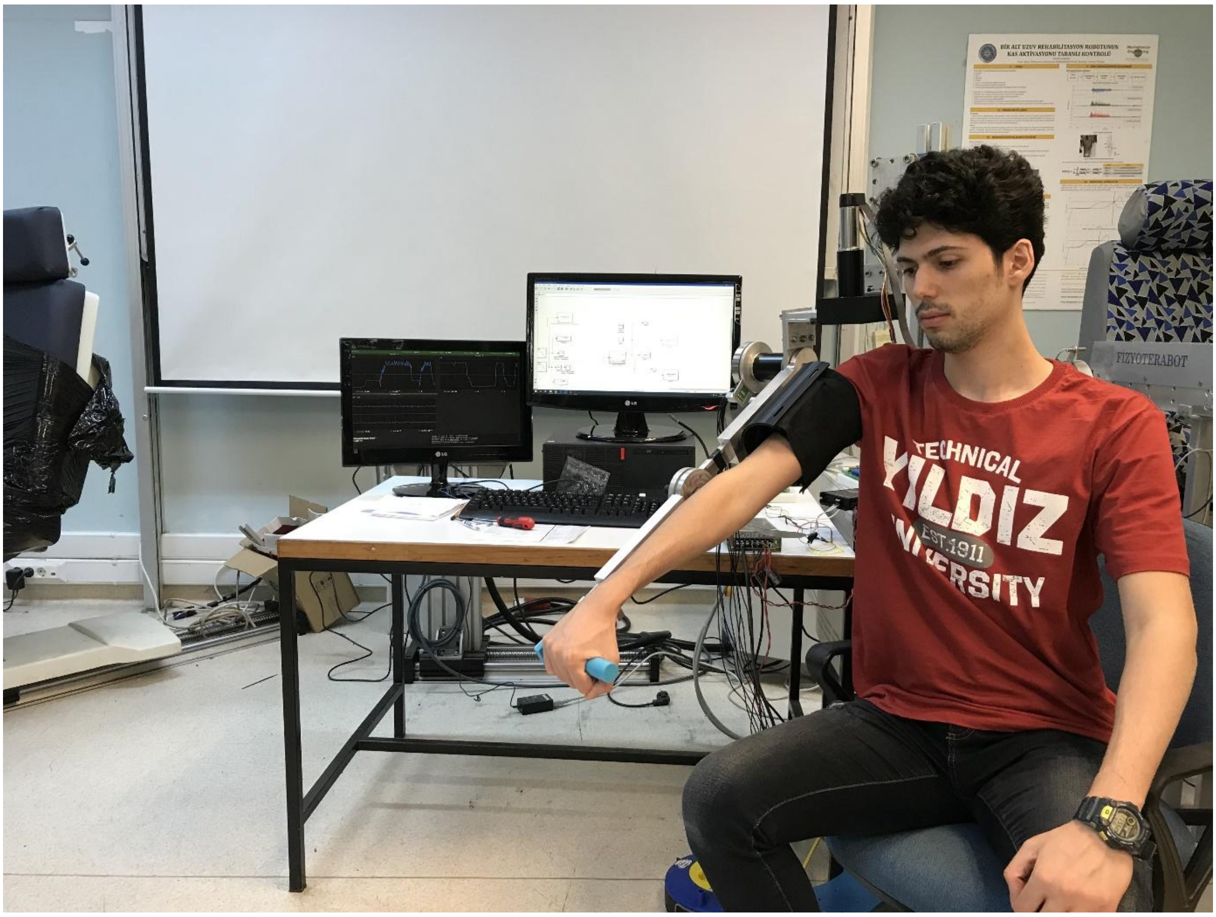

(b)

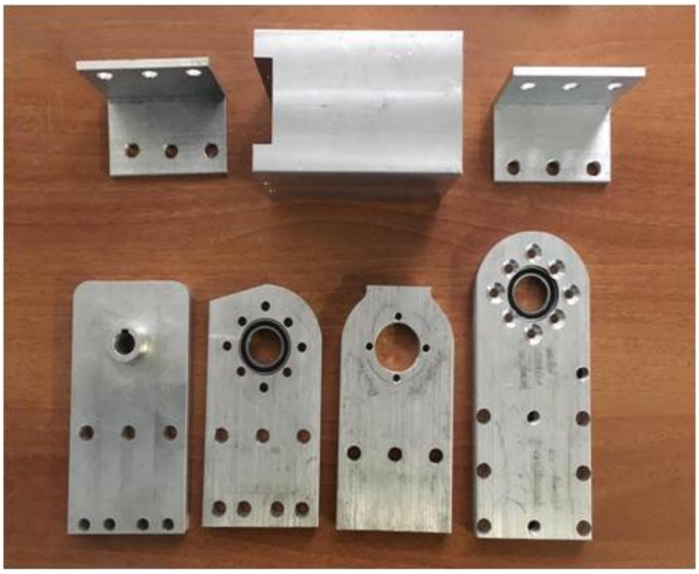

(c)

Figure 5: Produced prototype; (a) Completed status, (b) Using by a patient, (c) Produced Aluminum parts

3.3. Electronic Hardware

The system block diagram can be seen in Fig.6. Raw muscle signals are taken from patients arm by Rapidan Tester branded surface electrodes. These signals are transmitted with surface electrodes to EMG circuit. In EMG circuit, these signals are amplified, filtered and rectified respectively. Raw muscle signals are come out from the EMG circuit as muscle activation levels. Force applied by the patient when performing manual exercises are measured by two force sensors that are both tension-compression micro load cell CZL635 from robot manipulator. Then, muscle activation levels and measured force data are transmitted to main controller by PCI-6025E DAQ which has 16 channels (eight differential) of analog input with 12-bit resolution, two channels of analog output with 12-bit resolution, a 100-pin connector, and 32 lines of digital I/O. The sampling time is 1 ms. Moreover, torque and velocity data are transmitted to motor drivers (ESCON) by DAQ from main controller. According to these data, three brushless dc motors are actuated by motor drives. Maxon EC-Flat 60(100 Watt), EC-Max 30(40 Watt) and EC-Flat 45(30 Watt) are used as motors and ESCON 50/5 is used as motor controller. In response to the rotational movement of these motors' shafts, digital electrical signals are generated by incremental encoders (integrated with motor). Feedback is provided by the encoder to determine the position and direction information by monitoring the instantaneous positions of the motor shaft. Position information is sent to main controller by these incremental encoders by generating square signals in instant position. Then; position, force, and muscle activation level information are combined in MATLAB & Simulink inside the main controller. Furthermore, the rehabilitation robot is used conveniently by the human-machine interface in the main controller. Therefore, control of the manual exercises is done easily by the physiotherapists with the use of the human-machine interface. Additionally, patients are monitored in real time by physiotherapists during the manual exercises.

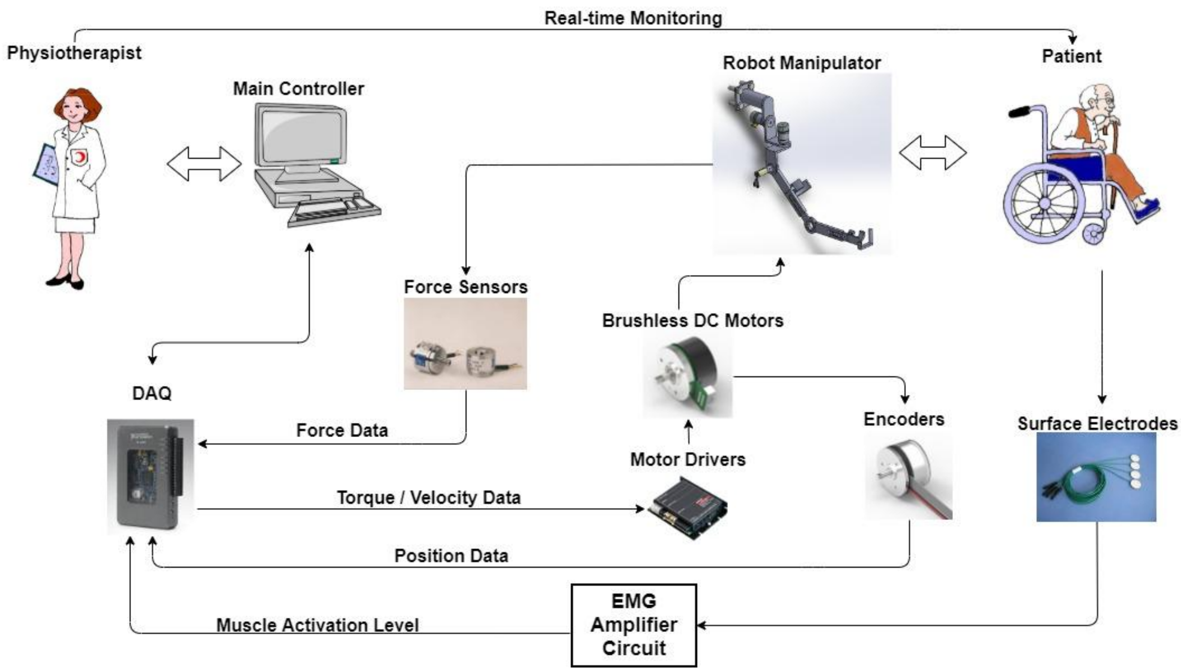

Figure 6: Block diagram of the system

3.3.1. Motor Selections and Calculations

Parallel Axis theorem was used to find the mass moment of inertia about desired axis.

3.3.1.1. Torque and Inertia Calculations for Motor 1

Torque Calculations:

The free body diagram for Motor 1 is given in Fig.7.

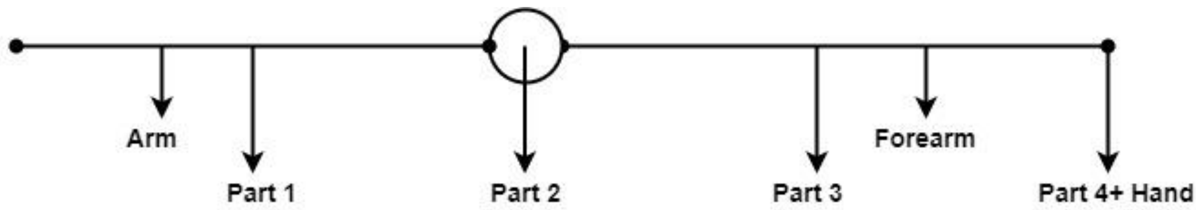

Figure 7: Free body diagram for motor 1 (joint 1)

The torque equation is given in (3.5);

$$T = F \times \Delta x = mg \times \Delta x \qquad (3.5)$$

where $T = Torque, F = Force, \Delta x = distance, g = gravity\ acceleration, m = mass$

$$Arm: 145{,}5\ mm \times 2{,}6\ kg = 378{,}3\ kgmm$$

$$Part\ 1: 186\ mm \times 0.554\ kg = 103{,}04\ kgmm$$

$$Part\ 2: 372\ mm\ \times 0{,}173\ kg = 64{,}36\ kgmm$$

$$Forearm: 664\ mm\ \times 1{,}6\ kg = 1062{,}4\ kgmm$$

$$Part\ 3: 518\ mm\ \times 0{,}28\ kg = 145{,}04\ kgmm$$

$$Hand + Part\ 4: 772mm\ \times 0{,}77kg = 594{,}44\ kgmm$$

$$Predicted\ Extra\ Load: 386\ mm\ \times 0{,}2\ kg = 77.2\ kgmm$$

$$\boldsymbol{Total : 2424{,}776\ kgmm = 23{,}79\ Nm}$$

Moment of Inertia Calculations for Parts:

Moment of inertia for hollow cylinder is given in (3.6) and for rectangular prisma in (3.7).

$$I = \frac{1}{2}M(R_1^2 + R_2^2) \qquad (3.6)$$

where $I = inertia\ , M = mass, R_1 = outer\ radius, R_2 = inner\ radius$

$$I = \frac{1}{12}M(a^2 + b^2) \qquad (3.7)$$

where $I = inertia, M = mass, a = long\ side, b = short\ side$

$$\frac{1}{12} \times 554 \times (265^2 + 50^2) + 554 \times 168^2 = 18993566\ grmm^2$$

$$\frac{1}{2} \times 162 \times (40^2 + 20^2) + 162 \times 340^2 = 18889200\ grmm^2$$

$$\frac{1}{12} \times 143 \times (180^2 + 40^2) + 143 \times 470^2 = 31993866\ grmm^2$$

$$\frac{1}{12} \times 137 \times (190^2 + 40^2) + 137 \times 590^2 = 48120108\ grmm^2$$

$$\boldsymbol{Total = 117996740\ \ grmm^2 = 0{,}1179\ kgm^2}$$

<u>Moment of Inertia Calculations for Human Body:</u>

Moment of inertia for solid cylinder is given in (3.8).

$$I = \frac{1}{12}M(3r^2 + h^2) \qquad (3.8)$$

where $I = inertia\ , M = mass, r = radius, h = height$

$$\frac{1}{12} \times 2600 \times (3 \times 60^2 + 372^2) + 2600 \times 191^2 = 32819800\ grmm^2$$

$$\frac{1}{12} \times 1600 \times (3 \times 50^2 + 292^2) + 1600 \times 446^2 = 13082133\ grmm^2$$

$$\frac{1}{12} \times 700 \times (3 \times 34^2 + 130^2) + 700 \times 685^2 = 1667633\ grmm^2$$

$$\boldsymbol{Total\ Inertia\ of\ human\ body + parts} : \mathbf{165556306}\ \boldsymbol{grmm^2} = \mathbf{0{,}165556}\ \boldsymbol{kgm^2}$$

3.3.1.2. Torque and Inertia Calculations for Motor 2:

<u>Torque Calculations:</u>

The free body diagram for Motor 2 is given in Fig.8.

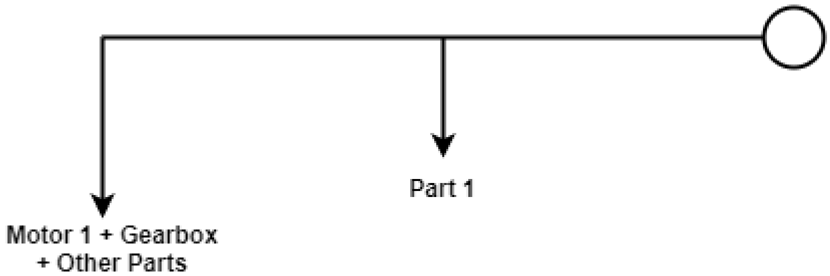

Figure 8: Free body diagram for motor 2 (joint 2)

The torque equation is given in (3.5);

$$T = F \times \Delta x = mg \times \Delta x \qquad (3.9)$$

where $T = Torque, F = Force, \Delta x = distance, g = gravity\ acceleration, m = mass$

$$Part\ 1: 0.176kg\ \times 30\ mm = 5.28\ kgmm$$

$$Motor1\ +\ Gearbox\ +\ Other\ Parts: 6kg\ \times 95\ mm = 570\ kgmm$$

$$\boldsymbol{Total:\ 575.28\ kgmm\ =\ 5.643\ Nm}$$

<u>Moment of Inertia Calculations for Parts:</u>

Moment of inertia for rectangular prisma in (3.10) and for solid cylinder about central axis in (3.11).

$$I = \frac{1}{12}M(a^2 + b^2) \qquad (3.10)$$

where $I = inertia, M = mass, a = long\ side, b = short\ side$

$$I = \frac{1}{2}MR^2 \qquad (3.11)$$

where $I = inertia\ , M = mass, R = radius$

$$\frac{1}{12} \times 225 \times (130^2 + 70^2) + 225 \times 30^2 = 611250\ grmm^2$$

$$\frac{1}{12} \times 231 \times (10^2 + 70^2) + 231 \times 100^2 = 2406250\ grmm^2$$

$$-\frac{1}{2} \times 49 \times 48^2 = -56448\ grmm^2$$

$$\frac{1}{12} \times 554 \times (265^2 + 16^2) + 554 \times 193^2 = 23889818\ grmm^2$$

$$\frac{1}{12} \times 143 \times (180^2 + 8^2) + 143 \times 478^2 = 33060074\ grmm^2$$

$$\frac{1}{12} \times 137 \times (190^2 + 8^2) + 137 \times 598^2 = 49404620\ grmm^2$$

$$\frac{1}{4} \times 162 \times (40^2 + 20^2) + 162 \times 352^2 = 20153448 \; grmm^2$$

$$\boldsymbol{Total = 129469012 \;\; grmm^2 = 0,1294 \; kgm^2}$$

Moment of Inertia Calculations for Human Body:

Moment of inertia for solid cylinder is given in (3.12) and for solid cylinder about central axis in (3.13).

$$I = \frac{1}{12} M(3r^2 + h^2) \qquad (3.12)$$

where $I = inertia \, , M = mass, r = radius, h = height$

$$I = \frac{1}{2} MR^2 \qquad (3.13)$$

where $I = inertia \, , M = mass, R = radius$

$$\frac{1}{12} \times 2600 \times (3 \times 60^2 + 372^2) + 2600 \times 194^2 = 130176800 \; grmm^2$$

$$\frac{1}{12} \times 2600 \times (3 \times 50^2 + 292^2) + 1600 \times 450^2 = 336368533 \; grmm^2$$

$$\frac{700}{2} \times 34^2 + 700 \times 687^2 = 330782900 grmm^2$$

Moment of Inertia Calculations for Motor 1 w.r.t Motor 2:

Moment of inertia for solid cylinder is given in (3.14).

$$I = \frac{1}{12} M(3r^2 + h^2) \qquad (3.14)$$

where $I = inertia \, , M = mass, r = radius, h = height$

$$\frac{1}{12} \times 700 \times (3 \times 26^2 + 80^2) + 700 \times 145^2 = 15209133 \; grmm^2$$

$$\frac{1}{12} \times 624 \times (3 \times 45^2 + 27^2) + 624 \times 199^2 = 25064832 \; grmm^2$$

$$\boldsymbol{Total\ Inertia\ of\ human\ body + parts + Motor1\ w.r.t\ Motor2 = 967071210 \;\; grmm^2}$$

$$\boldsymbol{Total\ Inertia\ of\ human\ body + parts + Motor1\ w.r.t\ Motor2 = 0,967071 \; kgm^2}$$

3.3.1.3. Torque and Inertia Calculations for Motor 3

Torque Calculations:

The free body diagram for Motor 3 is given in Fig.9.

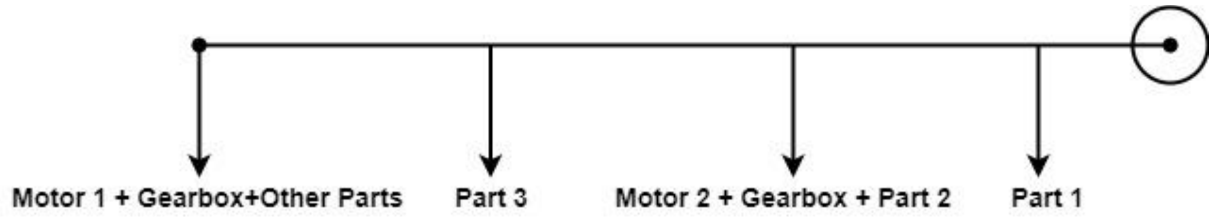

Figure 9: Free body diagram for motor 3 (joint 3)

The torque equation is given in (3.15);

$$T = F \times \Delta x = mg \times \Delta x \qquad (3.15)$$

where $T = Torque, F = Force, \Delta x = distance, g = gravity\ acceleration, m = mass$

$$Part\ 1: 0.247\ kg\ \times 38\ mm = 9{,}38\ kgmm$$

$$Motor2 + Gearbox + Part\ 2 : 0{,}887\ kg\ \times 95\ mm = 84{,}26\ kgmm$$

$$Part\ 3: 0.184\ kg\ \times 143\ mm = 26{,}31\ kgmm$$

$$Motor1 + Gearbox + Other\ parts: 3{,}00\ kg\ \times 190\ mm = 570\ kgmm$$

$$\boldsymbol{Total: 690, 14\ kgmm = 6, 77\ Nm}$$

Moment of Inertia Calculations for Parts:

Moment of inertia for rectangular prisma in (3.16) and for solid cylinder about central axis in (3.17).

$$I = \frac{1}{12} M(a^2 + b^2) \qquad (3.16)$$

where $I = inertia, M = mass, a = long\ side, b = short\ side$

$$I = \frac{1}{2} MR^2 \qquad (3.17)$$

where $I = inertia\ , M = mass, R = radius$

$$\frac{1}{12} \times 247 \times (130^2 + 70^2) + 247 \times 30^2 = 671016\ grmm^2$$

$$\frac{1}{12} \times 278 \times (10^2 + 70^2) + 278 \times 90^2 = 2367633\ grmm^2$$

$$-\frac{1}{4} \times 2 \times 49 \times 48^2 - 2 \times 49 \times 95^2 = -940898\ grmm^2$$

$$\frac{1}{12} \times 225 \times (130^2 + 10^2) + 225 \times 109^2 = 2991975\ grmm^2$$

$$\frac{1}{12} \times 231 \times (130^2 + 10^2) + 231 \times 191^2 = 8754361\ grmm^2$$

$$\frac{1}{12} \times 554 \times (50^2 + 16^2) + 554 \times 212^2 = 25026211\ grmm^2$$

$$\frac{1}{4} \times 162 \times (40^2 + 20^2) + 162 \times 211^2 = 7293402\ grmm^2$$

$$\frac{1}{12} \times 143 \times (8^2 + 40^2) + 143 \times 209^2 = 6266212\ grmm^2$$

$$\frac{1}{12} \times 137 \times (8^2 + 40^2) + 137 \times 212^2 = 6176325\ grmm^2$$

$$\boldsymbol{Total = 58606237\ \ grmm^2 = 0,058606237\ kgm^2}$$

Moment of Inertia Calculations for Human Body:

Moment of inertia for solid cylinder is given in (3.18) and for solid cylinder about central axis in (3.19).

$$I = \frac{1}{12} M(3r^2 + h^2) \qquad (3.18)$$

where $I = inertia\ , M = mass, r = radius, h = height$

$$I = \frac{1}{2} MR^2 \qquad (3.19)$$

where $I = inertia\ , M = mass, R = radius$

$$\frac{1}{12} \times 700 \times (3 \times 34^2 + 130^2) + 700 \times 200^2 = 29188133\ grmm^2$$

$$\frac{2600}{2} \times 60^2 + 2600 \times 193^2 = 101527400\ grmm^2$$

$$\frac{1600}{2} \times 50^2 + 1600 \times 195^2 = 62840000\ grmm^2$$

<u>Moment of Inertia Calculations for Motor 1 and Motor 2 w.r.t Motor 3:</u>

Moment of inertia for solid cylinder is given in (3.20) and for solid cylinder about central axis in (3.19).

$$I = \frac{1}{12}M(3r^2 + h^2) \qquad (3.20)$$

where $I = inertia\ , M = mass, r = radius, h = height$

$$\frac{1}{12} \times 700 \times (3 \times 26^2 + 80^2) + 700 \times 240^2 = 40688725\ grmm^2$$

$$\frac{1}{12} \times 624 \times (3 \times 45^2 + 27^2) + 624 \times 275^2 = 47543808\ grmm^2$$

$$\frac{1}{12} \times 305 \times (3 \times 15^2 + 64^2) + 305 \times 95^2 = 2873888\ grmm^2$$

$$\frac{1}{12} \times 200 \times (3 \times 16^2 + 50^2) + 200 \times 95^2 = 1859467\ grmm^2$$

$$\boldsymbol{Total\ Inertia\ of\ human\ body + parts + Motor1\ and\ Motor2\ w.r.t\ Motor = 345127658\ grmm^2 = 0,345127\ kgm^2}$$

3.3.1.4. Calculations for Motor 1

First of all, the speed of exercise for patients at the end of robotic arm assumed as 1 m/sc. Then, the speed is found from (3.21) which is at gearbox output.

$$w = \frac{2\pi n}{60}$$

$$n_2 = \frac{1.295\ x\ 60}{2\ x\ \pi} \qquad (3.21)$$

$$n_2 = 13\ rpm$$

$$w = angular\ velocity, n = speed$$

This speed is approved for all motors.

$$\frac{n_1}{n_2} = \frac{T_2}{T_1}$$

$$T_1, T_2 = torque\ values$$

The input gearbox torque was assumed as nominal torque of motor and the gearbox ration was found with (3.22).

$$Gearbox\ ratio = \frac{25870\ mNm}{230\ mNm} = 112.4 \qquad (3.22)$$

Then, the closest gearbox ratio was selected as 113:1.

$$n_1 = 113\ x\ 13 = 1469\ rpm$$

The maximum acceleration of motor 1 is obtained from equation (3.23)

$$\alpha_{max} = 10^4 x \frac{4300}{835 + 1603870} = 26.8 \frac{rad}{sc^2} \quad (3.23)$$

$$\alpha_{max} = maximum\ acceleration\ from\ catalog$$

The acceleration time of our motor1 was chosen as 0.1 second.

$$\alpha_{max,our} = \frac{1.295\ rad/sc}{0.1\ sc} = 12.95\ rad/sc^2$$

$$\alpha_{max,our} = maximum\ acceleration\ from\ our\ calculations$$

Finally, the power and ampere usage was controlled from equations (3.24) and (3.25).

$$P_{max} = M_{max}\ x\ n_{max}\ x\ \frac{\pi}{30} \qquad (3.24)$$

$$P_{max,our} = 0.23\ x\ 1469\ x\ \frac{\pi}{30} = 36\ \text{W}$$

$$\text{P} = \text{I x V} \rightarrow \text{I} = 1.5\ \text{A} \qquad (3.25)$$

$$P = power, M = moment, n = speed, V = voltage, I = current$$

Optimum values are found for system and both of motor and gearbox.

3.3.1.5. Calculations for Motor 2

$$\frac{n_1}{n_2} = \frac{T_2}{T_1}$$

$$T_1, T_2 = torque\ values$$

The input gearbox torque was assumed as nominal torque of motor and the gearbox ration was found with (3.26).

$$Gearbox\ ratio = \frac{5747\ mNm}{25\ mNm} = 229.88 \qquad (3.26)$$

Then, the closest gearbox ratio was selected as 246:1.

The maximum acceleration of motor 2 is obtained from equation (3.27)

$$n_1 = 246\ x\ 13 = 3200\ rpm$$

$$\alpha_{max} = 10^4 x\ \frac{160}{11 + 9613869} = 0.166\frac{rad}{sc^2} \qquad (3.27)$$

$$\alpha_{max} = maximum\ acceleration\ from\ catalog$$

The acceleration time of our motor 2 was chosen as 8 seconds.

$$\alpha_{max,our} = \frac{1.295\ rad/sc}{8\ sc} = 0.162\ rad/sc^2$$

$$\alpha_{max,our} = maximum\ acceleration\ from\ our\ calculations$$

Finally, the power and ampere usage was controlled from equations (3.28) and (3.29).

$$P_{max} = M_{max}\ x\ n_{max}\ x\ \frac{\pi}{30} \qquad (3.28)$$

$$P_{max,our} = 0.025\ x\ 3200\ x\ \frac{\pi}{30} = 8.4\ \mathrm{W}$$

$$\mathrm{P} = \mathrm{I\,x\,V} \rightarrow \mathrm{I} = 0.35\ \mathrm{A} \qquad (3.29)$$

$$P = power, M = moment, n = speed, V = voltage, I = current$$

3.3.1.6. Calculations for Motor 3

$$\frac{n_1}{n_2} = \frac{T_2}{T_1}$$

The input gearbox torque was assumed as nominal torque of motor and the gearbox ration was found with (3.30).

$$Gearbos\ ratio = \frac{7000\ mNm}{55\ mNm} = 127.27 \qquad (3.30)$$

Then, the closest gearbox ratio was selected as 126:1.

The maximum acceleration of motor 3 is obtained from equation (3.31).

$$n_1 = 126\ x\ 13 = 1638\ rpm$$

$$\alpha_{max} = 10^4 x\ \frac{253}{92 + 3428790} = 0.737\frac{rad}{sc^2} \qquad (3.31)$$

(Max. acceleration of motor from catalog.)

The acceleration time of our motor 3 was chosen as 2 seconds.

$$\alpha_{max,our} = \frac{1.295\ rad/sc}{2\ sc} = 0.6475\ rad/sc^2$$

Finally, the our power and ampere usage was controlled from equations 3.32 and 3.33.

$$P_{max} = M_{max}\ x\ n_{max}\ x\ \frac{\pi}{30} \qquad (3.32)$$

$$P_{max,our} = 0.055\ x\ 1638\ x\ \frac{\pi}{30} = 9.5\ W$$

$$\mathrm{P} = \mathrm{I} \times \mathrm{V} \rightarrow \mathrm{I} = 0.4\ \mathrm{A} \qquad (3.33)$$

Optimum values are found for system and both of motor and gearbox. The total values are given below.

$$T_m = T_l + J\frac{dw}{dt}$$

$$for\ motor\ 1\ ; T_{m1} = 23{,}73\ Nm + 0{,}160387\ kgm^2 \times 12{,}95\frac{rad}{s^2} = 25{,}87\ Nm$$

$$for\ motor\ 2\ ; T_{m2} = 5.643\ Nm + 0{,}961369\ kgm^2 \times 0.476\frac{rad}{s^2} = 5.747\ Nm$$

$$for\ motor\ 3\ ; T_{m3} = 6{,}77\ Nm + 0{,}342879\ kgm^2 \times 0.6475\ \frac{rad}{s^2} = 7\ Nm$$

3.3.1.7. Selection of Brushless DC Motor

The movements of the rehabilitation robot is highly related with the movement capability of shoulder and elbow anatomy. Therefore, maximum torque capability values limit the motor selection criterias according to torque value. A motor which has torque value more than the Fig.10 values cannot be selected. For shoulder vertical flexion/extension movement (joint 1) motor 1 is used. For shoulder abduction/adduction movement (joint 2) motor 2 and for shoulder horizontal flexion/extension movement (joint 3) motor 3 is used. So, selected motor 1 should have less than 110 Nm, motor 2 should have less than 125 Nm and motor 3 should have less than 110 Nm torque.

DOF		Torque (Nm) [31]
Shoulder	Flexion/Extension	110
	Abduction/Adduction	125
	Medial/Lateral Rotation	-
Elbow	Flexion/Extension	72.5

Figure 10: Human Torque Limits of Shoulder and Elbow

3.3.1.8. Motor Selections [22]

The specifications of the Maxon flat motors, rated operating point and operating ranges are given in Appendix A.

3.3.1.8.1. Motor 1 Selection

- For all motors, the supply voltage value was accepted 24 V.
- When considering the mass of the patient, the mass of the exoskeleton and additional loads, the torque value was found to be 23,79 Nm in the motor axis. In order to the selected motor reaches the desired speed in 0,1 second in this axis, the total torque coming to the motor axis was calculated to be 25,78 Nm. And, output torque of gearhead which was selected is 30 Nm. So, this motor is appropriate.
- In the engine catalog, there are 2 engine types in accordance with this torque value such as EC-flat 60 and EC-flat 90.
- Because of the the power value of EC-flat 90 type was much higher than required power value, the EC-flat 60 type was selected. Moreover, motors below this type of engine are not sufficient for the torque value which was found.
- At the output of the motor, the speed is 1469 rpm. And, the rpm value which was selected in the catalog, is 3730 rpm. Therefore, selected motor is suitable for the system.
- The maximum power the system consumes is 36 Watt. EC-flat 60 can withstand up to 100 Watt. So, the selected motor is appropriate for the system.
- Moreover, the engine can accelerate the system in 0.1 seconds as can be seen in Fig.11.
- The motor is safe because the current drawn by the motor at the maximum torque as 1,5 A, is less than the rated current 5,14 A.

Therefore, EC-flat 60, 100 Watt type motor was selected as motor 1. Specifications of EC flat 60 motor are given in Appendix A.

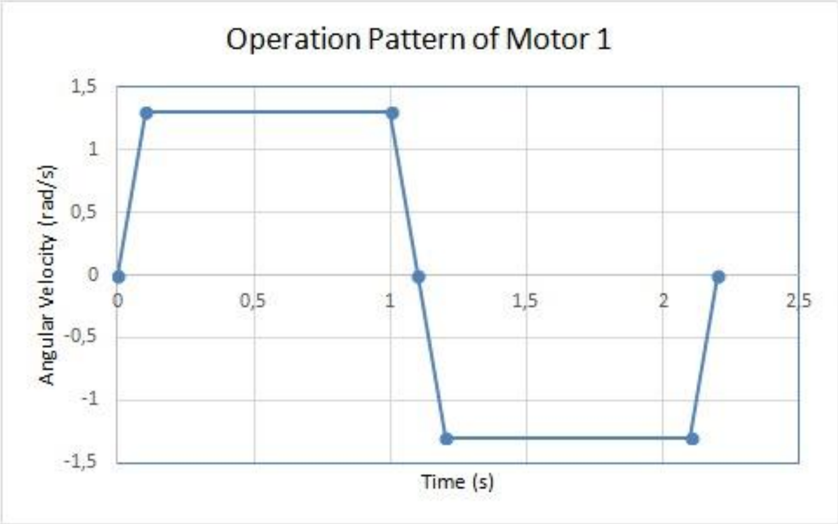

Figure 11: Operation pattern of motor 1 (joint 1)

3.3.1.8.2. Gearhead 1 Selection

- The torque value at the engine output was accepted slightly below the nominal torque value of the desired engine, gear ratio was found as 113:1. So, the gearhead was selected as this rate in GP-52 C gearhead type.
- Specifications of GP – 52 C is given in Appendix A.
- Fig. 12 shows that when the selected torque value is nominal, this motor is suitable for the system because this nominal torque value is under the curve.

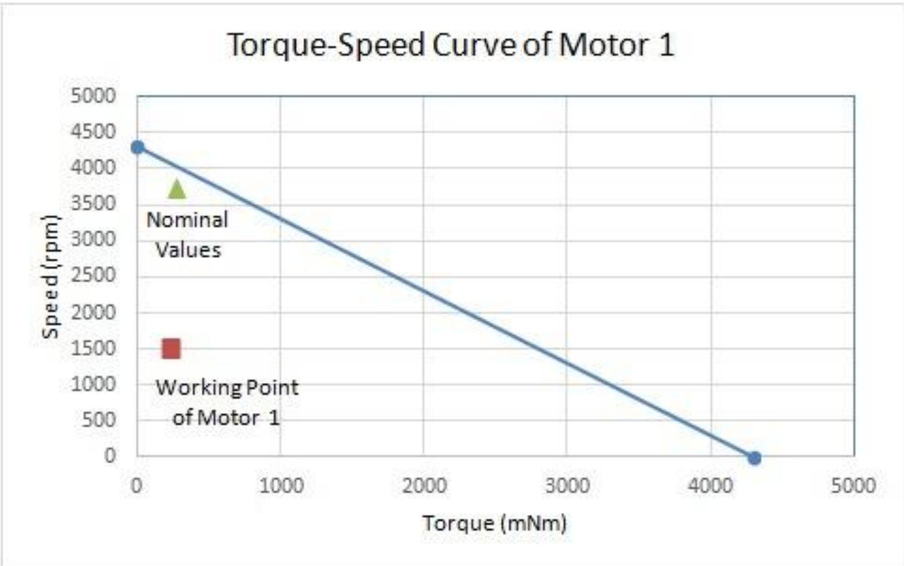

Figure 12: Torque-Speed curve of motor 1 (joint 1)

3.3.1.8.3. Motor 2 Selection

- When considering the mass of the patient, the mass of the exoskeleton and additional loads, the torque value was found to be 5,592 Nm in the motor axis. In the situation which the selected motor reaches the desired speed in 8 second in this axis, the total torque coming to the motor axis was calculated 5,747 Nm. And, output torque of gearhead which was selected is 6 Nm. So, this motor is appropriate.
- Because of the torque value which is taken from gearbox is the most suitable for the needed torque value, EC-max 30 motor was selected.
- At the output of the motor the speed was 3200 rpm. And, the rpm value which was selected in the catalog, is 7220 rpm. Therefore, selected motor is suitable for the system.
- The maximum power the system consumes was found 8,4 Watt. EC-max 30 can withstand up to 40 Watt. So, the selected motor is appropriate for the system.
- Moreover, the engine can accelerate the system in 8 seconds.
- The motor is safe because the current drawn by the motor at the maximum torque as 0,35 A, is less than the rated current 1,49 A.

Therefore, EC-max 30, 40 Watt type motor was selected as motor 1. Specifications of EC max 30 motor are given in Appendix A.

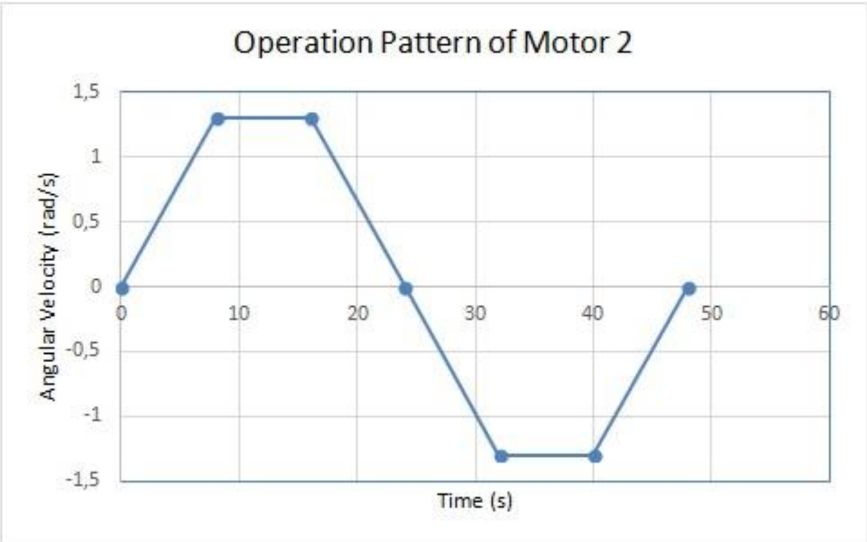

Figure 13: Operation pattern of motor 2 (joint 2)

3.3.1.8.4. Gearhead 2 Selection

- The torque value at the engine output was selected slightly below the nominal torque value of the desired engine, Gear ratio was found as 246:1. So, GP-32 C gearhead type was selected.
- Specifications of GP – 32 C is given in Appendix A.

- Fig. 14 shows that when the selected torque value is nominal, this motor is suitable for the system because this nominal torque value is under the curve.

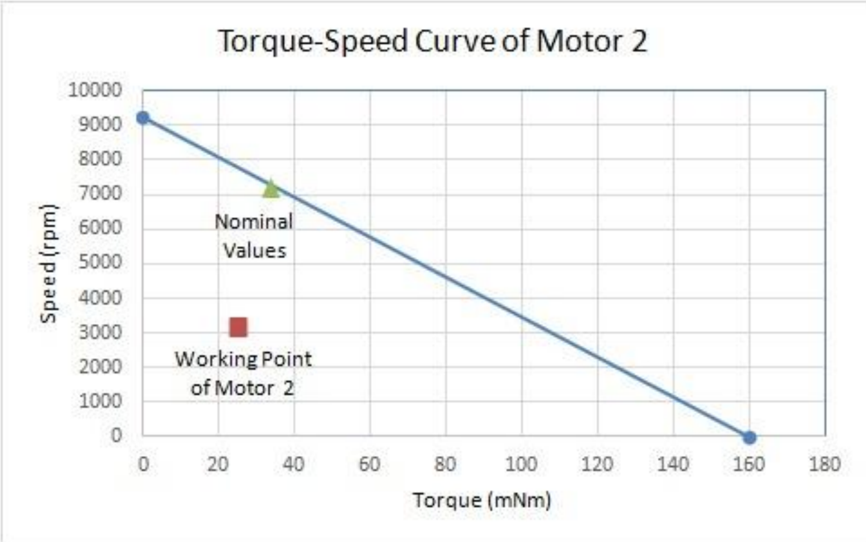

Figure 14: Torque-Speed curve of motor 2 (joint 2)

3.3.1.8.5. Motor 3 Selection

- When considering the mass of the patient, the mass of the exoskeleton and additional loads, the torque value was found 6,77 Nm in the motor axis. In order to the motor reaches the desired speed in 2 seconds in this axis, the total torque coming to the motor axis was calculated to be 7 Nm. And, output torque of gearhead which was selected is 15 Nm. So this motor is appropriate. Because of the torque value which is taken from gearbox is the most suitable for our torque value, EC-flat 45 motor was selected.
- At the output of the motor, the speed is 1638 rpm. And, the rpm value which was selected in the catalog, is 2930 rpm. Therefore, selected motor is suitable for the system.
- The maximum power the system consumes was found 9,43 Watt. EC-flat 45 can withstand up to 30 Watt. So, the selected motor is appropriate for the system.
- Moreover the motor can accelerate the system in 2 seconds.
- The motor is safe because the current drawn by the motor at the maximum torque as 0,394 A, is less than the rated current 1,01 A.

Therefore, EC-flat 45, 30 Watt type motor was selected as motor 1. Specifications of EC flat 45 motor are given in Appendix A.

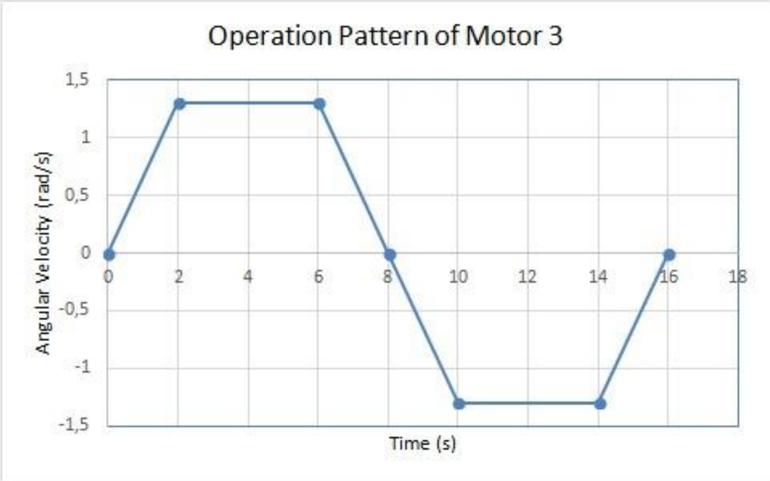

Figure 15: Operation pattern of motor 3 (joint 3)

3.3.1.8.6. Gearhead 3 Selection

- When the torque value at the engine output was accepted slightly below the nominal torque value of the desired motor, we found a gear ratio as 126:1. So, GP-42 C gearhead type was selected.
- Specifications of GP – 42 C is given in Appendix A.
- Fig.16 shows that when the selected torque value is nominal, this motor is suitable for the system because this nominal torque value is under the curve.

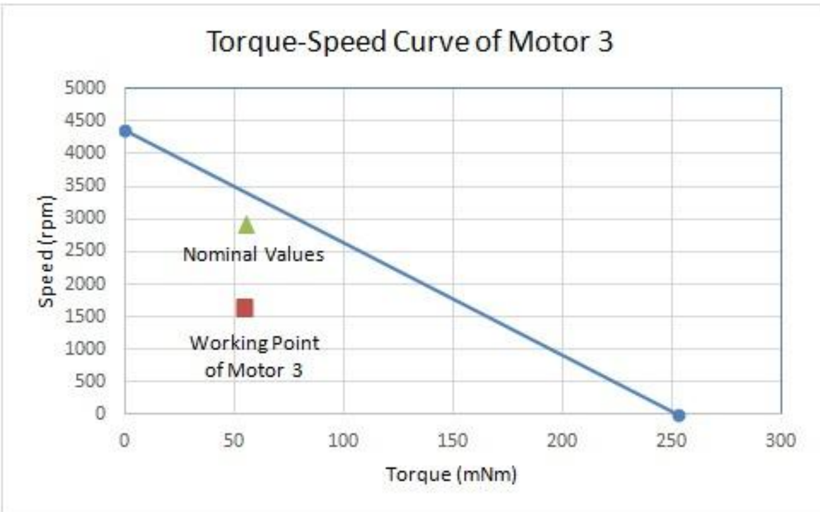

Figure 16: Torque-Speed curve of motor 3 (joint 3)

3.3.2. Sensor Selections

3.3.2.1. Electromyography (EMG)

The potential which is produced by the muscles is measured by this method. The EMG signals have 0-10 mV amplitude.

The EMG signals with low amplitude are amplified with the help of EMG circuits.

In rehabilitation robots EMG signals are used with other feedbacks to control the system more efficient and stable.

<u>Technical Requirements for Biological Sensor (EMG)</u>

In the rehabilitation robot, EMG based impedance control method was used. Therefore, an EMG circuit was needed to detect the muscle activation levels from arm muscles.

Frequency range of EMG: *0 Hz – 500 Hz.*

Usable energy of EMG signal: *50 Hz –150 Hz.*

Frequency range of muscle with slow twitch motor units: *75 Hz – 125 Hz.*

Frequency range of muscle with fast twitch motor units: *125 Hz – 250 Hz.*

Amplitude of EMG signals: 0-10 mV.

Stages of EMG Circuit: Rectification, Amplifying and Filtering stages.

3.3.2.2. Force Sensors

A force / torque sensor is a device which converts the mechanical force / torque effect to electrical output signals. These sensors can sense in 3 axis. This sensor is used in rehabilitation robots to measure the force amount from the patient or from the robot. This sensors are positioned in the direction of the rehabilitation movement.

<u>Technical Requirements for Force Sensors</u>

Range: 0 – 20 kg

Range: 0 – 196,2 N

Length: Less than 100 mm

Sensitivity: At least 10 bit

Accuracy: Less than 0,2

3.3.2.3. Position Sensors

This sensors can sense the position of the joints. The sensors can sense both linear and angular position. These are important to see and analyze the movements of the patient.

Technical Requirements for Encoder 1

Maximum Operating Frequency (kHz): 1000 kHz

Maximum Speed (rpm): More than 4000 rpm

Counts per Turn: Approximately 500

Suitability: It should be suitable for selected motor 1.

Technical Requirements for Encoder 2

Maximum Operating Frequency (kHz): 100 kHz

Maximum Speed (rpm): More than 8000 rpm

Counts per Turn: Approximately 500

Suitability: It should be suitable for selected motor 2.

Technical Requirements for Encoder 3

Maximum Operating Frequency (kHz): 1000 kHz

Maximum Speed (rpm): More than 3000 rpm

Counts per Turn: Approximately 500

Suitability: It should be suitable for selected motor 3.

3.3.2.4. Selection of Force Sensors

The required range is between 10 kg - 15 kg, so approximately range is between 98,1 N – 147,15 N. Moreover, range of load cell which was selected is between 0 kg – 20 kg, so it's range is approximately 0 N – 196,2 N. Therefore, selected load cell is suitable for the system.

Furthermore, according to the technical requirements, length of the load cell should be less than 100 mm. Length of selected load cell is 55 mm, so this load cell is appropriate for the system.

Therefore, Micro Load Cell CZL635 force sensors were selected. The specifications to Micro Load Cell CZL635 is given in Appendix B. Locations of force sensors are shown in the Fig.17. in red circles.

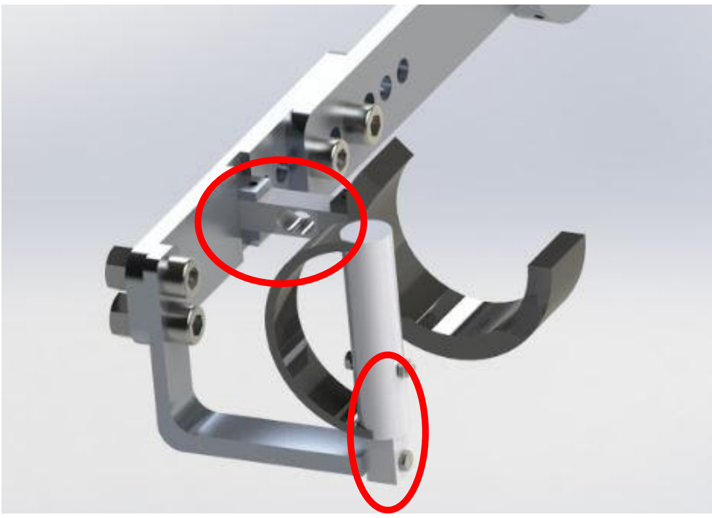

Figure 17: Locations of force sensors on the system

3.3.2.5. Selection of Encoders [22]

First of all, the selection for motors was made as suitable Maxon brushless dc motors. Because, these motors are more precise, vibration free and they have higher power value according to their size. After that, selection is made for motors according to calculated torque, power and speed values.

In MAXON motors, internal encoders are installed inside the motors. So, a selection was made for encoders according to motors which previously selected.

3.3.2.5.1. Selection of Encoder 1

FEATURES	CALCULATED VALUES	CATALOGUE VALUES
Torque	25,78 Nm	30 Nm
Power	36 Watt	100 Watt
Speed	1469 rpm	3730 rpm

Catalogue values are suitable. So, EC-flat 60 was selected as motor 1. Fig.18 represents the suitable encoder types for EC-flat 60. Therefore, encoder 1 was selected in suitable encoders for motor 1 according to the technical requirements.

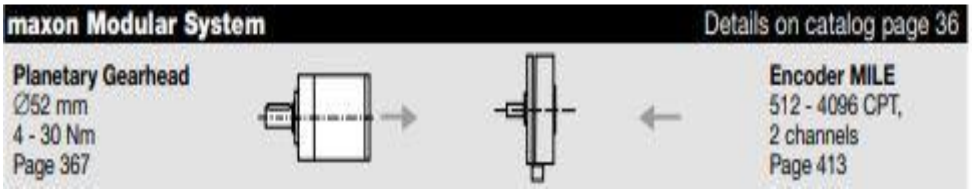

Figure 18: Suitable encoder types for EC-flat 60

The specifications to Encoder MILE, 512 CPT, 2 channel, with line driver is given in Appendix B.

3.3.2.5.2. Selection of Encoder 2

FEATURES	CALCULATED VALUES	CATALOGUE VALUES
Torque	5,747 Nm	6 Nm
Power	8,4 Watt	40 Watt
Speed	3200 rpm	7220 rpm

Catalogue values are suitable. So, EC-max 30 was selected as motor 2. Fig.19 shows that the suitable encoder types for EC-max 30. Therefore, encoder 2 was selected in suitable encoders for motor 2 according to the technical requirements.

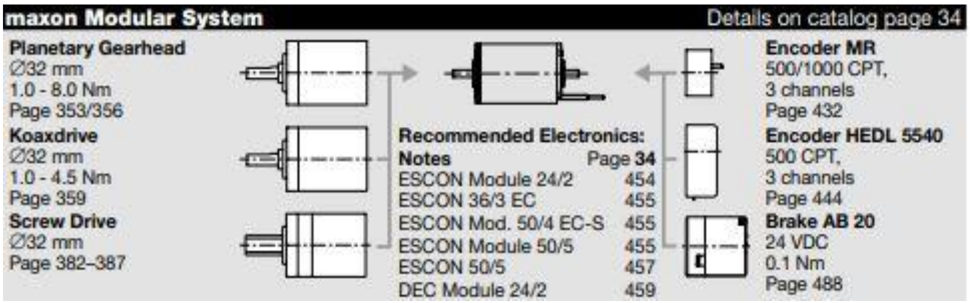

Figure 19 : Suitable encoder types for EC-max 30

The specifications to Encoder HEDL, 500 CPT, 2 channel, with line driver RS 422 is given in Appendix B.

3.3.2.5.3. Selection of Encoder 3

FEATURES	CALCULATED VALUES	CATALOGUE VALUES
Torque	7 Nm	15 Nm
Power	9,43 Watt	30 Watt
Speed	1638 rpm	2930 rpm

Catalogue values are suitable. So, EC-flat 45 was selected as motor 3. Fig. 20 demonstrates the suitable encoder types for EC-flat 45. Therefore, encoder 3 was selected in suitable encoders for motor 3 according to our technical requirements.

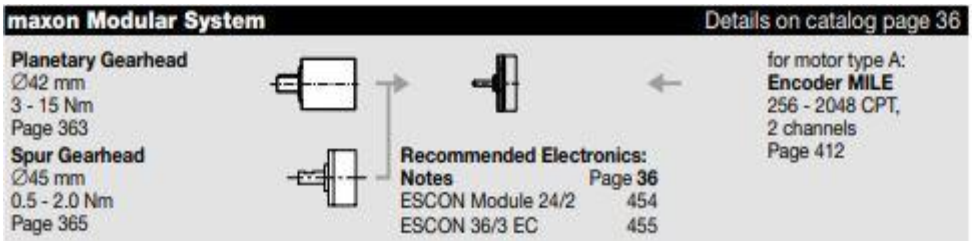

Figure 20: Suitable encoder types for EC-flat 45

The specifications to Encoder MILE, 512 CPT, 2 channel, with line driver is given in Appendix B.

3.3.3. EMG Circuit Design

The block diagram of EMG signal processing in the system is shown in Fig.21. Full-wave rectifier, instrumentation amplifier, one high-pass filter and one low-pass filter are used for rectification, amplifying and filtering stages. Negative portion of the muscle signal is turned into positive by full-wave rectifier. Therefore, the entire signal is fallen within the positive voltage region. Moreover, muscle signal is recovered from DC offset and low frequency noise by active high pass filter. Additionally, smooth signal is produced by active low pass filter. EMG circuit consist of one instrumentation amplifier and six operational amplifiers. Voltage differences between electrodes are measured by instrumentation amplifier.

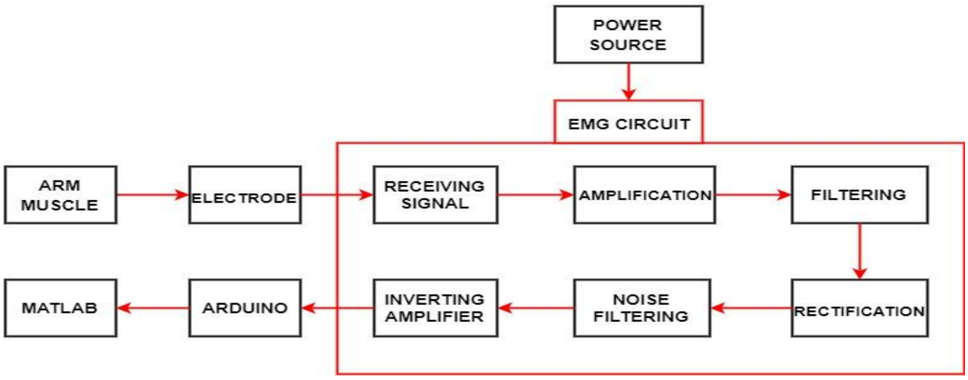

Figure 21: Block diagram of EMG circuit

At difference amplifier part, which is INA106 IC, voltage gain is difference between the electrodes:

$$R_1 = R_2 = 10\ k\Omega$$

$$R_3 = R_4 = 100\ k\Omega$$

R_1 *and* R_2: Difference amplifier's resistant values of op-amp 1.

R_3 *and* R_4: Instrumentation amplifier's resistant values of op-amp 2.

Therefore,

$$A_v = 110$$

At instrumentation amplifier part, voltage gain is:

$$A_v = -\frac{R_4}{R_3} = -\frac{150k\Omega}{10k\Omega} = -15 \qquad (3.34)$$

$$A_v = voltage\ gain$$

At *1st*. order high-pass filter part, voltage gain is:

$$A_v = -1$$

Cut-off frequency is:

$$f_c = \frac{1}{2 * \pi * R * C} = \frac{1}{6.28 * 15 * 10^4\Omega * 10^{-8}F} = 106.103\ Hz \qquad (3.35)$$

$$f_c = cut - off\ frequency$$

$$R = resistanve$$

$$C = capacitance$$

At full-wave rectifier part, negative portion of the signal turn into positive. Therefore, the entire signal falls within the positive voltage region**.**

At *1st.* order low-pass filter part, voltage gain is:

$$A_v = -1$$

Cut-off frequency is:

$$f_c = \frac{1}{2 * \pi * R * C} = \frac{1}{6.28 * 82 * 10^3 \Omega * 10^{-6} F} = 1.940\ Hz \qquad (3.36)$$

At inverting amplifier part, voltage gain is:

$$A_v = -\frac{R_f}{R_{in}} = -\frac{20k\Omega}{1k\Omega} = -20 \qquad (3.37)$$

$$R_f = final\ resistance$$

$$R_{in} = initial\ resistance$$

Proteus drawn of electronical circuit, which has rectification, filtering and amplification stages, is shown in Fig. 22. All electronical elements such as op-amps, diodes, resistances, capacitances were specified in the drawn.

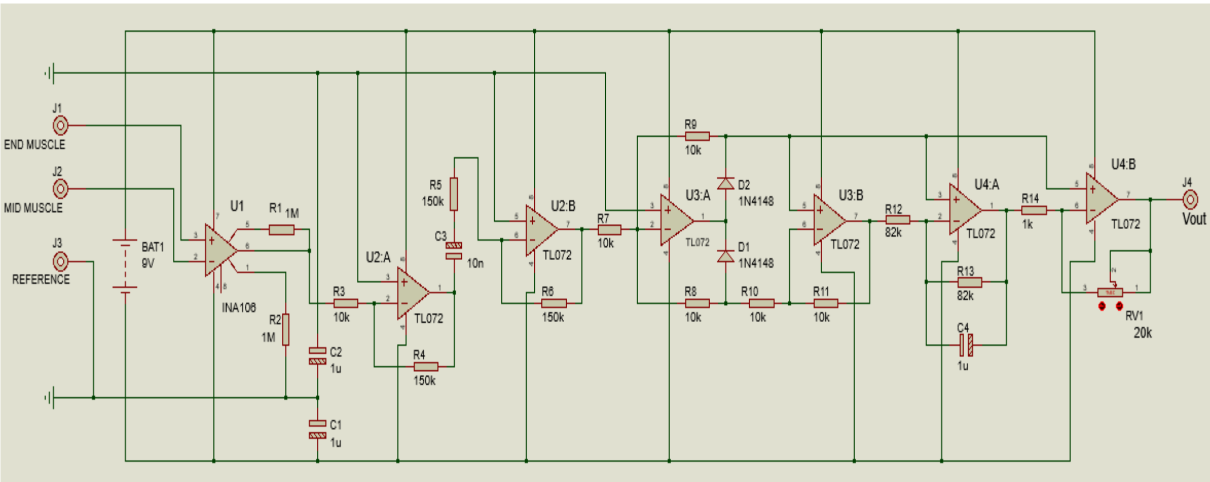

Figure 22: Electrical scheme of EMG circuit on PROTEUS

3.4. User Interface

When the user interface is operated, the menu in Fig.23 is displayed on the screen. In the first part, information such as the name, surname, weight, height and age of the patient are taken and saved with the save button. From the exercise types section, the type of exercise to be selected for the patient is selected. In the movement selection menu, it is possible to choose which joint to perform the movement. The rehabilitation robot starts with the start button and stops working with the stop button.

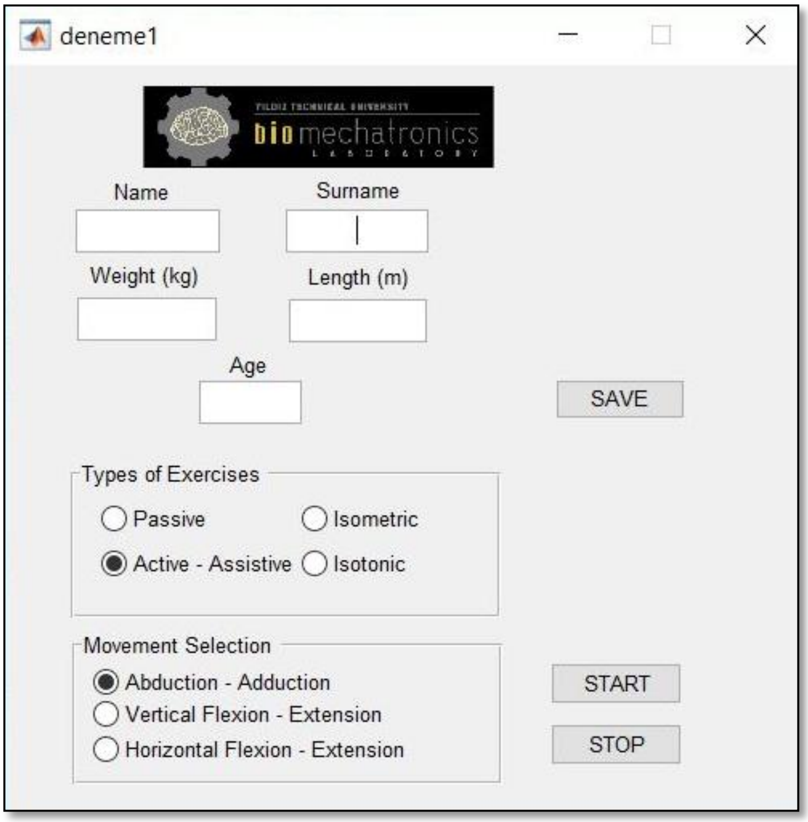

Figure 23: User interface

3.5. Kinematic Analysis

The link-frame attachment in Fig.24 is used to build-up the kinematic model of the rehabilitation robot. In this model joints 0, 1 and 2 together form the glenohumeral joint, where joint 0 corresponds to abduction-adduction, joint 1 horizontal flexion-extension and joint 2 to vertical flexion-extension. Joint 3, which fits to flexion-extension of the elbow joint is located outside the shoulder joint.

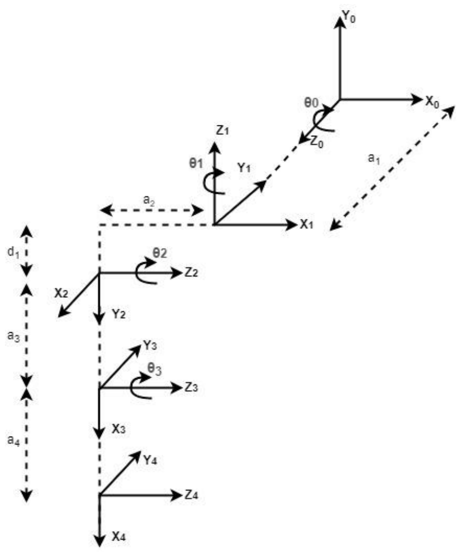

Figure 24: Link - Frame attachments

The DH (Denavit-Hartenberg) parameters are summarized in Tab. 5.

i	a	α	d	θ
1	a_1	$\pi/2$	0	θ_0
2	a_2	$\pi/2$	d_1	θ_1
3	a_3	0	0	θ_2
4	a_4	0	0	θ_3

Table 5: DH Parameter Table

We know that the general form of a link transformation that relates frame {i} relative to the frame {i-1} is in (3.38).

$$ {}^{i-1}_{i}T = \begin{bmatrix} & {}^{i-1}_{i}R^{3\times3} & & {}^{i-1}_{i}P^{3\times1} \\ 0 & 0 & 0 & 0 \end{bmatrix} \qquad (3.38)$$

Where, ${}^{i-1}_{i}R$ is the rotation matrix that describes frame {i} relative to frame {i-1} and can be expressed as in (3.39).

$$ {}^{i-1}_{i}R = \begin{bmatrix} cos\theta_i & -sin\theta_i & 0 \\ sin\theta_i cos\, a_{i-1} & cos\theta_i cos\, a_{i-1} & -sin\, a_{i-1} \\ sin\theta_i sin\, a_{i-1} & cos\theta_i sin\, a_{i-1} & cos\, a_{i-1} \end{bmatrix} \qquad (3.39)$$

And, ${}^{i-1}_{i}P$ is the vector that locates the origin of frame {i} relative to frame {I-1} and can be expressed as in (3.40).

$$ {}^{i-1}_{i}P = [a_{i-1} \quad -sa_{i-1}d_i \quad ca_{i-1}d_i]^T \qquad (3.40)$$

Using equation (3.37-3.40), the individual homogeneous transfer matrix that relates two successive frames can be found as:

$$A_i = T_i^{i-1} = \begin{bmatrix} cos\theta_i & -cos\alpha_i sin\theta_i & sin\alpha_i sin\theta_i & \mathrm{a}_i\, cos\theta_i \\ sin\theta_i & cos\alpha_i cos\theta_i & -sin\alpha_i cos\theta_i & \mathrm{a}_i\, sin\theta_i \\ 0 & sin\alpha_i & cos\alpha_i & d_i \\ 0 & 0 & 0 & 1 \end{bmatrix}$$

$$A_1 = T_1^0 = \begin{bmatrix} cos\theta_0 & 0 & sin\theta_0 & a_1 cos\theta_0 \\ sin\theta_0 & 0 & -cos\theta_0 & a_1 sin\theta_0 \\ 0 & 1 & 0 & 0 \\ 0 & 0 & 0 & 1 \end{bmatrix}$$

$$A_2 = T_2^1 = \begin{bmatrix} cos\theta_1 & 0 & sin\theta_1 & a_2cos\theta_1 \\ sin\theta_1 & 0 & -cos\theta_1 & a_2sin\theta_1 \\ 0 & 1 & 0 & d_1 \\ 0 & 0 & 0 & 1 \end{bmatrix}$$

$$A_3 = T_3^2 = \begin{bmatrix} cos\theta_2 & -sin\theta_2 & 0 & a_3cos\theta_0 \\ sin\theta_2 & cos\theta_2 & 0 & a_3sin\theta_0 \\ 0 & 0 & 1 & 0 \\ 0 & 0 & 0 & 1 \end{bmatrix}$$

$$A_4 = T_4^3 = \begin{bmatrix} cos\theta_3 & -sin\theta_3 & 0 & a_3cos\theta_3 \\ sin\theta_3 & cos\theta_3 & 0 & a_3sin\theta_3 \\ 0 & 0 & 1 & 0 \\ 0 & 0 & 0 & 1 \end{bmatrix}$$

The homogeneous transformation matrix that relates frame {4} to frame {0} can be obtained by multiplying individual transformation matrices. Where "*c*" represents cosine and "*s*" represents sine.

$$T_4^0 = T_1^0 T_2^1 T_3^2 T_4^3 = \begin{bmatrix} r_{11} & r_{12} & r_{13} & r_{14} \\ r_{21} & r_{22} & r_{23} & r_{24} \\ r_{31} & r_{32} & r_{33} & r_{34} \\ r_{41} & r_{42} & r_{43} & r_{44} \end{bmatrix} \quad (3.41)$$

$$r_{11} = c3s0s2 + c0c1c2 + s3c2s0 - c0c1s2$$
$$r_{12} = c3c2s0 - c0c1s2 - s3s0s2 + c0c1c2$$
$$r_{13} = c0s1$$
$$r_{14} = a1c0 + d1s0 + a4c3s0s2 + c0c1c2 + a4s3c2s0 - c0c1s2 + a2c0c1 + a3s0s2 + a3c0c1c2$$
$$r_{21} = -c3c0s2 - c1c2s0 - s3c0c2 + c1s0s2$$
$$r_{22} = s3c0s2 - c1c2s0 - c3c0c2 + c1s0s2$$
$$r_{23} = s0s1$$
$$r_{24} = a1s0 - d1c0 - a4c3c0s2 - c1c2s0 - a4s3c0c2 + c1s0s2 + a2c1s0 - a3c0s2 + a3c1c2s0$$
$$r_{31} = c(theta\_2 + theta\_3) * s1$$
$$r_{32} = -s(theta\_2 + theta\_3) * s1$$
$$r_{33} = -c1$$
$$r_{34} = s(1) * (a2 + a4 * cos(theta\_2 + theta\_3) + a3 * cos(theta\_2)$$
$$r_{41} = 0$$
$$r_{42} = 0$$
$$r_{43} = 0$$
$$r_{44} = 1$$

The single transformation matrix thus found from (3.41) represents the positions and orientations of the reference frame attached to the end – effector with respect to the fixed reference frame {0}.

3.6. Dynamic Analysis

Euler – Lagrangian method is used to determine the dynamics of the rehabilitation robot. This method handles both the joint velocities and position of the system together. With this data potential energy and kinetic energy of the system can be found easiliy. For a certain restriction class systems it generalizes the Newtonian mechanics.

In this study all three motors are accepted as pendulum systems. Equation (3.42) represents the dynamic model of pendulum.

$$I\ddot{\theta} + mglsin\theta + F\left(\theta, \dot{\theta}\right) = \tau \qquad (3.42)$$

where τ is torque, I is inertia, m is mass, g is gravitational acceleration constant, l is length of pendulum and θ is angle of pendulum. External forces (Coriolis and fraction forces) are neglected because of slow-motion of the system. The dynamic equation of the system for a joint is given in (3.43) and location of motors is shown in Fig. 29.

$$\theta(s)\left[I(s)s^2 + mgl\frac{1}{(s^2+1)}\right] = \tau(s) \qquad (3.43)$$

Transfer Function of Motor 1;

The transfer function for joint angle 1 is given in (3.44);

$$\frac{\theta_1(s)}{\tau(s)} = \frac{s^2+1}{0{,}160s^2(s^2+1)+7{,}62} \qquad (3.44)$$

where θ_1 is shaft angle of motor 1.

Transfer Function of Motor 2;

The transfer function for joint angle 1 is given in (3.45);

$$\frac{\theta_2(s)}{\tau(s)} = \frac{1}{0{,}961s^2} \qquad (3.45)$$

where θ_2 is shaft angle of motor 2.

Transfer Function of Motor 3;

The transfer function for joint angle 1 is given in (3.46);

$$\frac{\theta_3(s)}{\tau(s)} = \frac{s^2+1}{0{,}343s^2(s^2+1)+22{,}07} \qquad (3.46)$$

where θ_3 is shaft angle of motor 3.

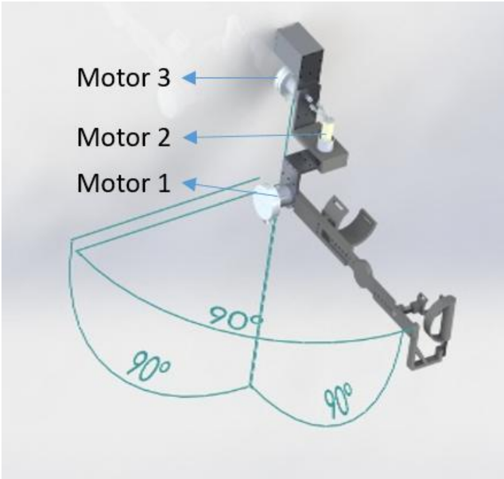

Figure 25: Location of motors and joint angles

3.7. Control Strategy

Exercise types and related control methods are shown in Tab. 6.

Table 6: Exercise types & control methods

Exercise Types	Control Methods
Passive	PID Control
Active-assistive	Force and Position Based Impedance Control
Isometric	Force Based Impedance Control
Isotonic	Force Based Impedance Control

In all of these exercises instant position of the robot is needed to control the system properly. To get the position correctly and continuously an encoder is used and the data obtained from the encoder. The data is converted to degree with some mathematical operations which can be seen in Fig.26.

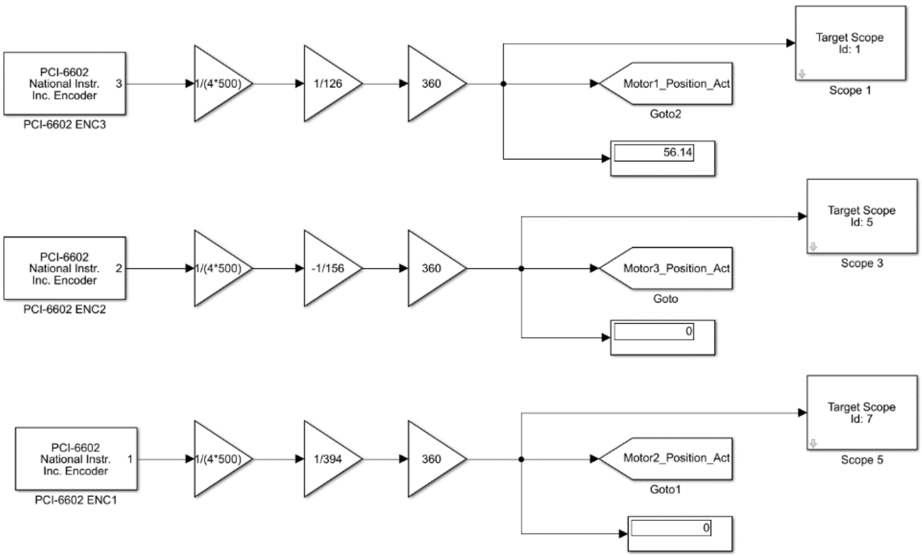

Figure 26: Position reading model

3.7.1. PID Control

PID control method ensures the ability to use the three control terms of the proportional, integral and derivative effect on the controller output to apply accurate control. Systematic parameter exchange method to determine PID parameters was used on the rehabilitation robot. The PID Control law is given in (3.47).

$$G_{PID}(s) = K_p + \frac{K_I}{s} + K_d s \quad (3.47)$$

where Kp, Kd, Ki represents proportion constant, derivative constant and integral constant, respectively.

3.7.2. Impedance Control [23]

In rehabilitation systems impedance control method is used extensively because of effectiveness in human-robot interaction systems [20]. Force and position are used together or separately in Impedance control by tuning the mechanical impedance of the end effector of the robot. The regulation of force or position is maintained in a complex way. The relationship between force and position is regulated in one side meanwhile, velocity and acceleration is regulated on the other side. As a input it needs position and the output will be a resulting force. Mechanical impedance is the response of mechanism elasticity against external force applied. Mechanical impedance is adjustable and can be changed during the exercises while the robot tracks the desired force or position continuously. Therefore, impedance control tends to be position based or force based. Force based impedance control method is suitable for isometric and isotonic exercise because desired force is required. Because of the both position and force control are necessary for active-assistive exercise, both position and force-based impedance controller are used. Impedance control model is given in Fig.26.

The robot dynamic equation is expressed by the following nonlinear equation:

$$\tau = M(q)\ddot{q} + C(q,\dot{q}) + G(q) + F(\dot{q}) - J^T(q)F_e \quad (3.48)$$

3.7.2.1. Position Based Impedance Control

The desired dynamic behaviour of the robot manipulator after applying position based impedance control can be given as:

$$M_d(\ddot{x} - \ddot{x_d}) + B_d(\dot{x} - \dot{x_d}) + K_d(x - x_d) = -F_e \quad (3.49)$$

Where M_d, B_d and K_d are symmetrical matrices that represents desired inertia, damping and stiffness matrices. The vector x denotes the end-effector position and orientation, and x_d denotes the desired end-effector position and orientation.

$$\ddot{x} = \ddot{x_d} + M_d^{-1}[-B_d(\dot{x} - \dot{x_d}) - K_d(x - x_d) - F_e] \quad (3.50)$$

The velocity of the end-effector is;

$$\dot{x} = J(q)\dot{q} \qquad (3.51)$$

And the acceleration is;

$$\ddot{x} = J(q)\ddot{q} + J(\dot{q})\dot{q} \qquad (3.52)$$

Consider the robot dynamics in Equation 3.48 and choose the control input as;

$$\tau = M(q)u + C(q,\dot{q}) + G(q) + F(\dot{q}) - J^T(q)F_e \qquad (3.53)$$

Then the dynamic equation becomes $\ddot{q} = u$. Equation 3.52 becomes;

$$\ddot{x} = J(q)(\ddot{x} - \dot{J}(q)\dot{q}) = u \qquad (3.54)$$

The resulting control equation after combining these equations;

$$\tau = M(q)J(q)(\ddot{x_d} + M_d^{-1}[-B_d(\dot{x} - \dot{x_d}) - K_d(x - x_d) - F_e] - J(q)\dot{q})$$
$$+ C(q,\dot{q}) + G(q) + F(q) - J(q)^T F_e \qquad (3.55)$$

The model designed according to Equation 3.55 is given in Fig.27.

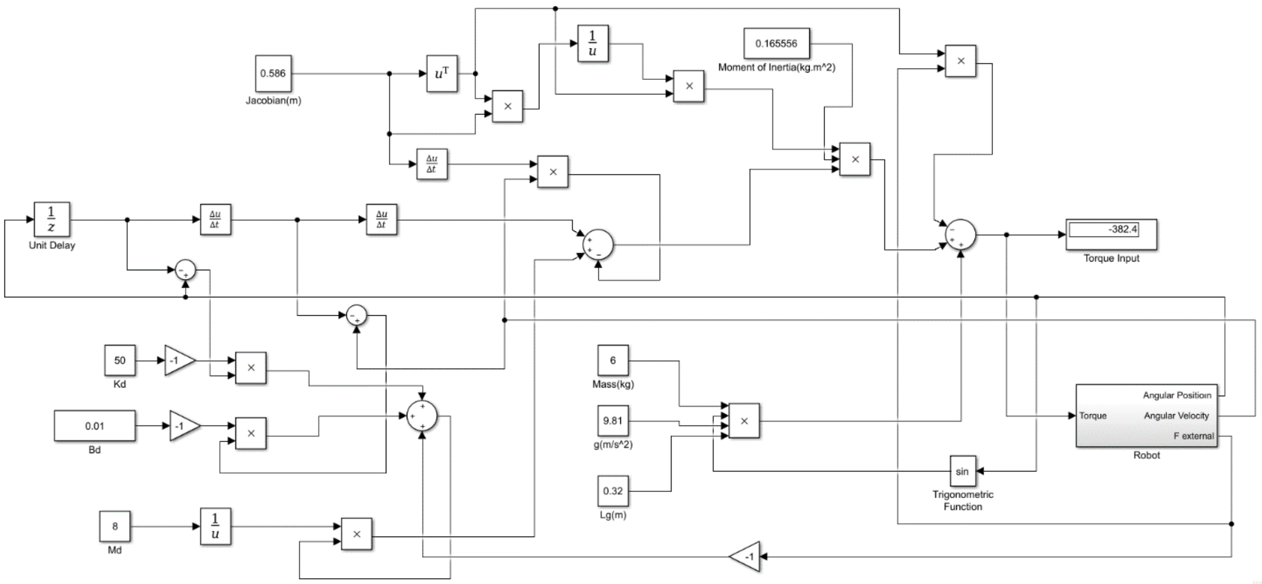

Figure 27: Position based impedance control model

3.7.2.2. Force Based Impedance Control

To control the system with force based impedance control method, continues and correctly force data is needed. The required force data is filtered obtained from the system with the model which can be seen in Fig. 28.

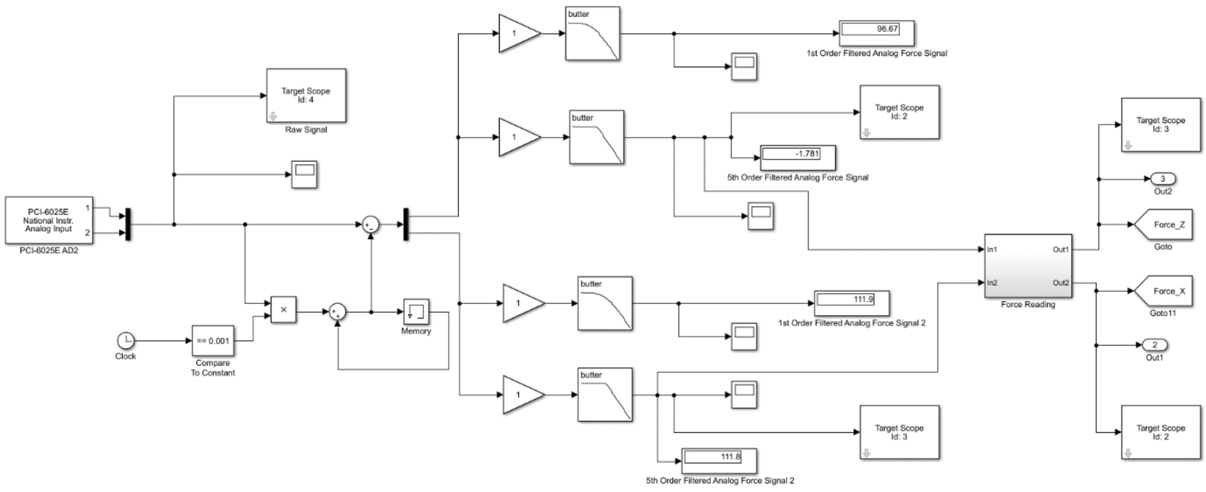

Figure 28: Reading - filtering force data

For the force based impedance control case, the desired dynamics behavior of the system can be given as:

$$M_d\ddot{x} + B_d\dot{x} - F_d = -F_e \qquad (3.56)$$

Which is equal to;

$$\ddot{x} = M_d^{-1}(-B_d(\dot{x} + F_d - F_e) \qquad (3.57)$$

Where F_d is the desired force. From The equations above we deduce the following control law:

$$\tau = M(q)J(q)\left(M_d^{-1}[F_d - F_e - B_d\dot{x}] - \dot{J}(q)\dot{q}\right) + C(q,\dot{q}) + G(q) + F(q) - J(q)^T F_e \qquad (3.58)$$

$$\tau = \tau_{gravity} - \left[\frac{1}{L_g M_d}\left(D_d\dot{\theta}_e + K_d\theta_e\right)\right] + [\frac{1}{L_g M_d} - L_g]F \qquad (3.59)$$

$$\tau_{gravity} = mgsin\theta L_g \qquad (3.60)$$

The model designed according to Equations 3.58 and 3.60 is given in Fig.29.

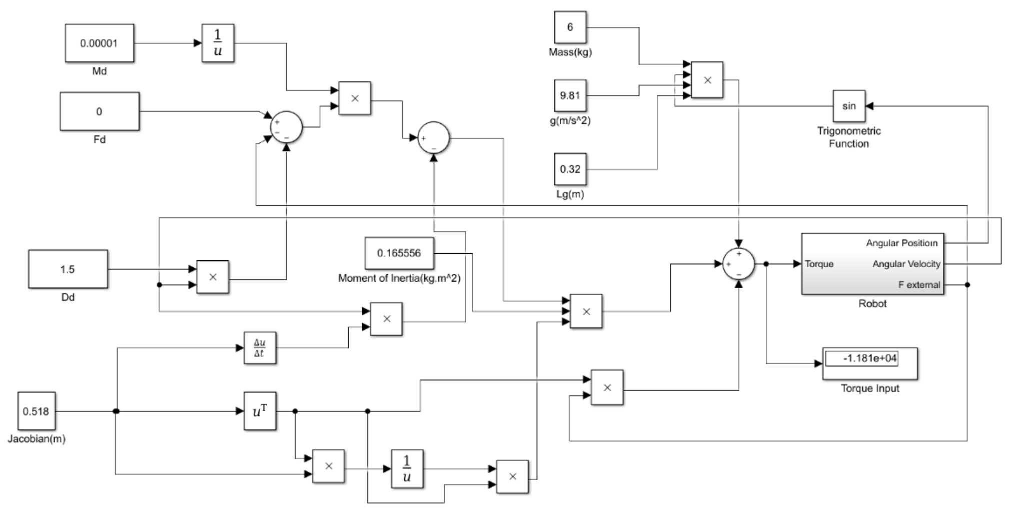

Figure 29: Force based impedance control model

3.8. Exercise Types and Algorithms

3.8.1. Passive Exercise

Patient Types: Passive exercise is applied to zero scale (scale-0) or poor scale (scale-1) patients.

Control Methods: PID control method was used for this type of exercise.

Algorithm of passive exercise for zero scale and poor scale patients and usage of PID control for this exercise are presented in Fig.30.

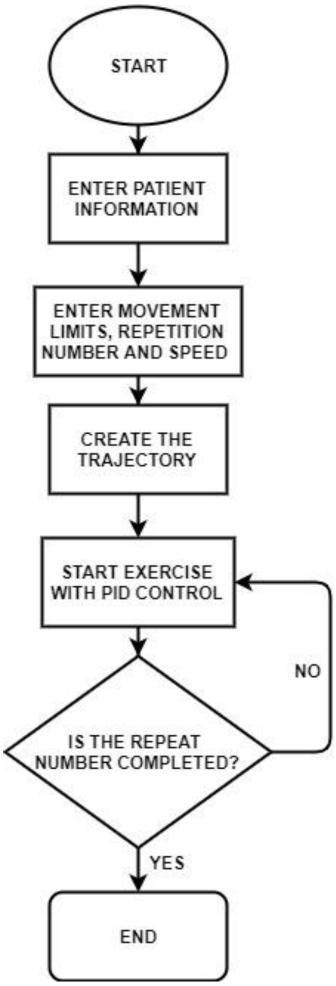

Figure 30: Algorithm of passive exercise

3.8.2. Active – Assistive Exercise

Patient Types: Active-assistive exercise is applied to trace scale (scale-2) or fair scale (scale-3) patients.

Control Methods: PD position control and impedance control will be used for this type of exercise.

Algorithm of active-assistive exercise for trace scale and fair scale patients and usage of PD position and impedance control methods for this exercise are shown in Fig.31.

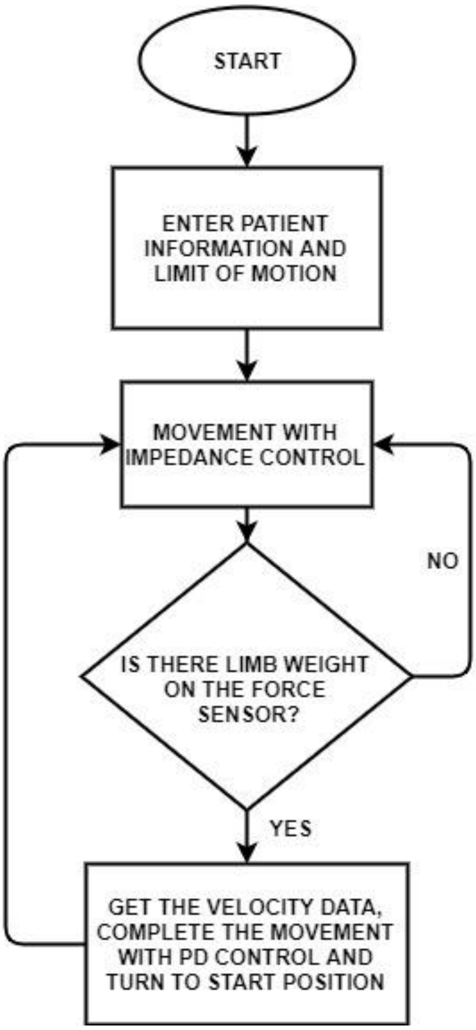

Figure 31: Algorithm of active-assistive exercise

3.8.3. Isometric Exercise

Patient Types: Isometric exercise is applied to good scale (scale-4) patients.

Control Methods: Impedance control and torque control will be used for this type of exercise.

Algorithm of isometric exercise for good scale patients and usage of impedance and torque control methods for this exercise are demonstrates in Fig.32.

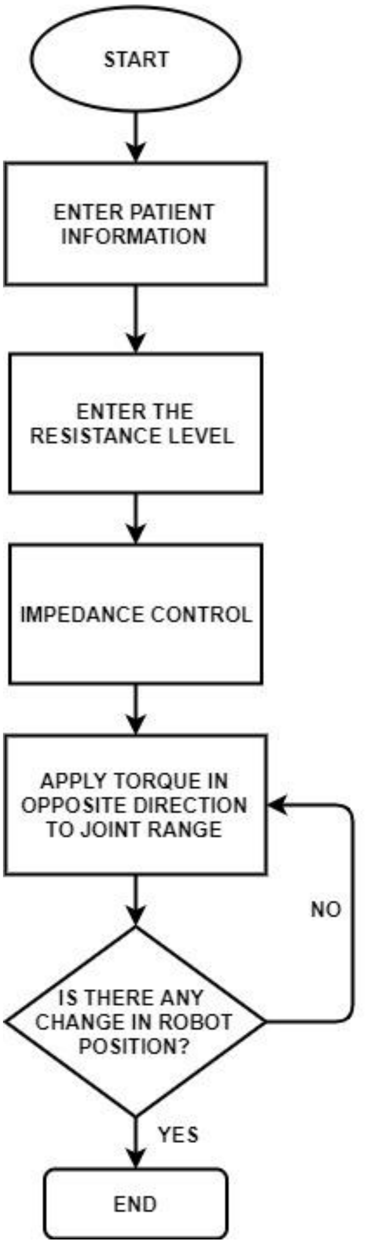

Figure 32: Algorithm of isometric exercise

3.8.4. Isotonic Exercise

Patient Types: Isotonic exercise is applied to good scale (scale-4) patients.

Control Methods: Impedance control will be used for this type of exercise.

Algorithm of isotonic exercise for good scale patients and usage of impedance control method for this exercise are presented in Fig.33.

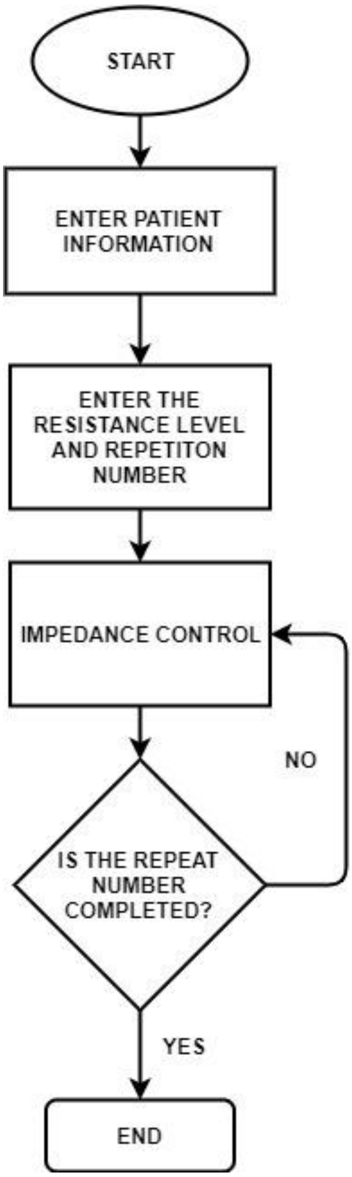

Figure 33: Algorithm of isotonic exercise

4. RESULTS

4.1. Strength Analysis

Approximate force and torque values were applied to the robot arm according to the maximum mass and dimensions expected from the patients who would use the system. Strength analysis is performed with respect to the load capacity of the system. The static calculations are performed to all system from the end effector where the system meets with patient's hand. According to the strength analysis, the connection point where the robot connects to the stand needs primary consideration because of the extra bending. As a result of the calculations based on the yield strength for aluminum material, the thicknesses on the connection part are increased to make the system safer. The system is all in blue and strong enough as shown in Fig.34.

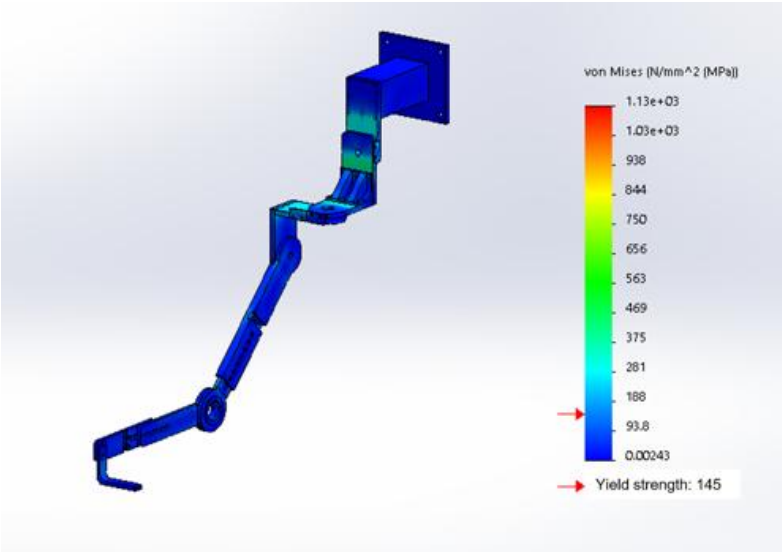

Figure 34: Strength analysis

4.2. EMG Circuit Outcomes

This circuit was used with Simulink to detect muscle movements. These detection graphs are obtained with the help of the system shown in Fig. 35. Muscle activation level condition is written under the graphs according to the muscle activation level. Also, the activation level is written under the graph in the unit of mV.

The block diagram and operating stages of EMG circuit is shown in Fig.21. Full-wave rectifier for rectification stage, instrumentation amplifier for amplifying stage, one high-pass filter and one low-pass filter for filtering stages were selected. The muscle signals can be seen in Figures 54 – 56.

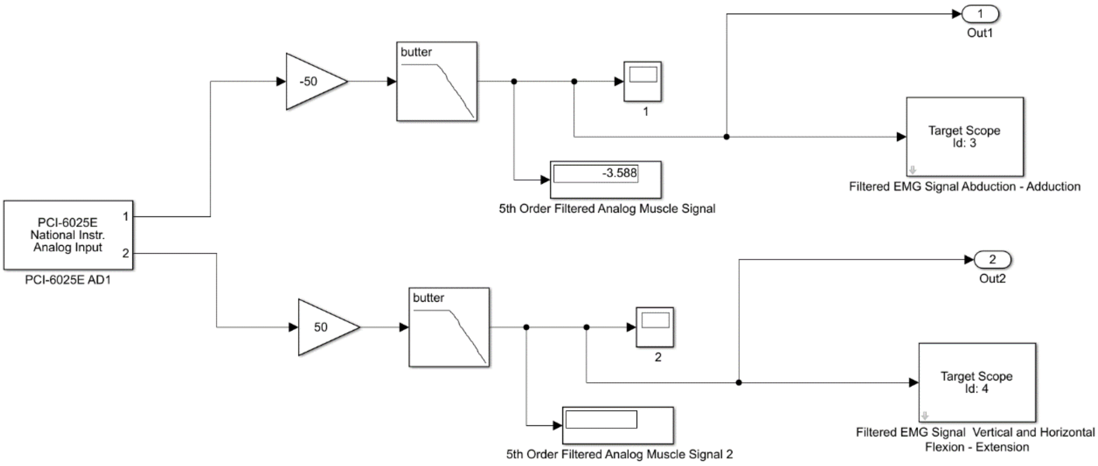

Figure 35: EMG System Diagram

Shoulder Horizontal Flexion–Extension Movement:

In Fig. 36 horizontal flexion and extension movements can be seen in black circles. Anterior deltoid and posterior deltoid muscles are mainly used in this exercise.

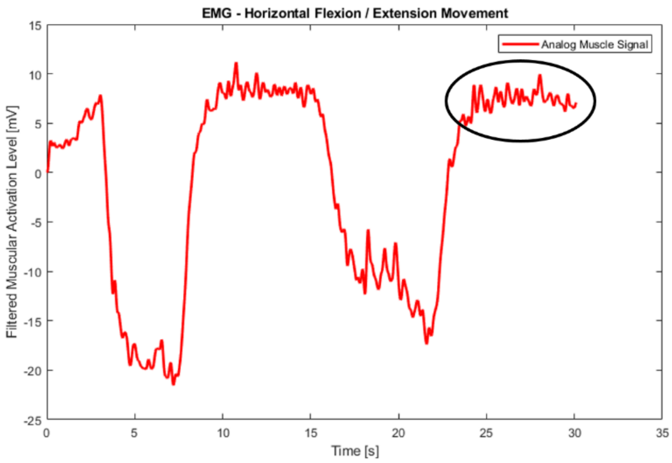

(a)

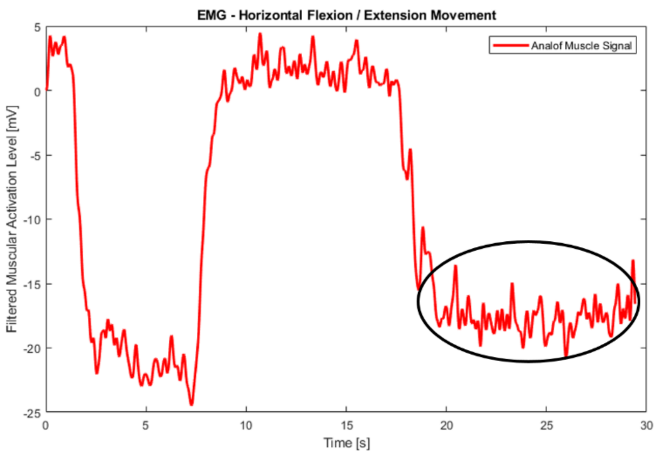

(b)

Figure 36: Horizontal (a) flexion, (b)extension

Shoulder Vertical Flexion-Extension Movement:

In Fig. 37 vertical flexion and extension movements can be seen in black circles. Anterior deltoid and posterior deltoid muscles are mainly used in this exercise.

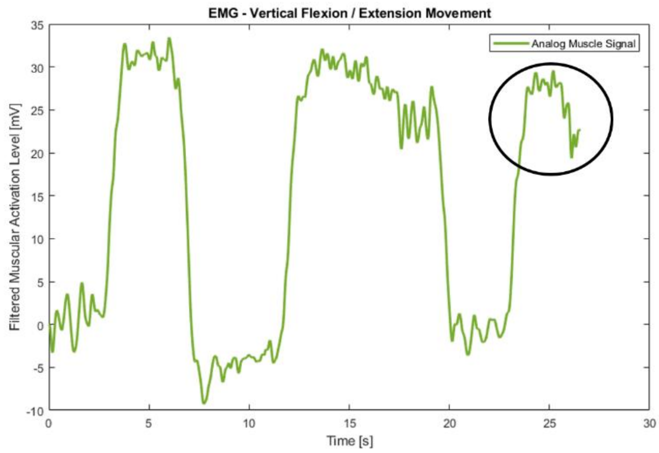

(a)

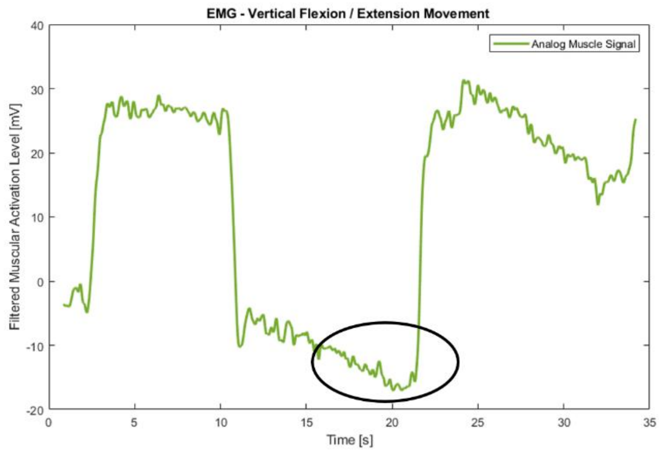

(b)

Figure 37: Vertical (a) Flexion, (b) Extension movement

Shoulder Abduction-Adduction Movement:

In Fig. 38 abduction and adduction movements can be seen in black circles. Medial deltoid and latissimus dorsi muscles are used in this exercise.

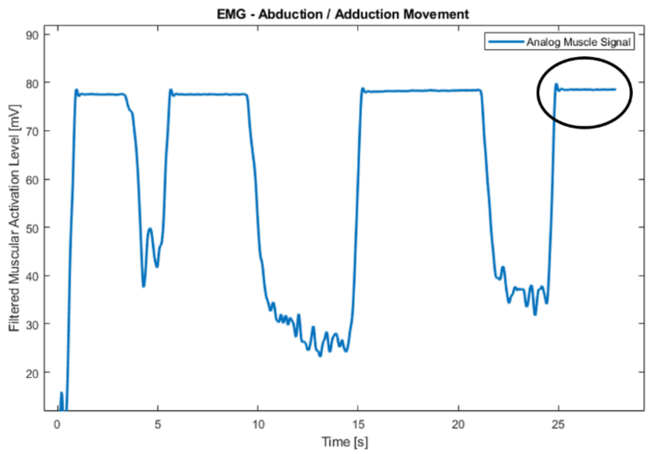

(a)

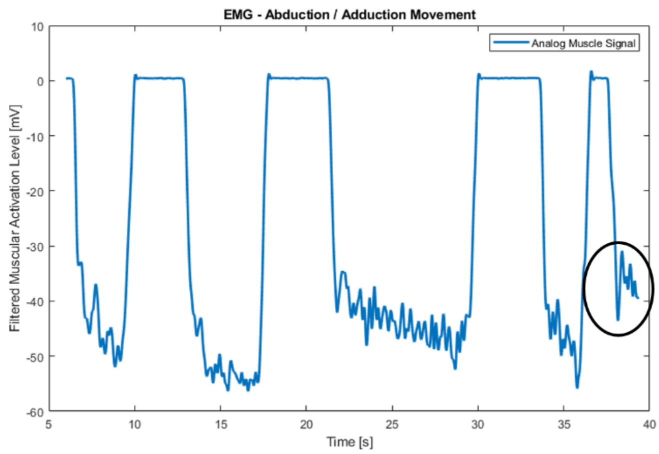

(b)

Figure 38: (a) abduction, (b) adduction movement

4.3. Simulation Result with Simscape Model

The passive exercise was simulated by using PID control method for each motor. The system mechanical 3D model was transferred from Solidworks to Simulink with the help of Simscape tool. In the Simulink environment, this model was controlled via PID control method. Two types of inputs are given to these systems. One of them was a step function and the other one was a sine function.

In Fig.39.a the response of joint 1 to the sine input can be seen. According to this figure, the robot manipulator follows the reference sinusoidal trajectory with high accuracy. Step response of joint 1 is given in Fig.35.b for the step function. The robot manipulator fitted on the step wave in five seconds which was acceptable and the slope was appropriate. There is no steady state error.

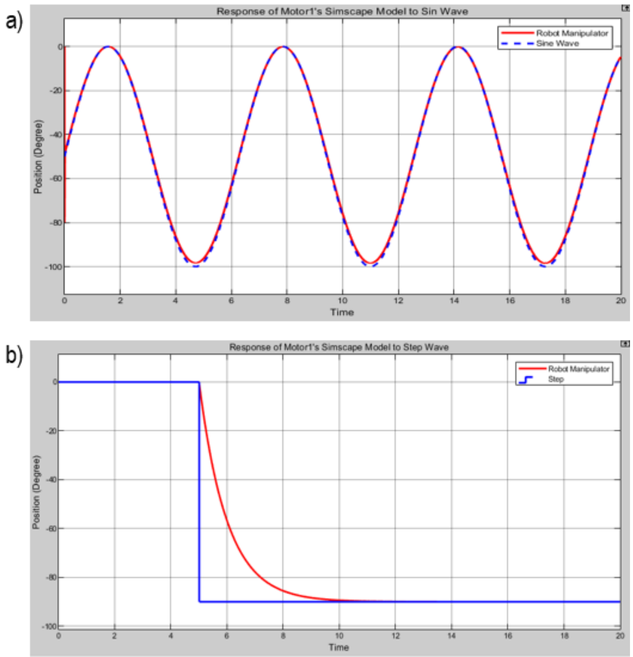

Figure 39: Joint 1 response a) sinus input, b) step input

The response of joint 1 for the sinusoidal trajectory can be seen from Fig.40.a. According to this result, the robot manipulator follows the sinusoidal reference trajectory with high accuracy. The step response of joint 1 is shown in Fig.40.b. The robot manipulator fitted on the step wave in five seconds which is acceptable and the rising time is appropriate for application.

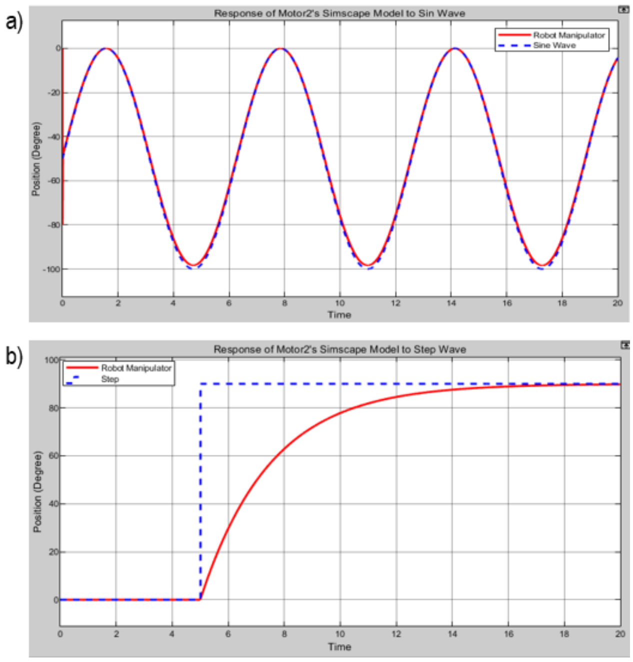

Figure 40: Joint 2 response a) sinus input, b) step input

In Fig.41.a the response of joint 3 to the sine function can be seen. As can be seen from Fig.41.a the robot manipulator tracks the sine wave as expected. In Fig.41.b the response of joint 1 to the step function. The robot manipulator fitted on the step wave in five seconds which was acceptable and the slope was appropriate.

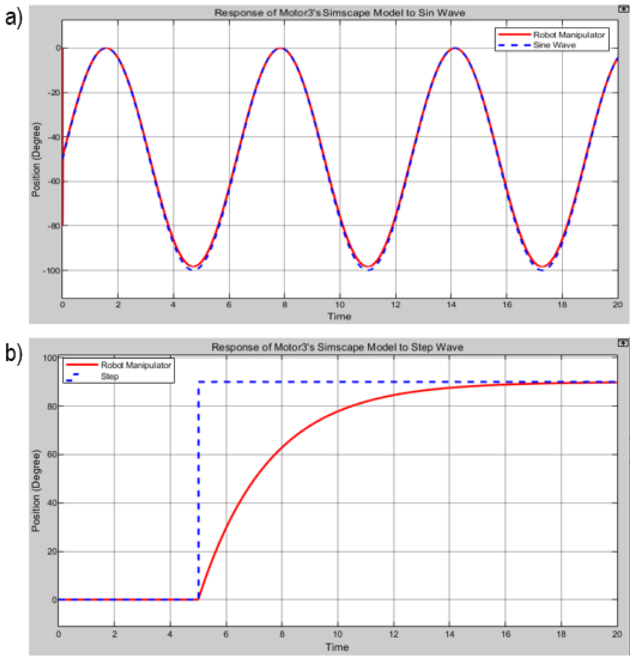

Figure 41: Joint 3 response a) sinus input, b) step input

4.4. Simulation Result with Dynamic Models of the System

The transfer functions of the dynamic models for all joints were placed in three separate control systems as a subsystem in the control diagrams in Simulink. The PID values were tuned by the Heuristic approach. Step and sine wave trajectory command were sent to the systems shown in Fig. 42 for testing and simulation.

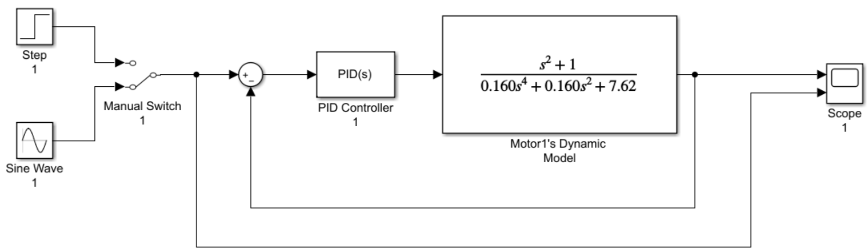

(a)

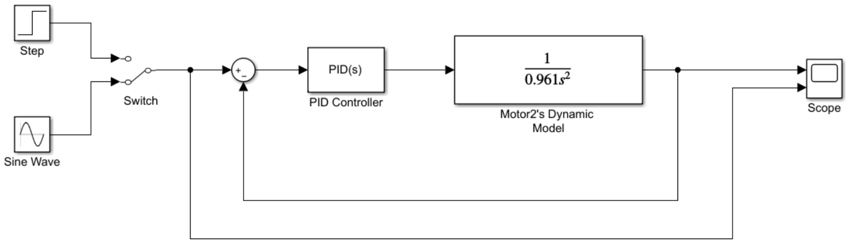

(b)

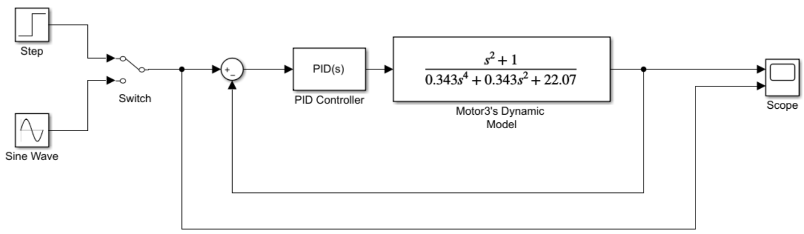

(c)

Figure 42: Dynamic Model of; a) Joint 1, b) Joint 2, c) Joint 3

As shown in Fig.43 the dynamic model for motor 1 is tracking the sine wave and step wave properly without delays and vibration in simulation.

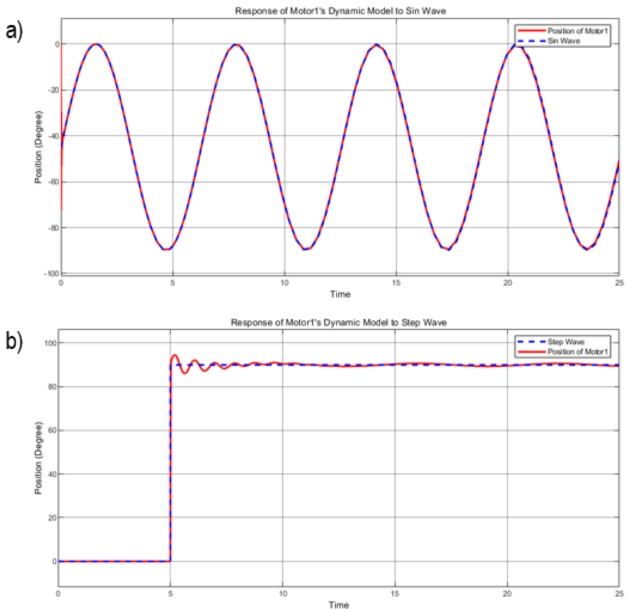

Figure 43: Joint 1 response a) sinus input, b) step input

As shown in Fig.44 the dynamic model for joint 2 is tracking the sine wave and step wave properly without delays and vibration in simulation.

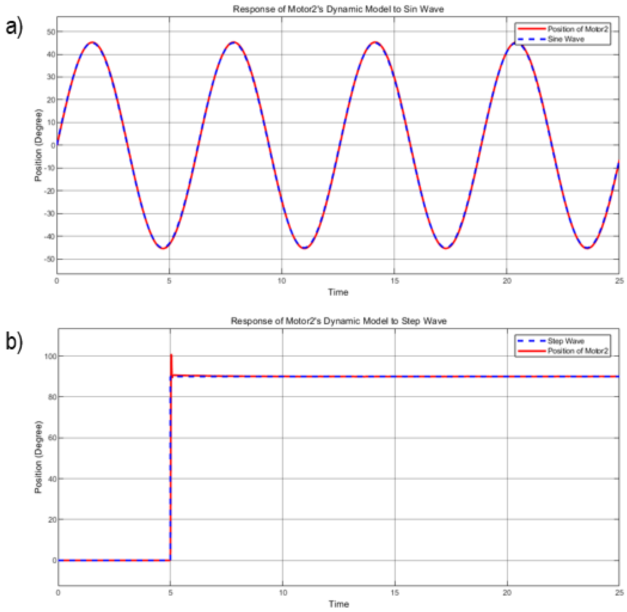

Figure 44: Joint 2 response a) sinus input, b) step input

As shown in Fig.45 the dynamic model for joint 3 is tracking the sine wave and step wave properly without delays and vibration in simulation.

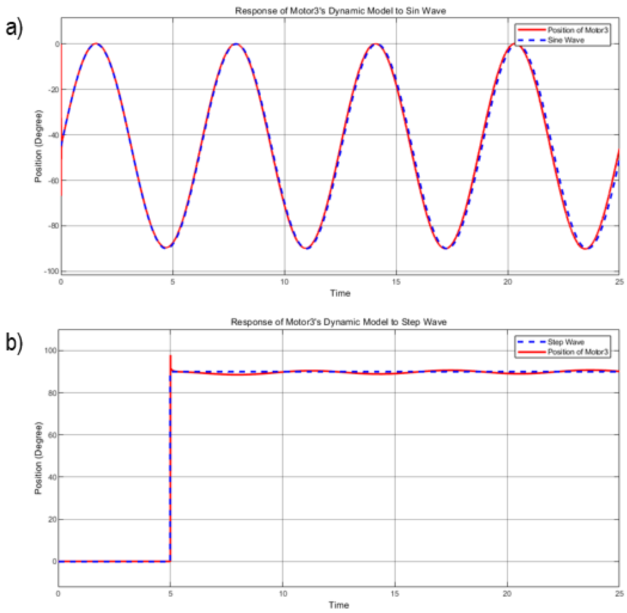

Figure 45: Joint 3 response a) sinus input, b) step input

4.5. Simulation of Passive Exercise

In the Simscape model, a trajectory was determined to require the use of all three motors in sequence. This trajectory was transferred to the system using switches and step functions as can be seen from Fig.46. The switches are used to obtain a continuous trajectory tracking of all three movements. As can be seen from Fig. 47 the joint 1 can follow the reference step trajectory between 5-10 seconds. The joint 2 between 10-15 seconds and joint 3 between 20-

25 seconds. These results show that the PID constants were determined as correct. Therefore, this controller can be used for any desired trajectory.

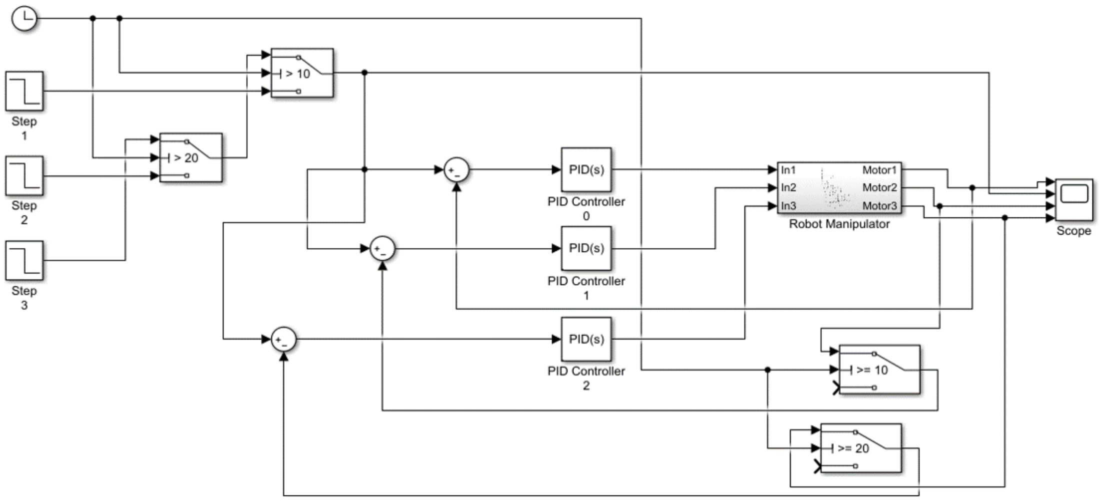

Figure 46: Circuit diagram

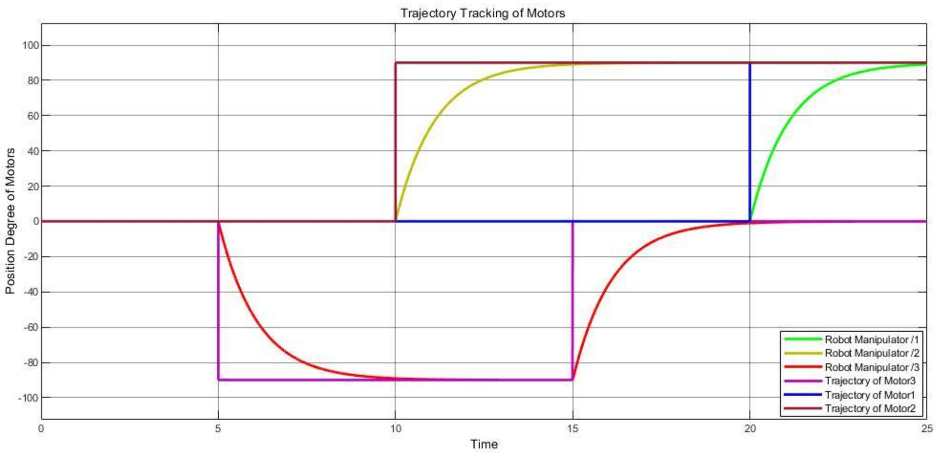

Figure 47: Trajectory of passive exercise

4.6. Passive Exercise with Prototype

This exercise can be applied on patients with no muscle activity in physical medicine and rehabilitation. The limbs of the patient move with any resistance. Physiotherapist can manage the exercise via graphical user interface. EMG data can be monitored and recorded for the muscle activity of the patient. In order to generate desired trajectory, a Simulink real-time model is developed. In this system the encoder gets the position data from the robot as feedback. This data goes into the system as feedback and helps for positioning in desired position. PID controller controls the signal and gives the needed torque value into the subsystem which converts the torque value into voltage value to drive the motors properly after that the voltage value passes a saturation value for safety. Finally, after the last saturation the output signal exits the control system from the analog output port of the data acquisition card. The PID control system can be seen in Fig.48.

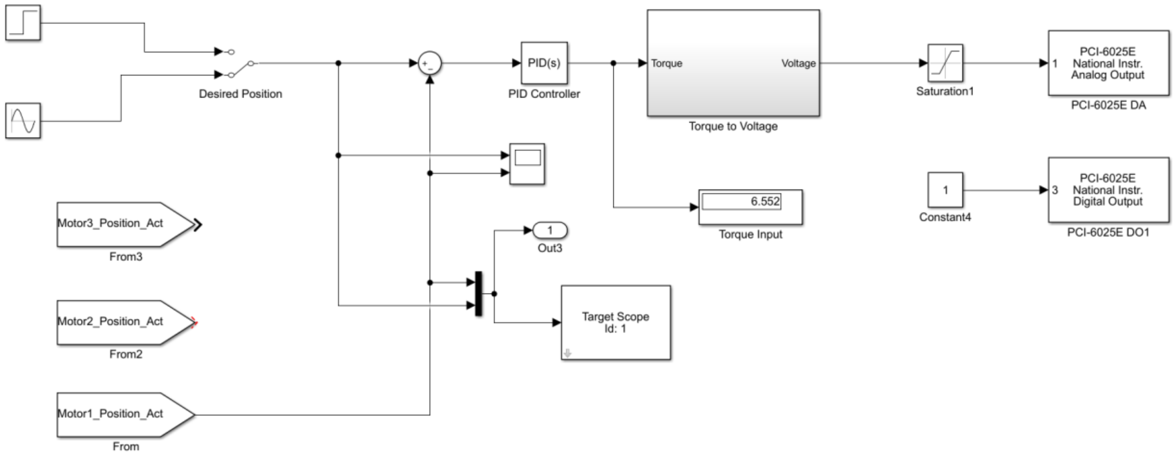

Figure 48: PID Control Diagram

The responses for all three motors to a step function are given in Fig.49. As can been from the figures all three motors are working stable. All three motors have acceptable settling times which is around 3 seconds.

The P, I and D parameters for the Joints are as follow;

Joint 1: P = 50, I = 35, D = 5

Joint 2: P = 20, I = 0, D = 5

Joint 3: P = 70, I = 37, D = 5

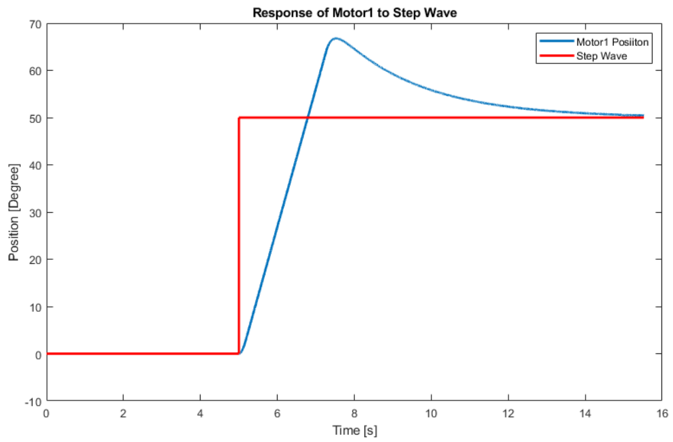

(a)

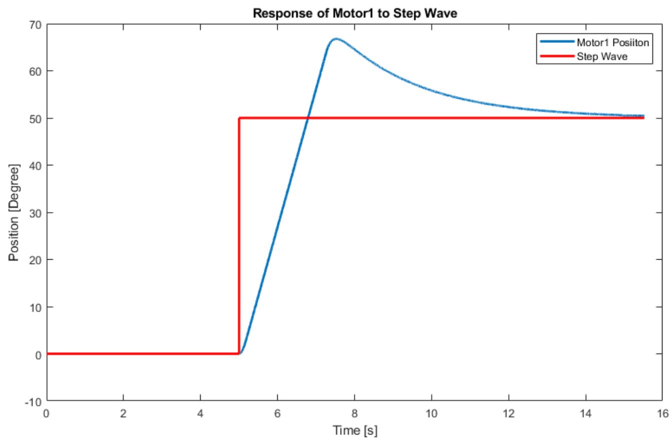

(b)

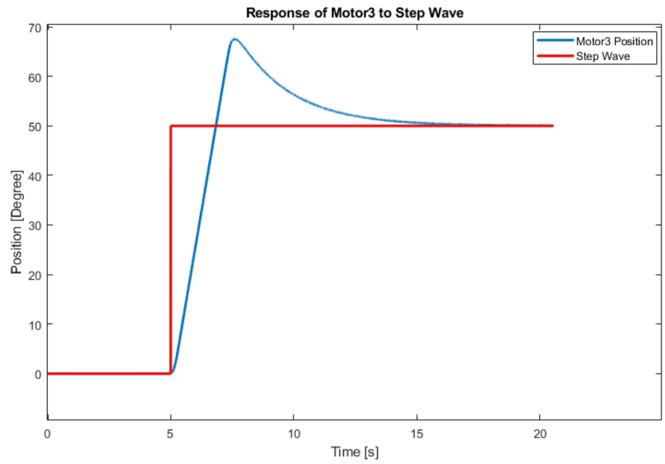

(c)

Figure 49: Step response of the system, a)Joint 1, b)Joint 2 c)Joint 3

The results of the passive exercise experiment with the robot are given in Fig.50 for three joints. The robot can follow the given sinusoidal trajectory with very high accuracy.

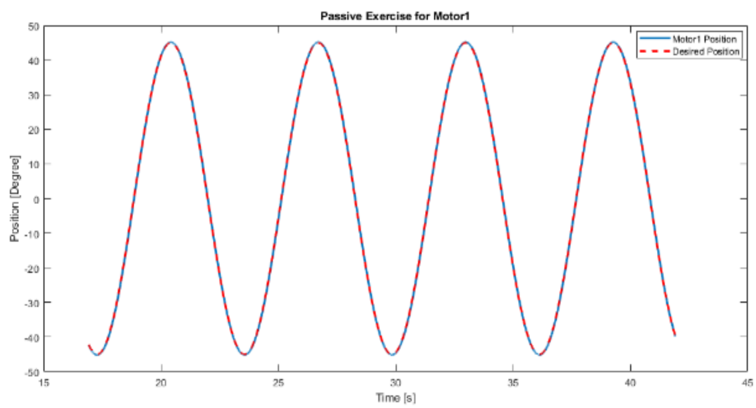

(a)

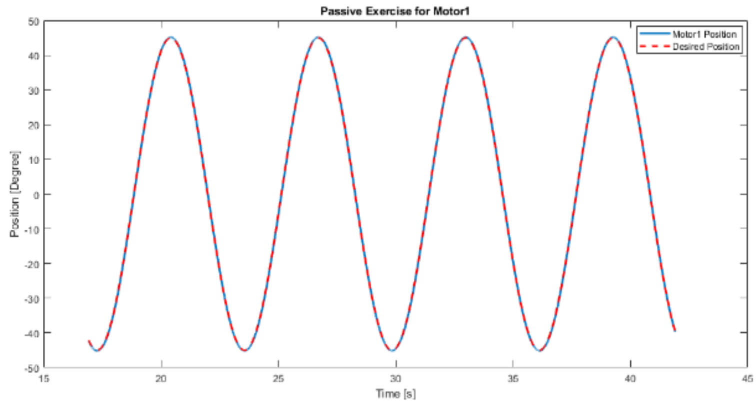

(b)

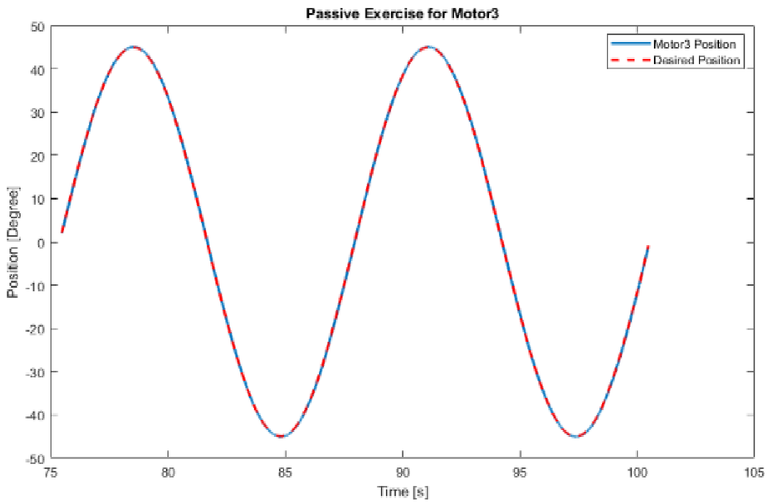

(c)

Figure 50: Sine response of the system (a) Joint 1, (b) Joint 2, (c) Joint 3

4.7. Impedance Control Effect

Different impedance control parameter values are applied on a subject, who is 65 kg, are shown in Table 6. These experiments are realized at medium speed that 5 seconds period with 90 degrees by the subject.

Tablo 6: Values of Impedance Paramters

M_d	0.01	0.2	4
D_d	0	10	20
F_d	0.00001	0.01	0.5

4.7.1. M_d, Inertia Coefficient Parameter Effect

For realize the importance of inertia coefficient effect on impedance control, we set the desired force and damping coefficient as fixed as shown in the Fig. 51-53. According to these three figures, when the inertia coefficient increases, resistance of the system will increase. Moreover, because of the patients' limb weight is added to the external force on flexion direction, robot applies higher resistance on flexion direction than extension direction.

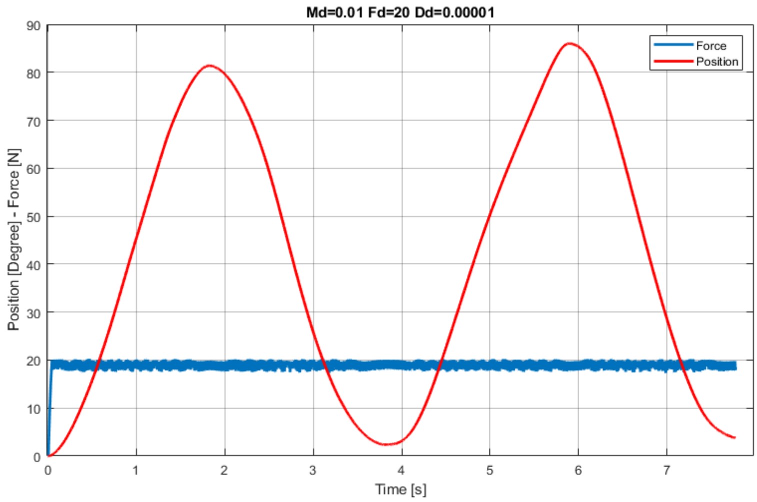

(a)

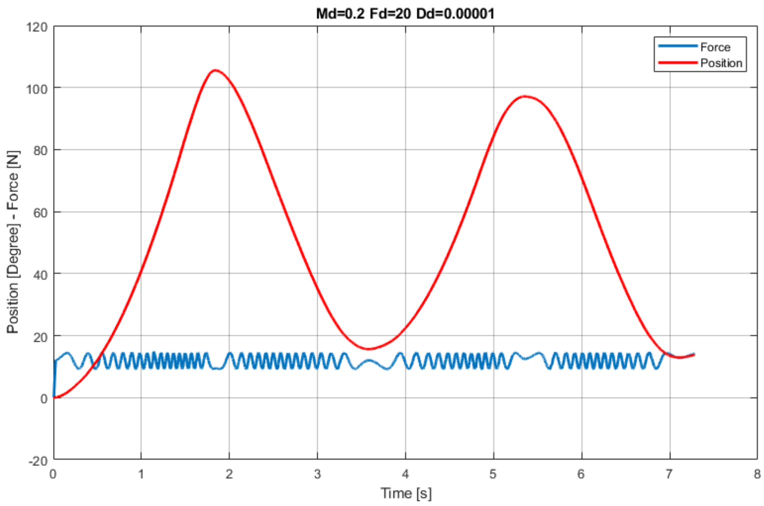

(b)

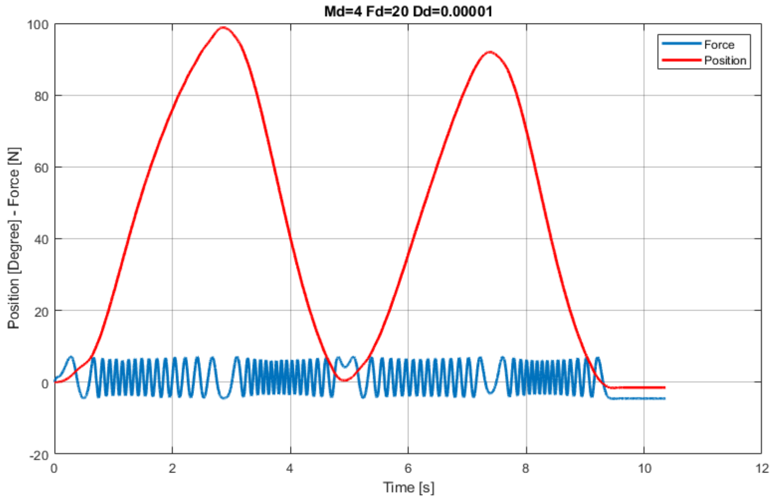

(c)

Figure 51: Fd=20 ; Dd=0.00001 ; (a) Md=0.01, (b) Md=0.2, (c) Md=4

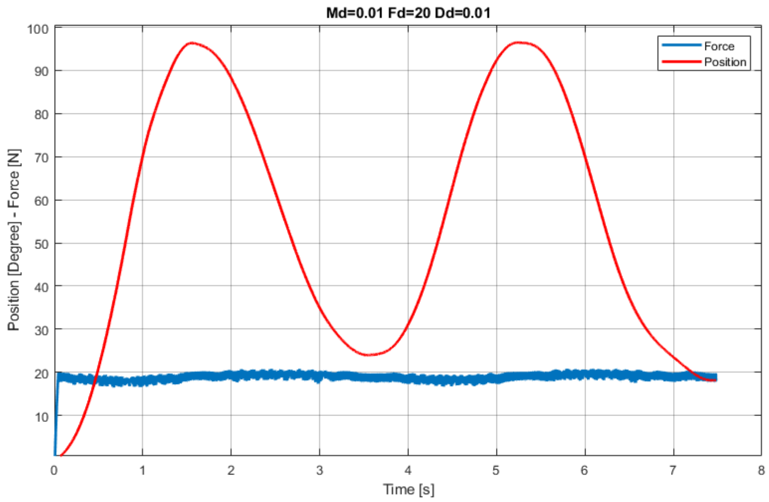

(a)

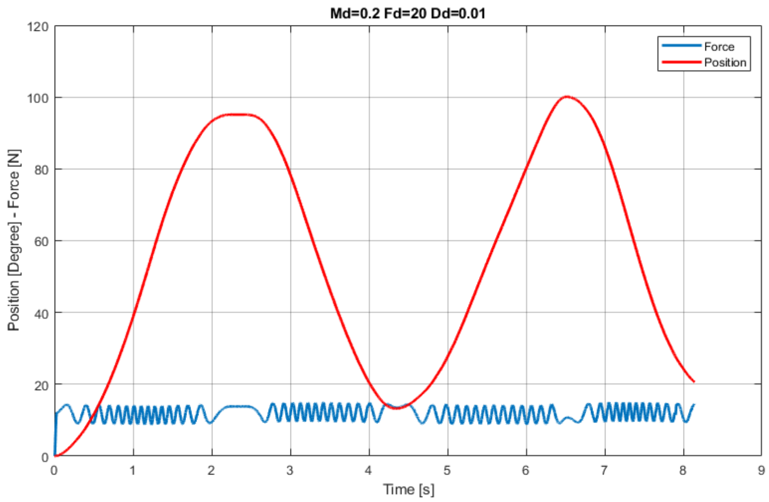

(b)

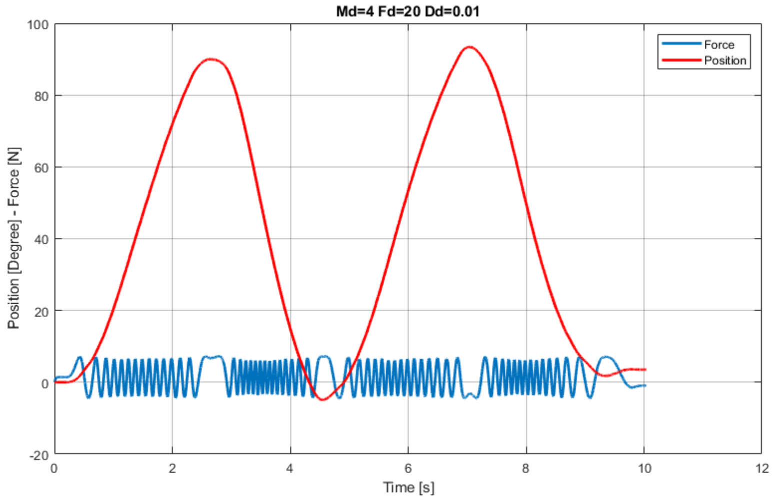

(c)

Figure 52: Fd=20 ; Dd=0.01 ; (a) Md=0.01, (b) Md=0.2, (c) Md=4

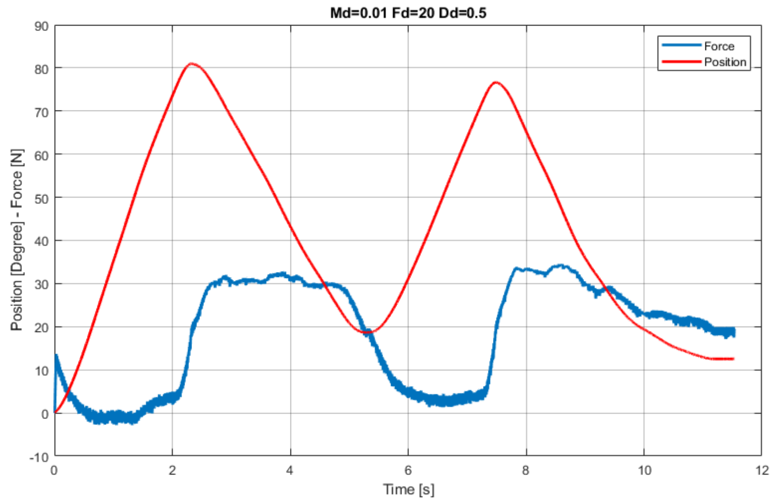

(a)

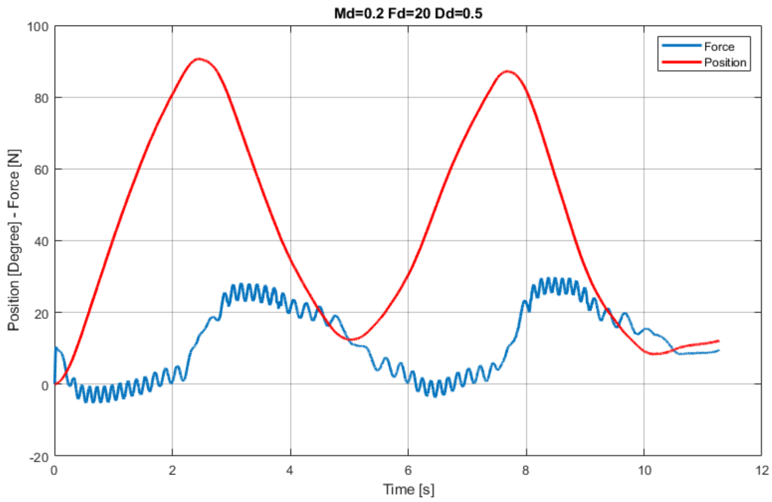

(b)

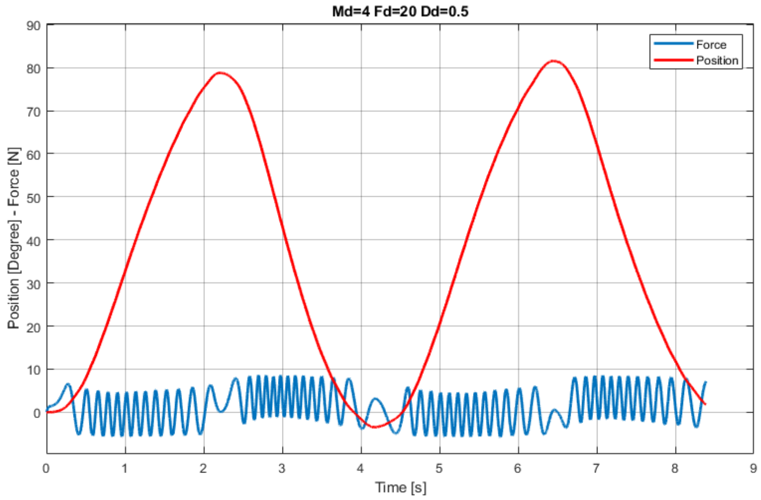

(c)

Figure 53: Fd=20 ; Dd=0.5 ; (a) Md=0.01, (b) Md=0.2, (c) Md=4

4.7.2. D_d, Damping Coefficient Parameter Effect

For realize the importance of damping coefficient effect on impedance control, we set the inertia coefficient and desired force as fixed as shown in the Fig. 54-56. According to these three figures, we realized that the damping coefficient is directly related to movement speed. Furthermore, if the damping coefficient increases, the resistance of the system will increase. Therefore, when D_d is 0.5, the subject has more difficulty in applying force to robotic arm than D_d is 0.01 and 0.00001.

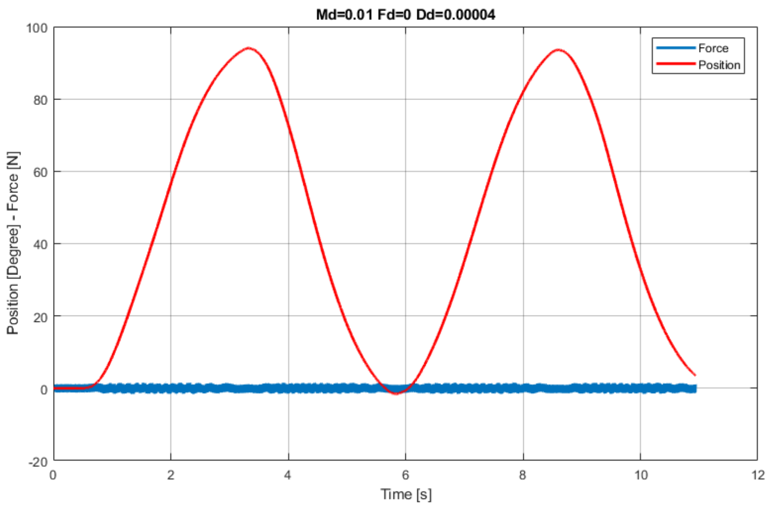

(a)

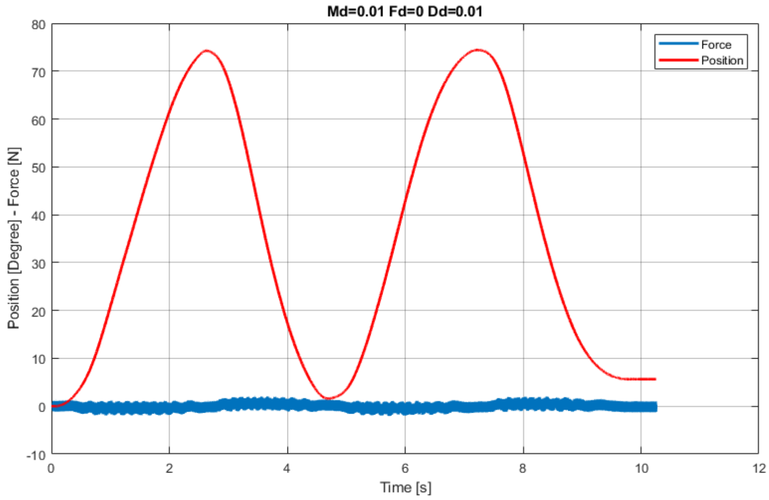

(b)

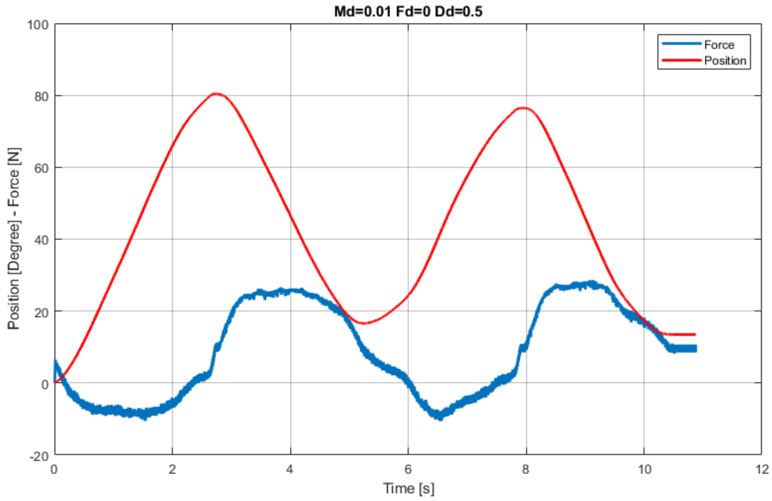

(c)

Figure 54: Md=0.01 ; Fd=0 ; (a) Dd=0.00001, (b) Dd=0.01, (c) Dd=0.5

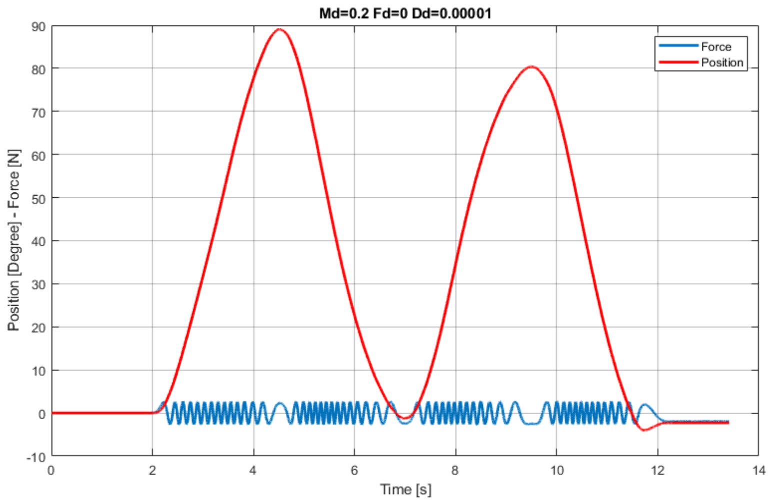

(a)

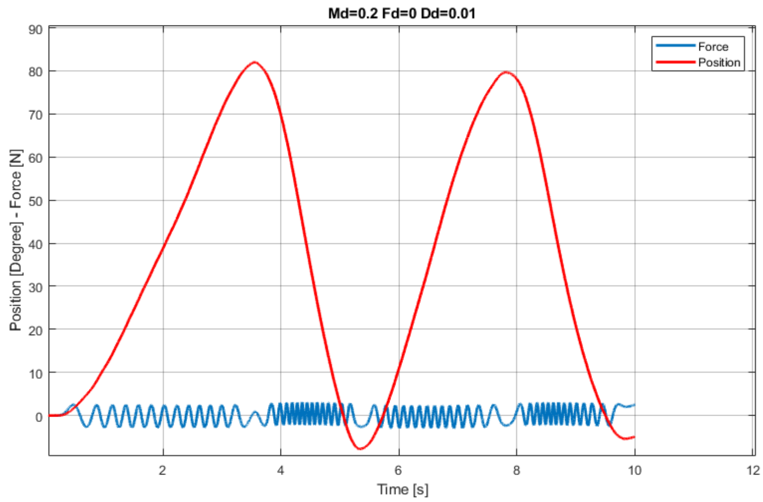

(b)

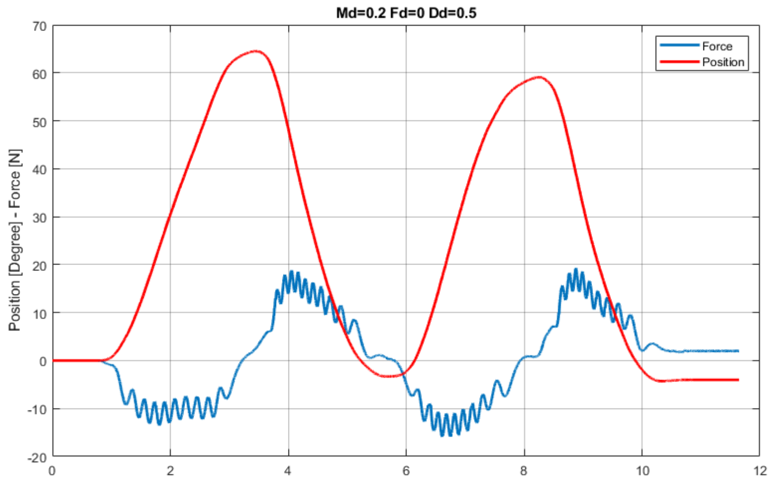

(c)

Figure 55: Md=0.01 ; Fd=10 ; (a) Dd=0.00001, (b) Dd=0.01, (c) Dd=0.5

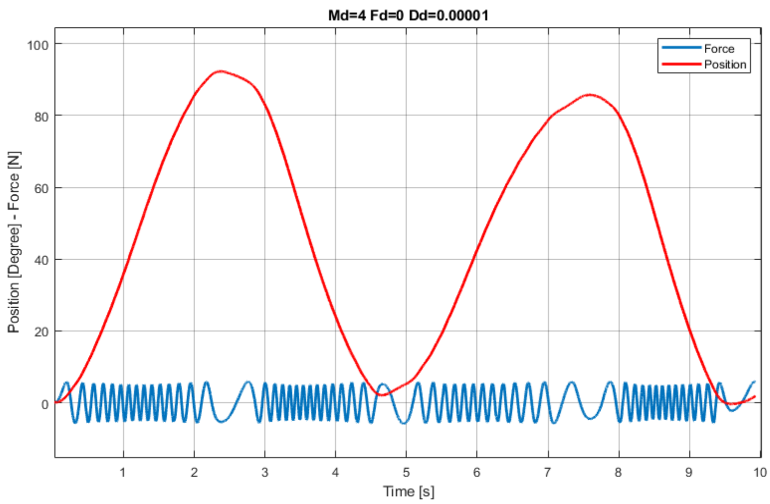

(a)

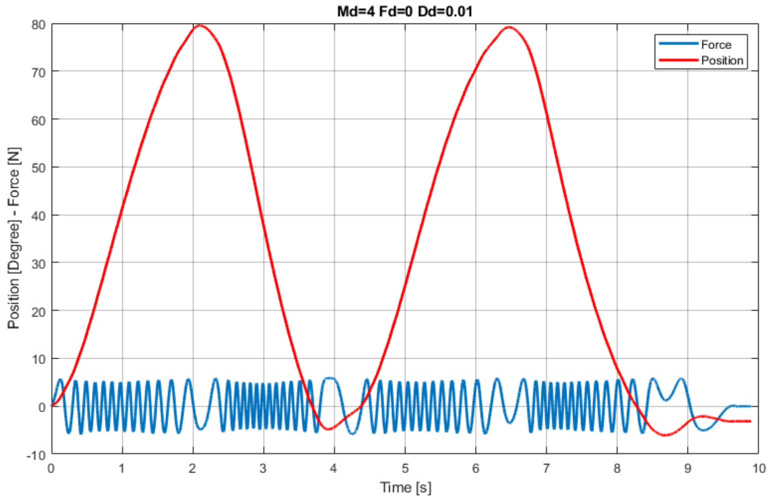

(b)

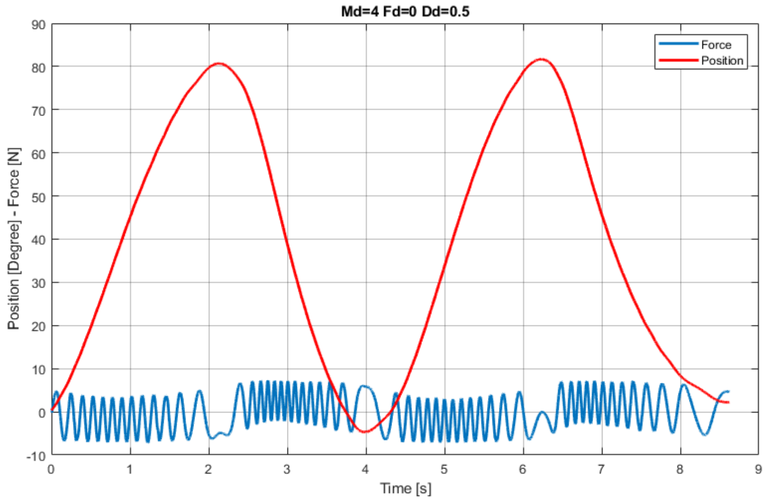

(c)

Figure 56: Md=0.01 ; Fd=20 ; (a) Dd=0.00001, (b) Dd=0.01, (c) Dd=0.5

4.7.3. F_d, Desired Force Parameter Effect

For realize the importance of desired force effect on impedance control, we set the inertia coefficient and damping coefficient as fixed as shown in the Fig. 57-59. According to these three figures, when the desired force increases, the applied force to the patients' arm will increase. Therefore, the patients' must apply the desired force to robotic arm continuously in one direction. Moreover, when the position of the motor reaches to peak points, there will be delay on force signal as can be seen in the all figures.

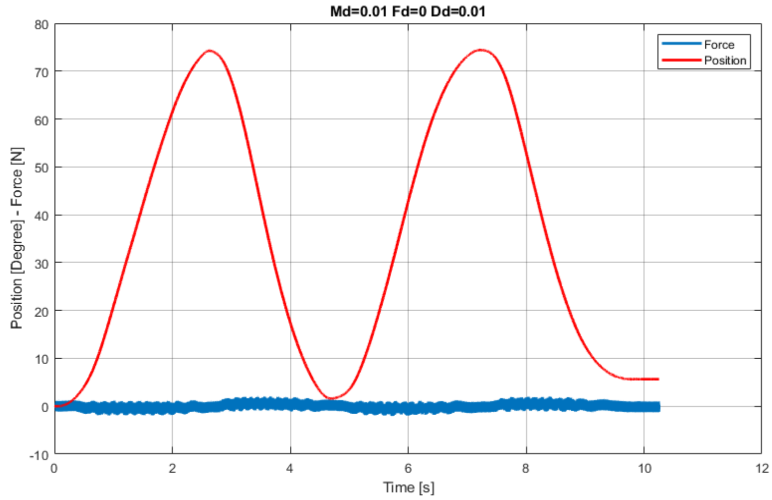

(a)

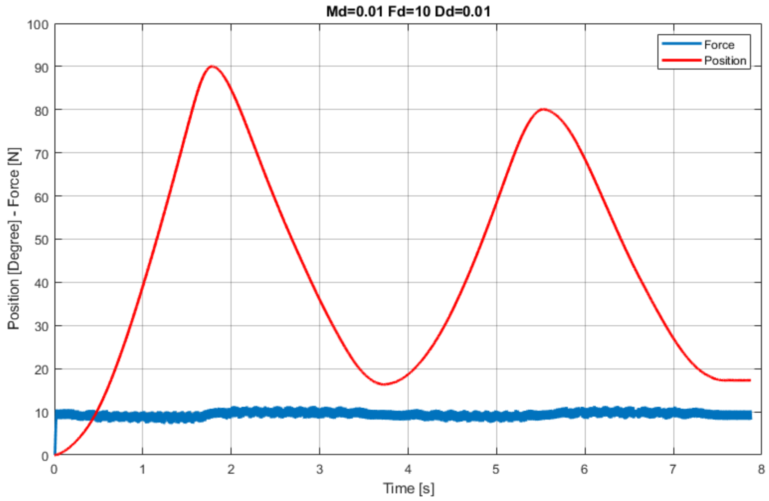

(b)

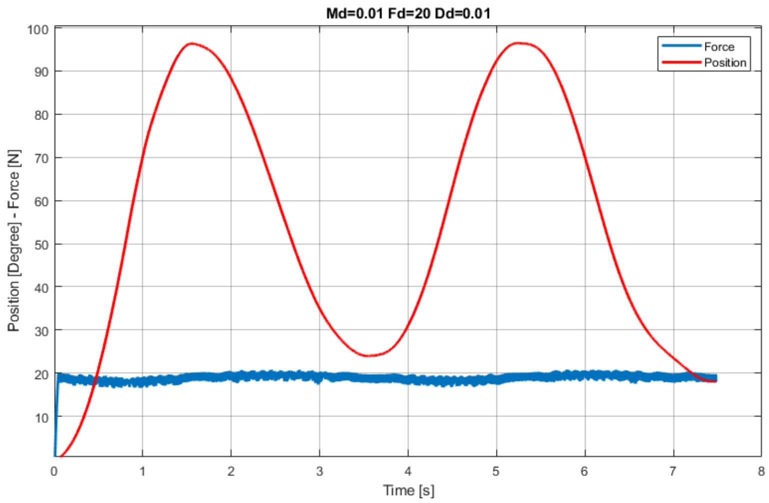

(c)

Figure 57: Md=0.01 ; Dd=0.01 ; (a) Fd=0, (b) Fd=10, (c) Fd=20

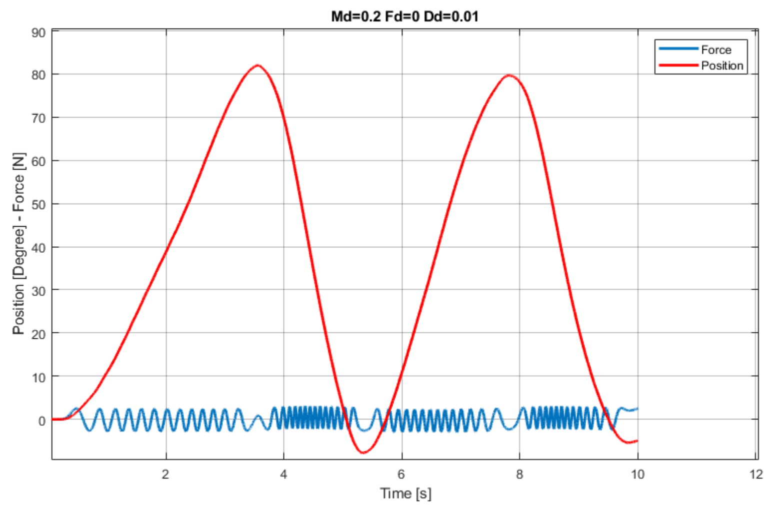

(a)

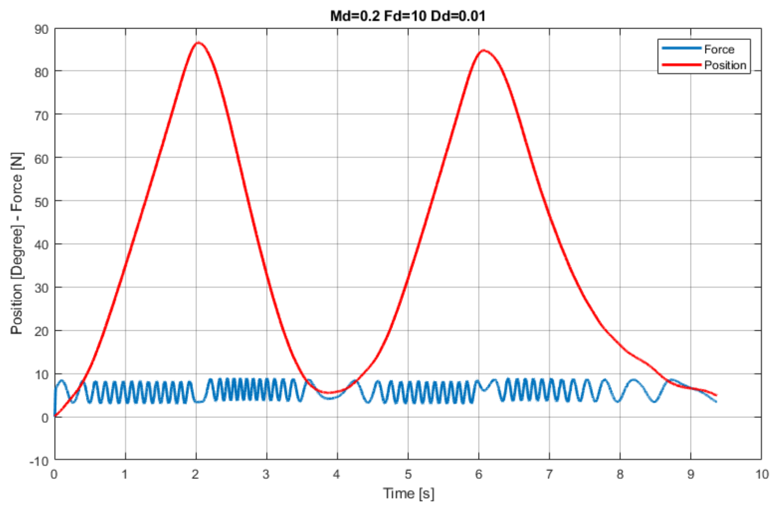

(b)

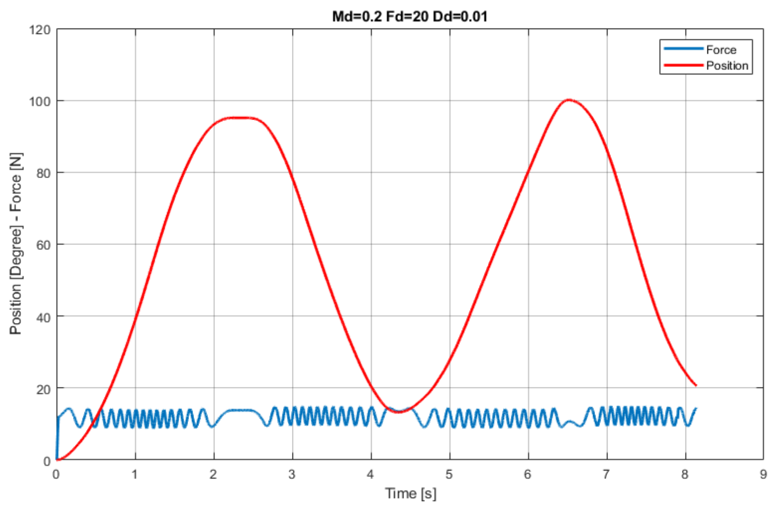

(c)

Figure 58: Md=0.2 ; Dd=0.01 ; (a) Fd=0, (b) Fd=10, (c) Fd=20

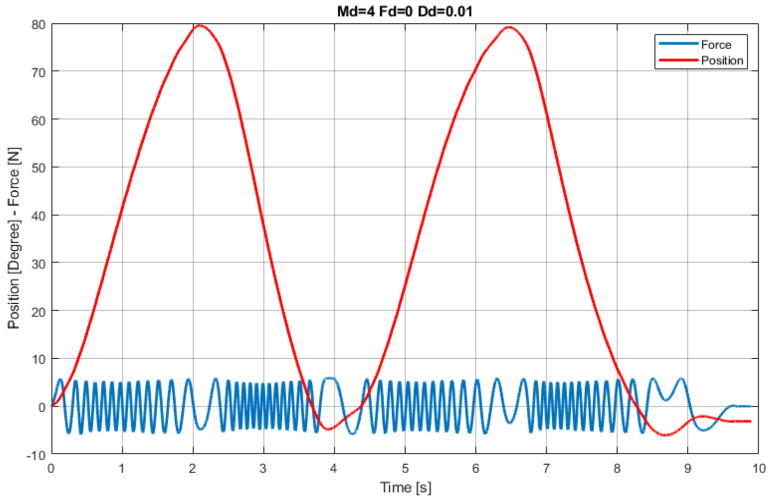

(a)

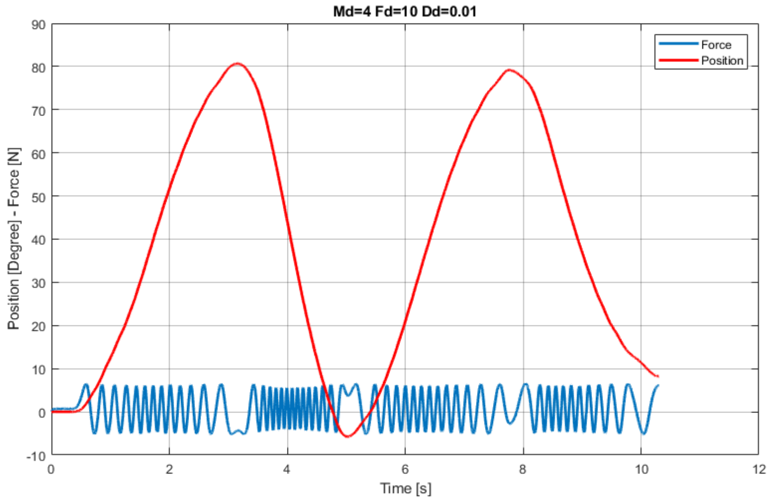

(b)

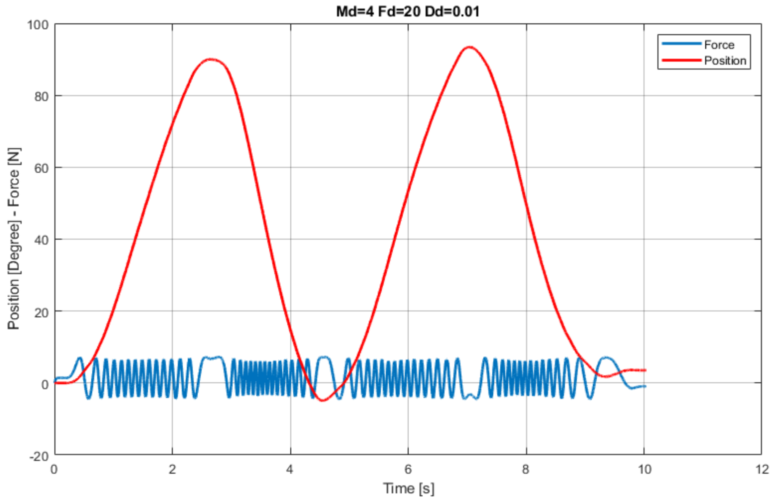

(c)

Figure 59: Md=4 ; Dd=0.01 ; (a) Fd=0, (b) Fd=10, (c) Fd=20

4.8. Isometric Exercise with Prototype

Through this exercise, the level of muscle contraction is increased without causing a change in the length of the muscle. It can be performed by pressing a stationary object, by opposing the manual act of the physiotherapist or by holding a weight in a static condition. The robot applies a force to the patient's limb. The task of the subject is to keep the limb constant against this external force. To perform these tasks the M_d must be high and D_d value must be low. Otherwise the system oscillates too much.

As can be seen in Fig. 60-61 the position of the robot is steady but the force is changing during the exercise. In this exercise the parameters were:

$M_d = 100, F_d = 0{,}1, D_d = 0{,}00001.$

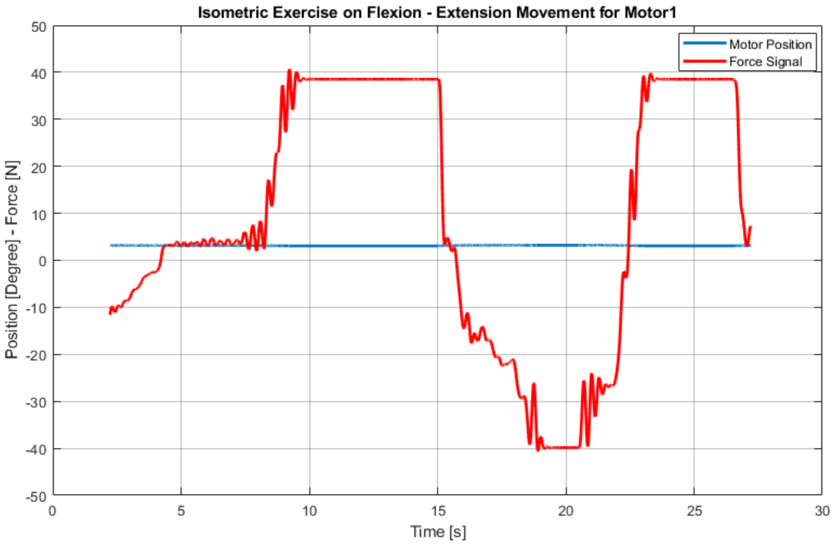

Figure 60: Isometric exercise on flexion-extension movement result

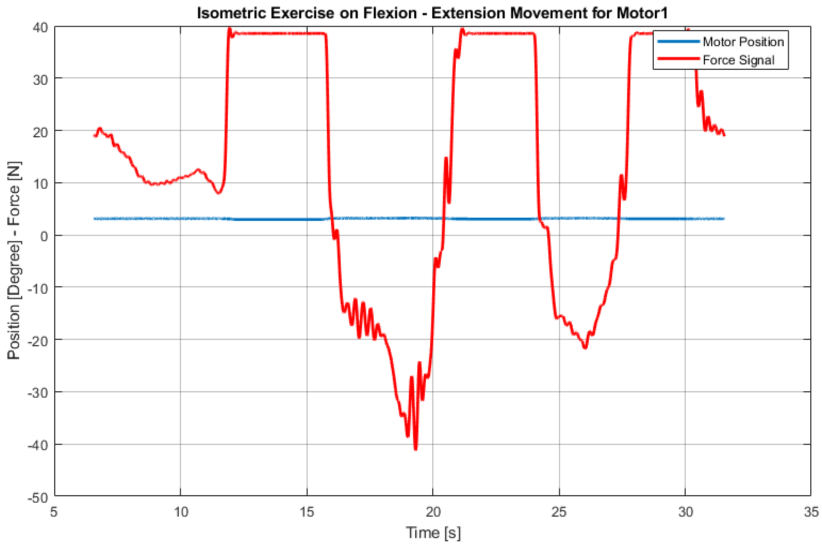

Figure 61: Isometric on flexion-extension movement result

4.9. Isotonic Exercise with Prototype

The patient works againts a constant force which the robot produces. The input of the controller is the target force. The main point is to move patient's limb at a constant force within a certain angle range. To achieve this task the the M_d must be low because with the increase of M_d the resistance increases too. D_d value must be high. Otherwise the system oscillates too much.

In Fig.62 extension movement can be seen. During the exercise the force is always steady at 20 N and when the movement reaches to the end position the force decreases to zero. IN this exercise the parameter values were: $M_d = 0{,}00001, F_d = 0, D_d = 2$.

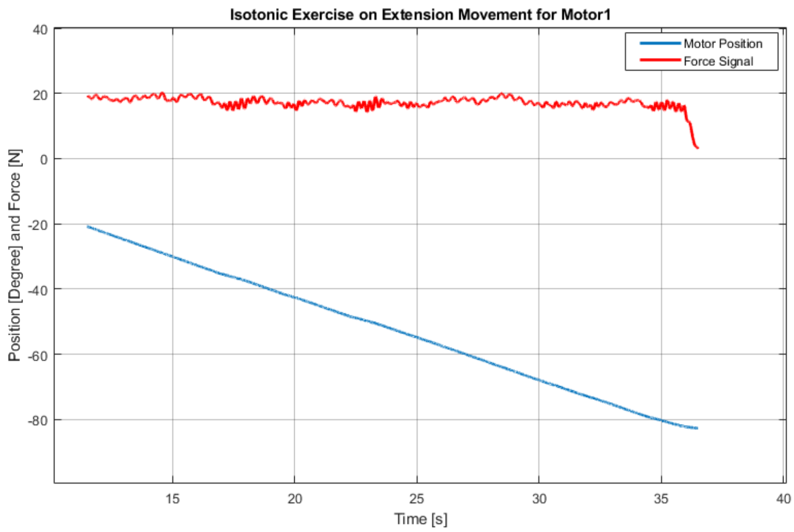

Figure 62: Isotonic exercise on extension movement result

In Fig.63 flexion movement can be seen. During the exercise the force is always steady at 20 N and when the movement reaches to the end position the force decreases to zero.

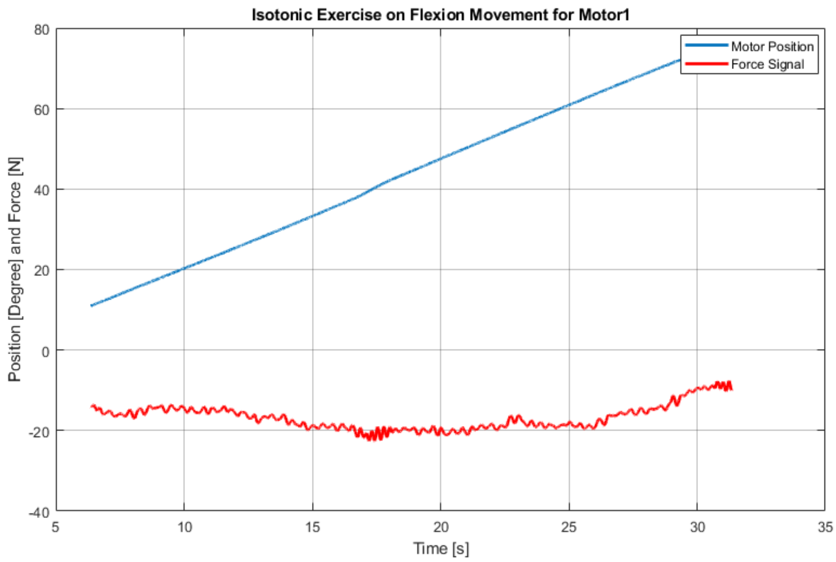

Figure 63: Isotonic exercise on flexion movement result

4.10. Isotonic Exercise with EMG on Prototype

The isotonic exercise was tried on the patient. As can be seen in Fig. 64 the EMG sigal is very wavy and the system doesn't work properly. The reason of this problem is the parameters.

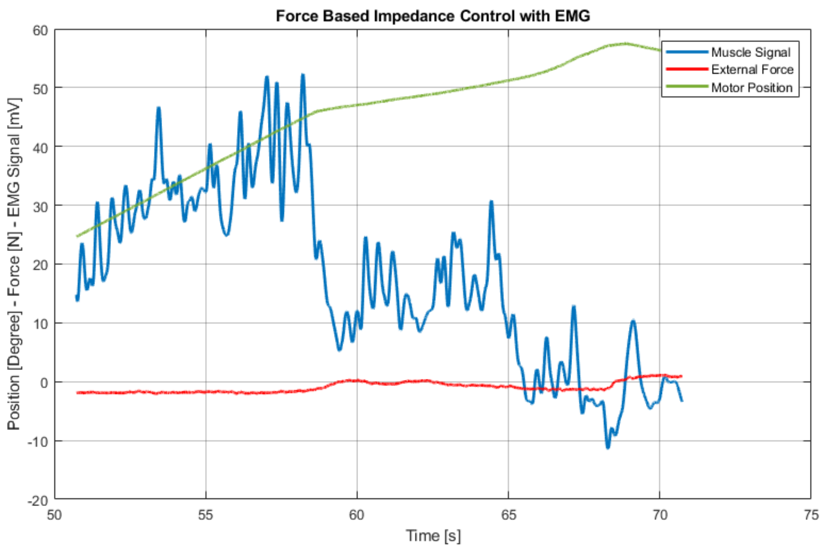

Figure 64: Flexion movement with EMG in Isotonic exercise

After the alignment of the damping ratio the system began to work smoothly. Position of the system changes when the patient applies force on the robot. But the force is always steady in this type of exercises. The flexion movement can be seen in Fig. 65.

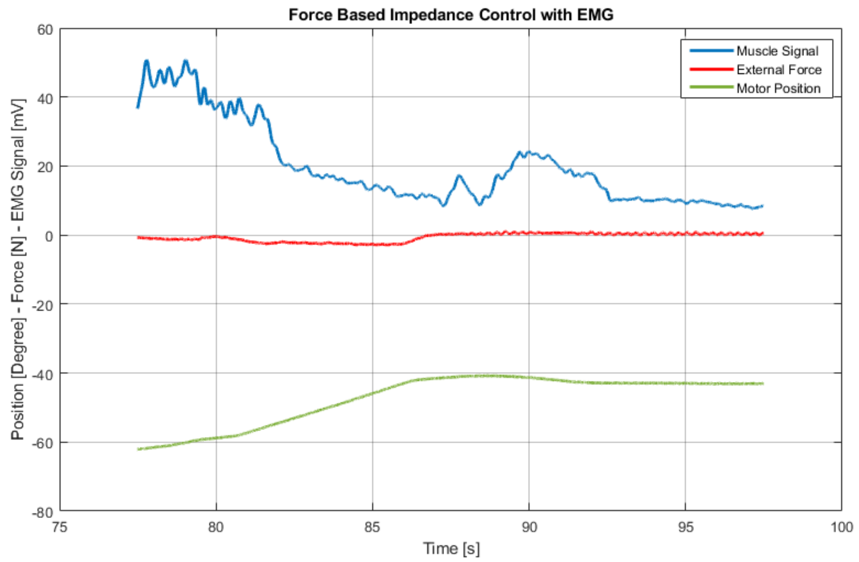

Figure 65: Flexion movement with EMG in Isotonic exercise

Position of the system increases when the patient applies force on the robot but the force stays steady during the exercise. The extension movement can be seen in Fig. 66.

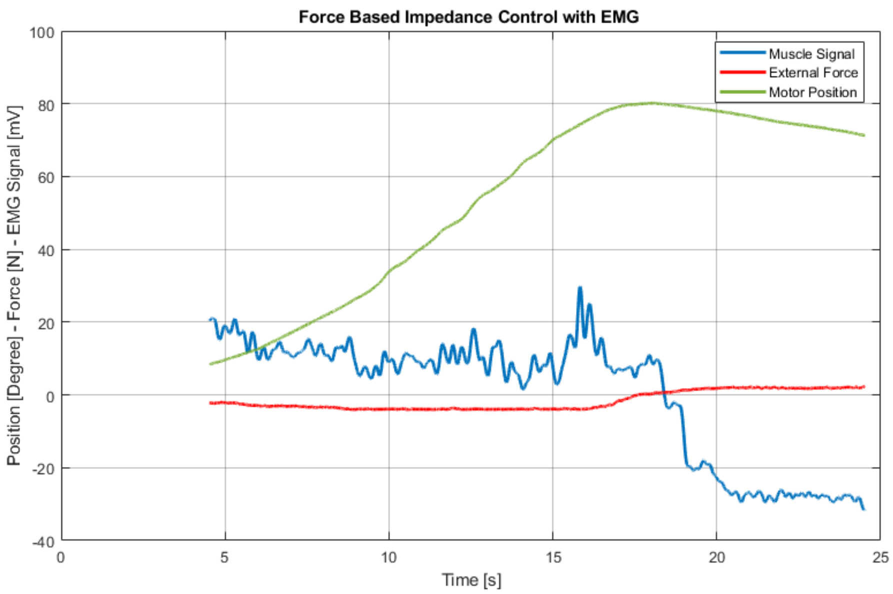

Figure 66: Extension movement with EMG in Isotonic exercise

4.11. Mass Properties

In the SOLIDWORKS environment, the mass properties of our design including weight, center of mass, volume and inertia as are shown in Fig.67 - 69.

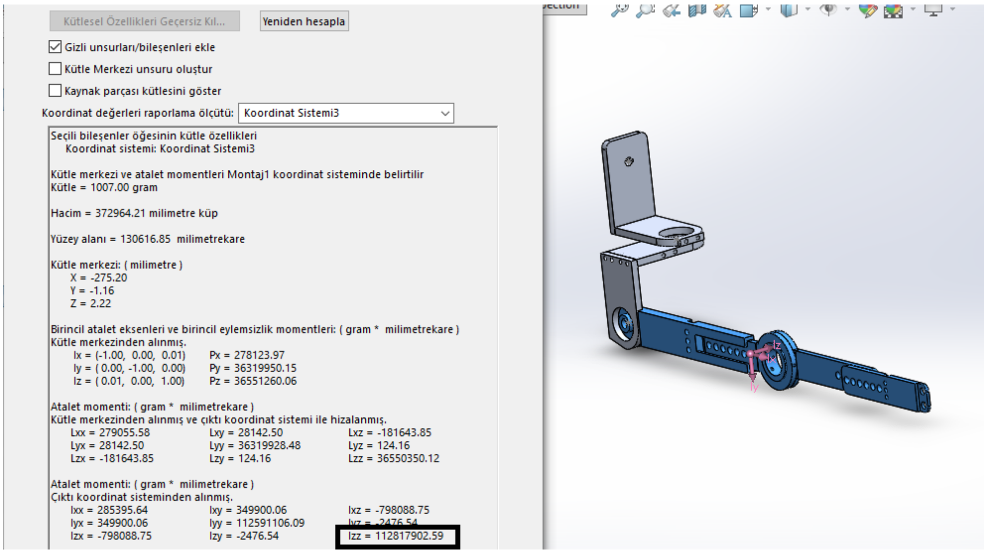

Figure 67: Moment of inertia value of joint 1

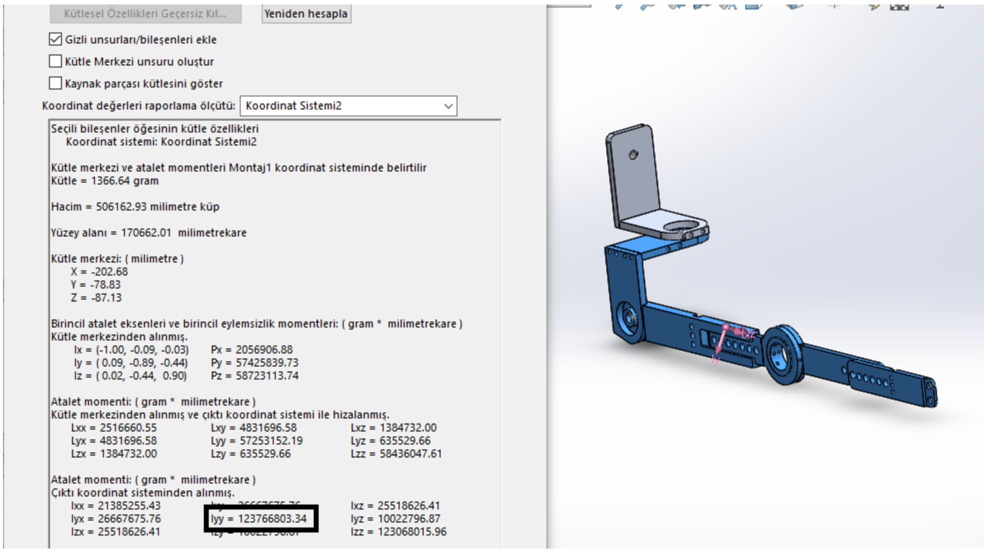

Figure 68: Moment of inertia value of joint 2

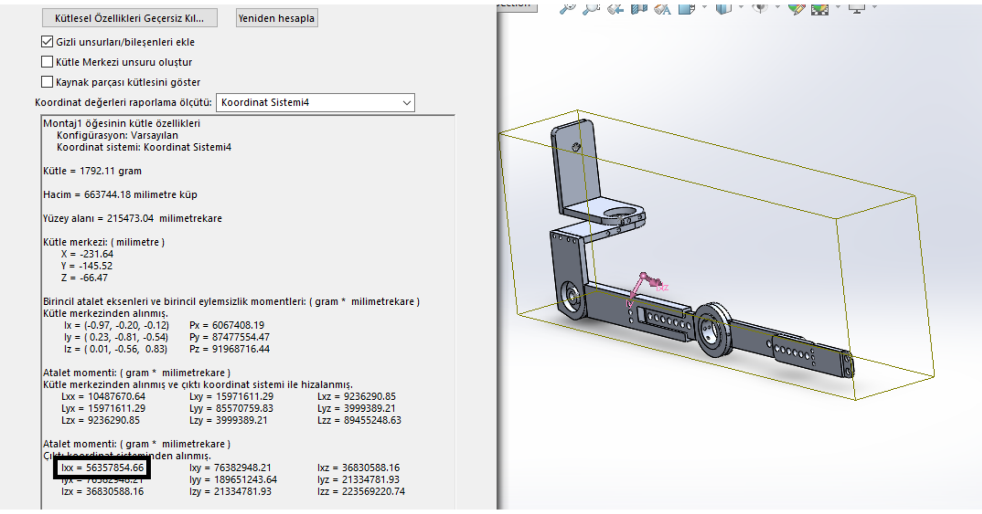

Figure 69: Moment of inertia value of joint 3

The data from Solidworks and calculated compared in the Tab.7. As can be seen from the table, the manual calculations and Solidworks inertia values are very close to each other. This means our calculated values are calculated correctly.

Table 7: Moment of inertia comparison

	Movement Axis	**Manuel**	**Solidworks**
Motor 1	I_{zz}	0,1179 kgm²	0,1128 kgm²
Motor 2	I_{yy}	0,1294 kgm²	0,1276 kgm²
Motor 3	I_{xx}	0,0586 kgm²	0,0563 kgm²

5. WORKING SCHEDULE

This study started with literature review. However, progress has also been made in mechanical design. Analysis and electronic design were completed by December. Equipment selection and control algorithm was carried out by December but the procurement process has not yet started. After that programming the system partly was completed. Lastly the system has been integrated and tested. The results are documented.

The working schedule is shown below.

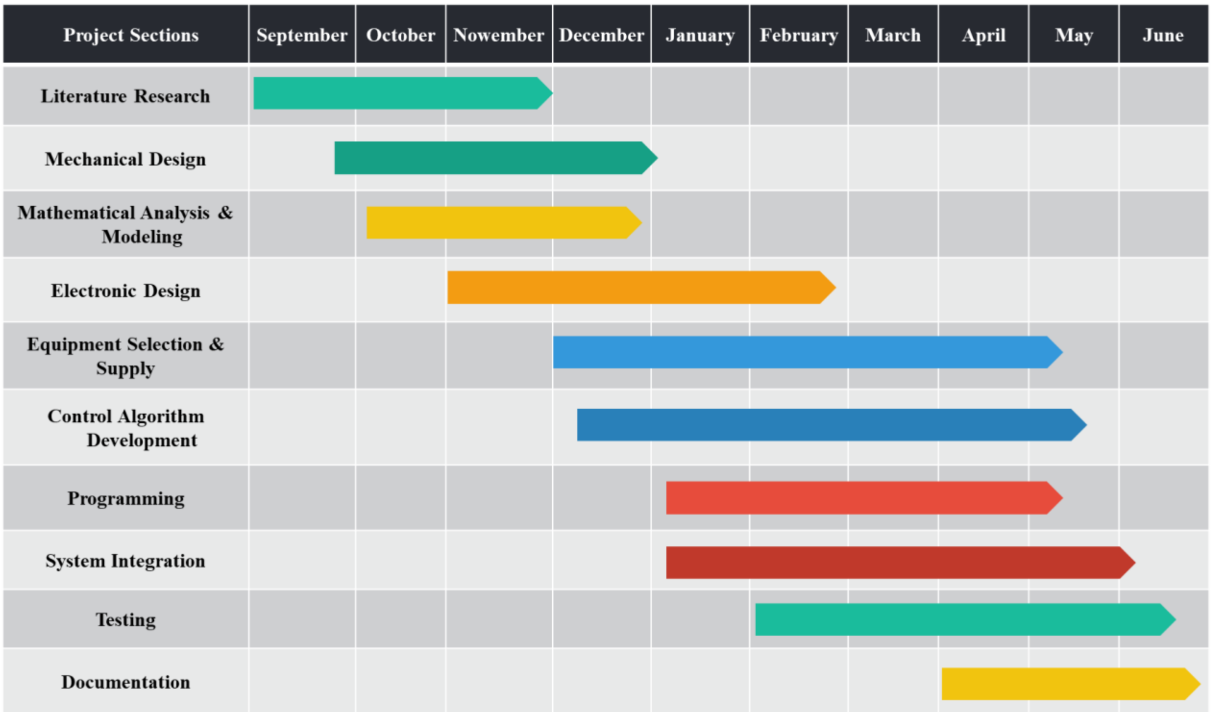

6. BUDGET

The materials and their cost's which used in this project are given in the Tab.8.

Table 8: Product – Cost

Product Type	Product Model	Quantity	Cost
Body material	6013 Aluminum	*1 m^3*	*200 TL*
Prothesis material	for fore arm and rear arm	*2*	*100 TL*
Bolts	M4×30×14	*1*	*0,3 TL*
Bolts	M4×25×14		*1*
Bolts	M6×30×18		*18*
Bolts	M6×12		*4*
Nut	M4		*5*
Nut	M10		*3*
Motor 1	EC Flat 60, 100 Watt with Hall Sensors	*1*	*685 TL*
Gearhead 1	Planetary Gearhead GP-52C 52mm 4-30 Nm, Ceramic Version	*1*	*1260 TL*
Motor 2	EC Max 30, 40 Watt with Hall Sensors	*1*	*1200 TL*
Gearhead 2	Planetary Gearhead GP-32C 32mm 1.0-6.0 Nm, Ceramic Version	*1*	*1330 TL*
Motor 3	EC Flat 45, brushless, 30 Watt with Hall Sensors	*1*	*485 TL*
Gearhead 3	Planetary Gearhead GP-42C 42mm 3-15 Nm -, Ceramic Version	*1*	*1650 TL*
EMG Circuit	PCB design and production handmade	*1*	*220 TL*
Surface Electrodes	Rapidan Tester Electrodes	*50*	*25 TL*
Force Sensors	Micro Load Cell CZL635	*2*	*70 TL*
Encoder 1	Encoder MILE, 512 CPT, 2 Channel with line driver	*1*	*870 TL*
Encoder 2	Encoder HEDL 5540, 500 CPT, 3 Channel with line driver	*1*	*565 TL*
Encoder 3	Encoder MILE, 512 CPT, 2 Channels with line driver	*1*	*870 TL*
Testing microcontroller	Arduino Uno Set	*1*	*40 TL*
Controller	STM32	*1*	*180 TL*

7. PRODUCT BACKLOG

Product Backlog						TEAM
Epic	**Sprint**	**User Story Role**	**User Story Name**	**Story Details**	**Acceptance Test Criteria**	**Tasks**
Design a Control System for Grounded Upper Limb Exoskeleton Rehabilitation Robot	1	Project Team (Mechatronics Enginner)	Design impedance control system	Design a impedance control system for manuel exercises which are active-assistive, isometric and isotonic. These exercises will be done by patients, patients' applied forces will be measured and controlled. According to taken datas from force sensors and limit switches, position control will be done.	1. Force should be measured in both x and y axis.	1. Analyse and select type and position of force sensors should be selected.
					2. Patient should apply maximum 10 N force.	2. Design hardware limitations.
					3. Position datas should be measured in real time.	3. Analyse select motor and encoder by manually and on SOLIDWORKS.
					4. Exercise senarios should be simulated as continuously and correct.	4. Simulate the impedance control systems on MATLAB SIMULINK.

Control System of Grounded Upper Limb Exoskeleton Rehabilitation Robot	2	Project Team (Mechatronics Engineer)	Integrate EMG Based Control System to Control Systems for Each Manuel Exercises	Integrate EMG based control system to PID control system for passive exercise, to PD and impedance control system for active-assistive exercise, to impedance and torque control system for isometric exercise and to impedance control system for isotonic exercise. These integrations are for more efficient human-robot interaction.	1. Muscle activation level should be less than 1kHz.	1. Design a EMG circuit with filtering,rectification and amplification stages.
					2. The muscle signal should get on a correct muscle.	2. Integrate surface electrodes to EMG circuits.
					3. Patients should be safe electronically when they use the robot.	3. Design a electrical switching mechanism.
					4. The efficiency of human-robot interaction should be more than 75%.	4. Integrate EMG based control system to other control systems.

Producible Final Form of Mechanical Design of Grounded Upper Limb Exoskeleton Rehabilitation Robot	3	Project Team (Mechanical Enginner)	Design producible final form of mechanical system	Design all parts of mechanical sysetm as producible. Moreover, design a final form of mechanical design.	1. All mechanical part should be produced easily in production companies.	1. Do dynamic analysis on Simscape.
					2. All parts should be durable.	2. Do strenght of material analysis should be done on SOLIDWORKS.
					3. Total cost of all parts should not be more than 1000 dollar.	3. Select a cost-effective materials from Solidworks, after the analysis.
					4. Mechanical system should be suitable for 1.5-2.0 meter height patients.	4. Design a 22 centimeter adjustable mechanism.
Human-Machine Interface of Grounded Upper Limb Exosekeleton Rehabilitation Robot	4	Project Team (Programmer)	Design safety human-machine interface	Control passive, active assistive, isometric and isotonic exercises on computer and write safety algorith.	1. Results of all manual exercises should be controlled on computer clearly.	1. Design a human-machine interface.
					2. Program of the robot should not be broken during the exercises.	2. Write a safety algorithm.
					3. Informations on ARDUINO should be transmitted to MATLAB.	3. Write a interface code for ARDUINO.

8. RISK ANALYSIS

We have identified the risks that we may face in the coming period. The effects, probability of occurrence and solution suggestions are given in the table below.

Potential Risk Occurence date (week)	Process Product People	Risks Definition	Probability (1-3)	Impact (1-3)	Effect	Open Closed Ongoing Status	Avoidance Reduction Sharing Transfer Deference Mitigation Contingency Insurance Acceptance RISK ACTION	Solution
1	People	Team communication problems	3	3	9	Open	Contingency	Motivation by project team leader
2	Process	Failure to supply motors and sensors	2	1	2	Open	Avoidance	Find a new supplier
3	Product	Some mechanical parts may not be produced	2	1	2	Open	Avoidance	Consult experts before production
4	Product	Some mechanical parts may not be available	2	1	2	Open	Avoidance	Supply of parts with similar characteristi cs
5	Product	Parts can be processed incorrectly	2	2	4	Open	Contingency	Check the product during production
6	Product	There may be assembly error	1	2	2	Open	Contingency	Check the product during production
7	Process	Cancellation of expected sponsorships from	2	3	6	Open	Contingency	Search for new sponsor
8	Process	Lack of time due to midterms	3	2	6	Open	Acceptance	Good time managemen t
9	Process	Increasing cost	2	3	6	Open	Deference	Search for more sponsor
10	People	Reduced motivation due to workload	2	3	6	Open	Acceptance	Getting consultant support
11	Process	Uncalibrated test equipments	1	3	3	Open	Contingency	Regular equipment control before testing
12	Process	Lower project objectives than expected	1	2	2	Open	Contingency	Good marketing
13	People	Dissatisfaction of stakeholders	1	3	3	Open	Sharing	Checking process and control feedbacks
14	People	Failure to meet users' expectation	1	2	2	Open	Sharing	Arrangement according to feedback

9. CONCLUSION

In this study, a 4 DOF grounded exoskeletal robot for shoulder and elbow rehabilitation was designed, produced and control. It can perform passive, active-assistive, isometric and isotonic exercises. The mechanical properties, system requirements, hardware, mathematical modelling were explained. A PID controller were developed for position-controlled exercises. Since the most known position-controlled exercise is passive exercise, simulation and test result with the prototype were given for passive exercise. Results for isotonic and isometric exercises with EMG signals are completed. The results also consist the system response for parameter modifications. According to test results, system can perform passive, active assistive, isometric and isotonic exercises with high accuracy.

10. REFERENCES

[1] E. Akdoğan, "Upper limb rehabilitation robot for physical therapy: design, control and testing," *Turkish Journal of Electrical Engineering & Computer Sciences*, 24(3), 911-934, 2016.

[2] http://iknow.stpi.narl.org.tw/Post/Files/policy/2012/policy_12_037_2.pdf[Accessed, April 21, 2020]

[3] http://www.who.int/mediacentre/factsheets/fs317/en/ [Accessed, April 21, 2020]

[4] C.G. Burgar, P.S. Lum, P.C. Shor and H.F.M. Van der Loos, "Development of robots for rehabilitation therapy: The Palo Alto VA/Stanford experience, " *Journal of Rehabilitation Research and Development 37*, 663-673, 2000.

[5] A. Gupta and M. K. O'Malley, "Design of a haptic arm exoskeleton for training and rehabilitation," *IEEE/ASME Transactions on Mechatronics*, 11(3), 280-289, 2006.

[6] R. Vertechy, A. Frisoli, A. Dettori, M. Solazzi and M. Bergamasco, "Development of a new exoskeleton for upper limb rehabilitation," *IEEE International Conference on Rehabilitation Robotics*, 188-193, 2009.

[7] Y. Ren, H. S. Park and L. Q. Zhang, "Developing a whole-arm exoskeleton robot with hand opening and closing mechanism for upper limb stroke rehabilitation," *IEEE International Conference on Rehabilitation Robotics*, 761-765, 2009.

[8] Y. Ganesan, S. Gobee and V. Durairajah., "Development of an Upper Limb Exoskeleton for Rehabilitation with Feedback from EMG and IMU Sensor," *Procedia Computer Science*, 76, 53-59, 2015.

[9] T. Lenzi, S.M.M. De Rossi, N. Vitiello and M.C. Carrozza, "Intention-based EMG control for powered exoskeletons," *IEEE Transactiıons Biomedical Engineering*, 59(8), 2180–2190, 2012.

[10] K. Kiguchi, K. Iwami, M. Yasuda, K. Watanabe and T. Fukuda, "An exoskeletal robot for human shoulder joint motion assist," *IEEE/ASME Transactions on Mechatronics*, 8 (1), 125–135, 2003.

[11] K. Kiguchi, T. Tanaka and T. Fukuda, "Neuro-fuzzy control of a robotic exoskeleton with EMG signals," *IEEE Transactions on Fuzzy Systems*, 12 (4), 481–490, 2004.

[12] H.C. Hsieh, D.F. Chen, L. Chien and C.C. Lan, "Design of a Parallel Actuated Exoskeleton for Adaptive and Safe Robotic Shoulder Rehabilitation," *IEEE/ASME Trans. Mechatron*., 22, 2034–2045, 2017.

[13] J. Hunt, H. Lee and P. Artemiadis, "A novel shoulder exoskeleton robot using parallel actuation and a passive slip interface," *Journal of Mechanisms and Robotics*, 9 (1), art. no. 011002, 2017.

[14] V.W. Oguntosin, Y. Mori, H. Kim, S.J. Nasuto, S. Kawamura and Y. Hayashi, "Design and Validation of Exoskeleton Actuated by Soft Modules toward Neurorehabilitation—Vision-Based Control for Precise Reaching Motion of Upper Limb," *Frontiers in Neuroscience*, 11, 352, 2017.

[15] Z. F. Shao, X. Tang and W. Yi, "Optimal design of a 3-DOF cable-driven upper arm exoskeleton," *Advanced Mechanical Engineering*, 6, 157096, 2014.

[16] Q. Wu, X. Wang and F. Du, "Development and analysis of a gravity-balanced exoskeleton for active rehabilitation training of upper limb," *Journal of Mechanical Engineering Science*, 230, 3777–3790, 2016.

[17] A. Accogli, L. Grazi, S. Crea, A. Panarese, J. Carpaneto, N. Vitiello and S. Micera , "EMG-based detection of user's intentions for human-machine shared control of an assistive upper-limb exoskeleton, " In Wearable Robotics: Challenges and Trends; Springer Berlin Germany, pp. 181–185, 2017.

[18] Yrd. Doç Dr. Hamza Sucuoğlu, ''Bölüm 1'', Robotik Rehabilitasyona Genel Bakış, haz. Dr. Hamza Sucuoğlu (İstanbul 2018)

[19] https://www.acefitness.org/ [Accessed, April 21, 2020]

[20]https://www.acefitness.org/fitness-certifications/ace-answers/exam-preparation-blog/3535/muscles-that-move-the-arm [Accessed, April 21, 2020]

[21] E. Akdoğan, E. Taçgın, M. Adli, A. "Knee rehabilitation using an intelligent robotic system," *Journal of Intellelligent Manufacturing*, 20(2), 195–202, 2009.

[22] Maxon Motor - Selection Guide 2017/2018

[23] E. Akdogan, M. Aktan, A. Koru, M. Arslan, M. Atlıhan, (2017). Hybrid impedance control of a robot manipulator for wrist and forearm rehabilitation: Performance analysis and clinical results. *Mechatronics*. 49. 10.1016/j.mechatronics.2017.12.001.

APPENDIX A

Maxon Flat Motors

Multipole EC motors, such as maxon flat motors require a greater number of commutation steps for a motor revolution. Due to the wound stator teeth, they have a higher terminal inductance than motors with an ironless winding. As a result, at higher speed, the current cannot develop fully during the correspondingly short commutation intervals. Therefore, the apparent torque produced is lower. Current is also fed back into the controller's power stage.

As a result, motor behavior deviates from the ideal linear speed-toque gradient. The apparent speed-torque gradient depends on voltage and speed. The gradient is steeper at higher speeds. Flat motors are operated in the continuous operation range the achievable where speed-torque gradient at nominal voltage tend to be approximated by a straight line between no load speed and nominal operating point.

Rated Operating Point

The rated operating point is an ideal operating for the motor and derives from operation at nominal voltage U_N and nominal current I_N.

Nominal speed n_N is reached in line with the speed gradient. The choice of nominal voltage follows from considerations of where the maximum no load speed should be. The nominal current derives from the motor's thermally maximum permission continues current.

The movements of our rehabilitation robot is highly related with the movement capability of shoulder and elbow anatomy. Therefore, maximum torque capability values limit our motor selection criterias according to torque value. We cannot select a motor which has torque value more than the figure 3 values. We use motor 1 for shoulder vertical flexion/extension movement. Motor 2 for shoulder abduction/adduction movement, motor 3 for shoulder horizontal flexion/extension movement. So, our selected motor 1 should have less than 110 Nm, motor 2 should have less than 125 Nm and motor 3 should have less than 110 Nm.

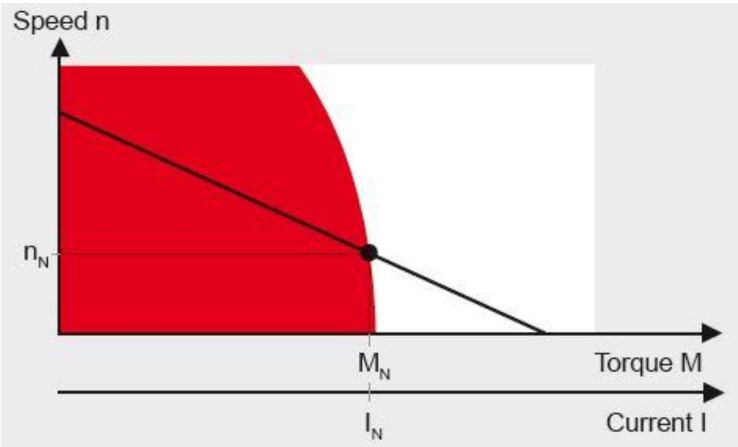

Figure 70: Rated Operating Diagram of Maxon Motors

Operating Ranges

Operating ranges diagram can be seen in Fig.48.

Permanent Operating Torque:

The two criteria "maximum continues torque" and "maximum permissible speed" limit the continues operating range. Operating points within this range are not critical thermally and do not generally cause increased wear of the commutation system.

Short-term Operating Range:

The motor may only be loaded with the maximum continues current for thermal reasons. However, temporary higher currents and torques are allowed. As long as the winding temperature is below the critical value, the winding will not be damaged. Phases with increased currents are time limited.

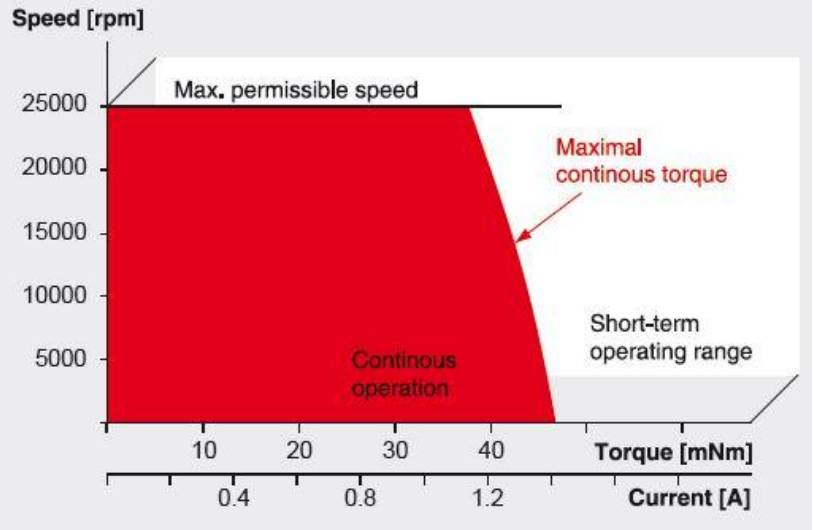

Figure 71: Operating Range Diagram of Maxon Motors

EC 60 Flat ∅60 mm, Brushless, 100 Watt, with Hall sensors:

Part No: 625855

Model of selected motor 1 is shown in Fig.49.

Figure 72: Maxon EC Flat 60

Technical drawing of selected motor 1 is shown in Fİg.50.

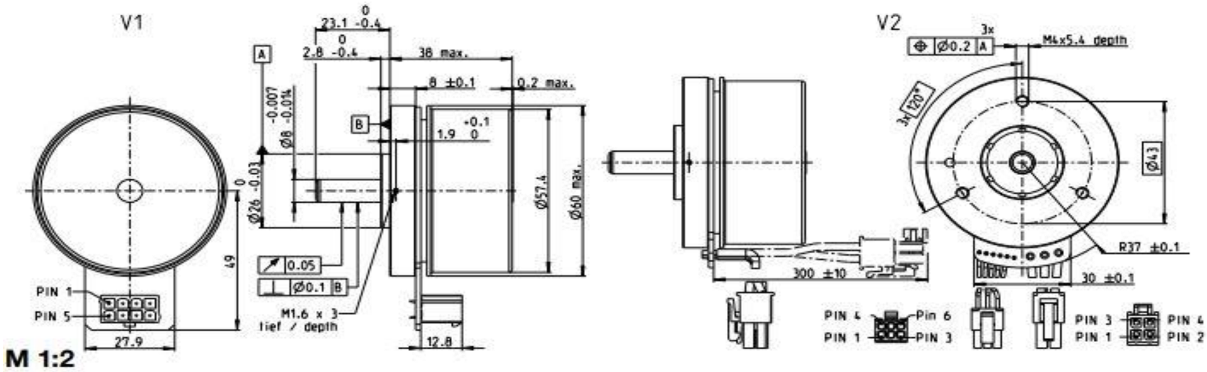

Figure 73: Drawing of EC Flat 60

Important characteristics of EC-flat 60 are represented in Fig.51.

VALUES AT NOMINAL VOLTAGE	
Nominal voltage	24 V
No load speed	4300 rpm
No load current	493 mA
Nominal speed	3730 rpm
Nominal torque (max. continuous torque)	269 mNm
Nominal current (max. continuous current)	5.14 A
Stall torque	4300 mNm
Stall current	81.9 A
Max. efficiency	85 %
CHARACTERISTICS	
Terminal resistance	0.293 Ω
Terminal inductance	0.279 mH
Torque constant	52.5 mNm/A
Speed constant	182 rpm/V
Speed / torque gradient	1.01 rpm/mNm
Mechanical time constant	8.86 ms
Rotor inertia	835 gcm²
THERMAL DATA	
Thermal resistance housing-ambient	2.5 K/W
Thermal resistance winding-housing	3.8 K/W
Thermal time constant winding	41.4 s
Thermal time constant motor	90 s
Ambient temperature	-40...+100 °C
Max. winding temperature	+125 °C
MECHANICAL DATA	
Bearing type	ball bearings
Max. speed	6000 rpm
Axial play	0 - 0.14 mm
Max. axial load (dynamic)	12 N
Max. force for press fits (static)	170 N
(static, shaft supported)	8000 N
Max. radial load	110 N, 5 mm from flange
OTHER SPECIFICATIONS	
Number of pole pairs	7
Number of phases	3
Number of autoclave cycles	0
PRODUCT	
Weight	350 g

Figure 74: Charecteristics of EC Flat 60

Data of motor 1 is represented in Fig.52.

Stock program
Standard program
Special program (on request)

		Part Numbers		
V1 with Hall sensors		625854	625855	625856
V2 with Hall sensors and cables		647691	645604	647692
Motor Data				
Values at nominal voltage				
1 Nominal voltage	V	12	24	48
2 No load speed	rpm	3760	4300	4020
3 No load current	mA	797	493	221
4 Nominal speed	rpm	3210	3730	3460
5 Nominal torque (max. continuous torque)	mNm	261	269	298
6 Nominal current (max. continuous current)	A	8.72	5.14	2.61
7 Stall torque[1]	mNm	3340	4300	4870
8 Stall current	A	111	81.9	43.2
9 Max. efficiency	%	84.1	85.3	86.4
Characteristics				
10 Terminal resistance phase to phase	Ω	0.108	0.293	1.11
11 Terminal inductance phase to phase	mH	0.0911	0.279	1.28
12 Torque constant	mNm/A	30	52.5	113
13 Speed constant	rpm/V	318	182	84.8
14 Speed/torque gradient	rpm/mNm	1.14	1.01	0.837
15 Mechanical time constant	ms	9.99	8.86	7.32
16 Rotor inertia	gcm²	835	835	835

Figure 75: Motor 1 Data

Operating range of EC-flat 60 is shown in figure 67.

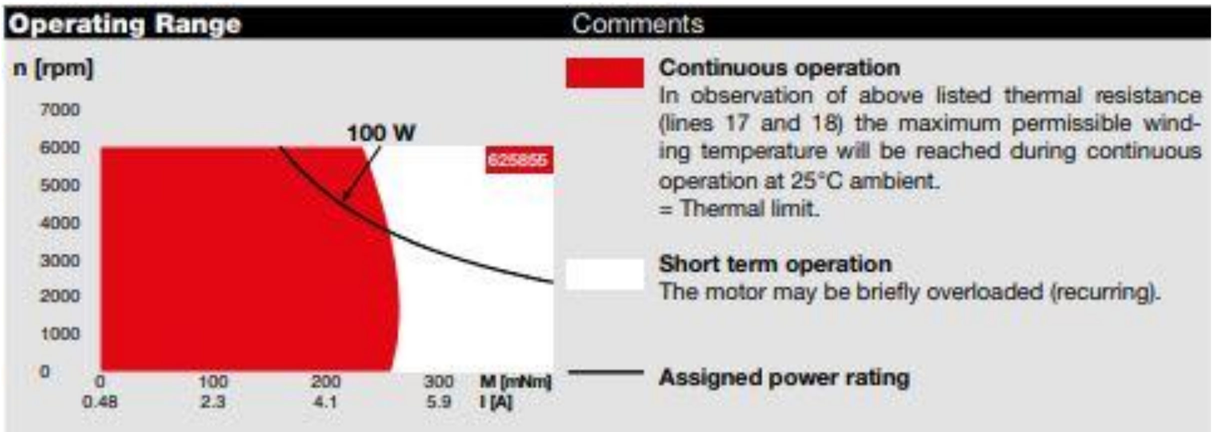

Figure 76: Operating Range of EC Flat 60

Suitable gearhead for motor 1 is represented in Fig.54.

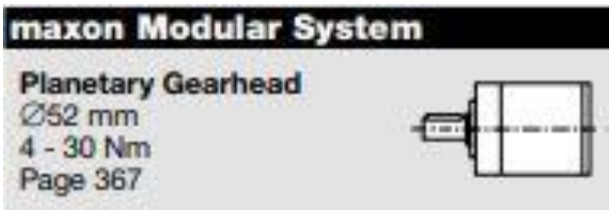

Figure 77: Suitable Gearhead for Motor 1

Planetary Gearhead GP-52 C Ø52 mm, 4-30Nm, Ceramic Version:

Part No: 223095

Model of selected gearhead 1 is represented in Fig.55.

Figure 78: GP-52C Gearhead

Technical drawing of selected gearhead 1 is shown in Fig.56.

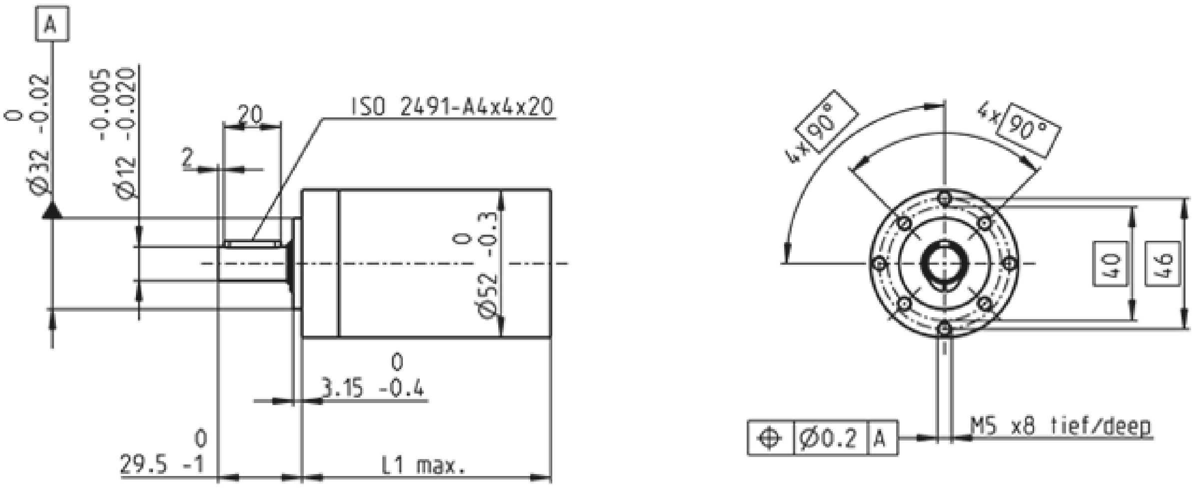

Figure 79: Drawing of GP-52 C

Important characteristics of GP-52 C is shown in Fig.57.

GENERAL INFORMATION	
Gearhead type	GP
Outer diameter	52 mm
Version	Ceramic version
GEARHEAD DATA	
Reduction	113 : 1
Absolute reduction	338/3
Max. motor shaft diameter	8 mm
Number of stages	3
Max. continuous torque	30 Nm
Max. intermittent torque	45 Nm
Direction of rotation, drive to output	=
Max. efficiency	75 %
Average backlash no load	1 °
Mass inertia	9.3 gcm²
Gearhead length (L1)	78.5 mm
Max. transmittable power (continuous)	170 W
Max. transmittable power (intermittent)	250 W
TECHNICAL DATA	
Radial play	max. 0.06 mm, 12 mm from flange
Axial play	0 - 0.3 mm
Max. radial load	900 N, 12 mm from flange
Max. axial load (dynamic)	200 N
Max. force for press fits	500 N
Max. continuous input speed	6000 rpm
Max. intermittent input speed	6000 rpm
Recommended temperature range	-15...+80 °C
Extended temperature range	-40...+100 °C
Number of autoclave cycles	0
PRODUCT	
Weight	770 g

Figure 80: Charecteristics of GP-52C

Data of selected gerahead 1 is represented in Fig.58.

	Stock program						
	Standard program						
	Special program (on request)						
	Part Numbers		223080	223083	223089	223094	223097
	Gearhead Data						
1	Reduction		3.5 : 1	12 : 1	43 : 1	91 : 1	150 : 1
2	Absolute reduction		7/2	49/4	343/8	91	2401/16
10	Mass inertia	gcm²	20.7	17.6	17.3	16.7	17.3
3	Max. motor shaft diameter	mm	10	10	10	10	10
	Part Numbers		223081	223084	223090	223095	223099
1	Reduction		4.3 : 1	15 : 1	53 : 1	113 : 1	186 : 1
2	Absolute reduction		13/3	91/6	637/12	338/3	4459/24
10	Mass inertia	gcm²	12	16.8	17.2	9.3	17.3
3	Max. motor shaft diameter	mm	8	10	10	8	10
	Part Numbers			223085	223091	223096	223101
1	Reduction			19 : 1	66 : 1	126 : 1	230 : 1
2	Absolute reduction			169/9	1183/18	126	8281/36
10	Mass inertia	gcm²		9.5	16.7	16.4	16.8
3	Max. motor shaft diameter	mm		8	10	10	10
	Part Numbers			223086	223092	223098	223102
1	Reduction			21 : 1	74 : 1	156 : 1	257 : 1
2	Absolute reduction			21	147/2	156	1029/4
10	Mass inertia	gcm²		16.5	17.2	9.1	17.3
3	Max. motor shaft diameter	mm		10	10	8	10
	Part Numbers			223087	223093		223103
1	Reduction			26 : 1	81 : 1		285 : 1
2	Absolute reduction			26	2197/27		15379/54
10	Mass inertia	gcm²		9.1	9.4		16.7
3	Max. motor shaft diameter	mm		8	8		10
4	Number of stages		1	2	3	3	4
5	Max. continuous torque	Nm	4	15	30	30	30
6	Max. intermittent torque at gear output	Nm	6	22.5	45	45	45
7	Max. efficiency	%	91	83	75	75	68
8	Weight	g	460	620	770	770	920
9	Average backlash no load	°	0.6	0.8	1.0	1.0	1.0
11	Gearhead length L1	mm	49.0	65.0	78.5	78.5	92.0

Figure 81: Gearhead 1 Data

Part number of our selected GP-52 C gearhead is 223095.

EC-Max 30 ∅30 mm, Brushless, 40 Watt, with Hall sensors:

Part No: 272768

Model of selected motor 2 is shown in Fig.59.

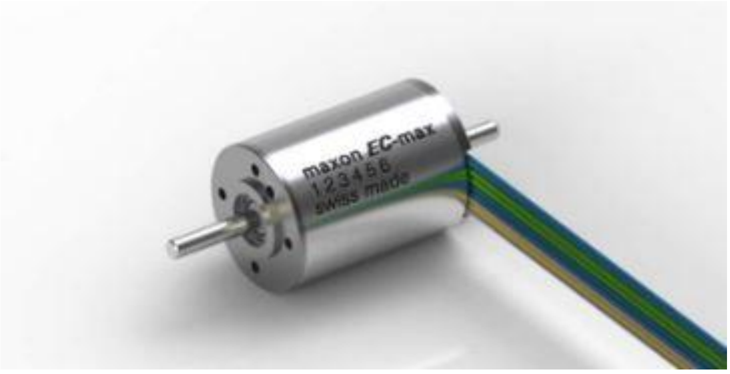

Figure 82: Maxon EC-Max 30

Technical drawing of selected motor 2 is shown in Fig.60.

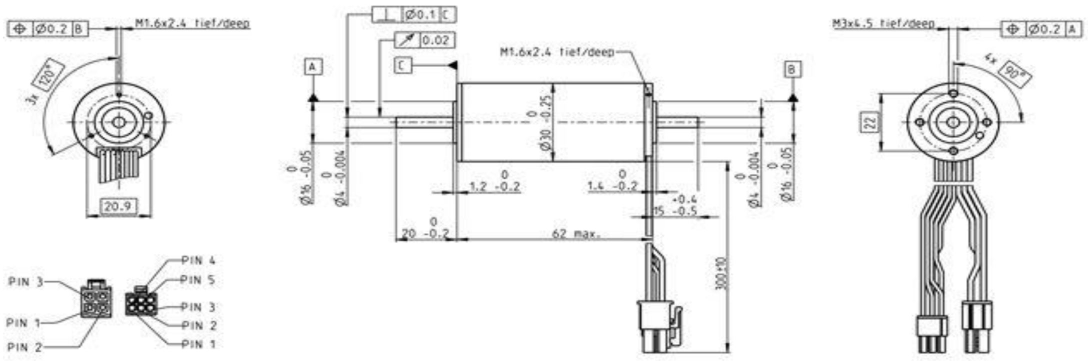

Figure 83: Drawing of Maxon EC-Max 30

Important characteristics of EC-max 30 are represented in Fig.61.

VALUES AT NOMINAL VOLTAGE	
Nominal voltage	24 V
No load speed	9250 rpm
No load current	151 mA
Nominal speed	7220 rpm
Nominal torque (max. continuous torque)	33.8 mNm
Nominal current (max. continuous current)	1.49 A
Stall torque	160 mNm
Stall current	6.57 A
Max. efficiency	75 %
CHARACTERISTICS	
Terminal resistance	3.65 Ω
Terminal inductance	0.31 mH
Torque constant	24.3 mNm/A
Speed constant	393 rpm/V
Speed / torque gradient	59.1 rpm/mNm
Mechanical time constant	6.81 ms
Rotor inertia	11 gcm²
MECHANICAL DATA	
Bearing type	ball bearings
Max. speed	15000 rpm
Axial play	0 - 0.14 mm
Max. axial load (dynamic)	5 N
Max. force for press fits (static)	98 N
(static, shaft supported)	2000 N
Max. radial load	25 N, 5 mm from flange
OTHER SPECIFICATIONS	
Number of pole pairs	1
Number of phases	3
Number of autoclave cycles	0
PRODUCT	
Weight	190 g

Data of selected motor 2 is shown in Fig.61.

Stock program
Standard program
Special program (on request)

Motor Data		Part Numbers 272766	272768	272769	272770
Values at nominal voltage					
1 Nominal voltage	V	12	24	36	48
2 No load speed	rpm	8680	9250	9150	9250
3 No load current	mA	223	123	80.5	61.4
4 Nominal speed	rpm	6630	7220	7090	7210
5 Nominal torque (max. continuous torque)	mNm	34.9	33.8	33.3	33.4
6 Nominal current (max. continuous current)	A	2.88	1.49	0.97	0.738
7 Stall torque	mNm	153	160	154	157
8 Stall current	A	11.8	6.57	4.18	3.24
9 Max. efficiency	%	75	75	75	75
Characteristics					
10 Terminal resistance phase to phase	Ω	1.01	3.65	8.61	14.8
11 Terminal inductance phase to phase	mH	0.088	0.31	0.713	1.24
12 Torque constant	mNm/A	12.9	24.3	36.8	48.6
13 Speed constant	rpm/V	738	393	259	197
14 Speed/torque gradient	rpm/mNm	57.8	59.1	60.6	59.9
15 Mechanical time constant	ms	6.66	6.81	6.98	6.9
16 Rotor inertia	gcm^2	11	11	11	11

Figure 84: Motor 2 Data

Part number of our selected EC-max 30 motor is 272768.

Operating range of motor 2 is shown in Fig.62.

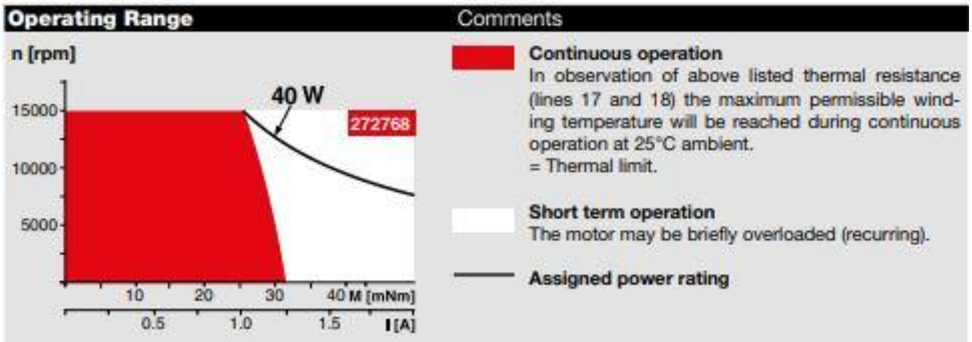

Figure 85. Operating Range of EC-Max 30

Suitable gearheads for motor 2 are shown in Fig.63.

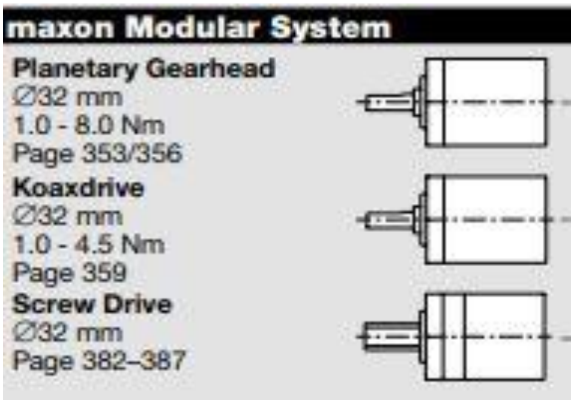

Figure 86: Suitable Gearbox for EC-Max 30

Planetary Gearhead GP-32 C Ø32 mm, 1.0 - 6.0 Nm, Ceramic Version:

Part No: 166949

Model of selected gearhead 2 is shown in Fig.64.

Figure 87: GP 32-C

Technical drawing of selected gearhead 2 is represented in Fig.65.

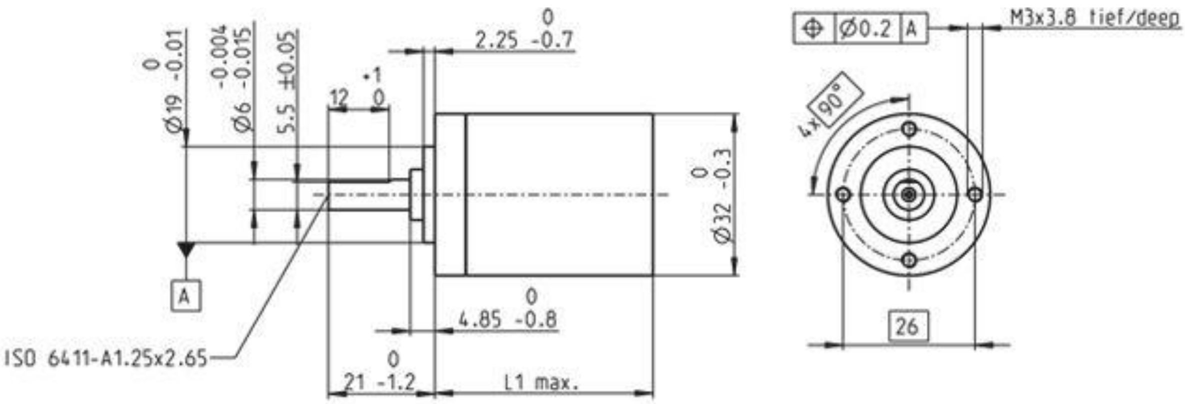

Figure 88: Drawing of GP-32C

Important characteristics of selectedare shown in Fig.66.

GENERAL INFORMATION	
Gearhead type	GP
Outer diameter	32 mm
Version	Ceramic version
GEARHEAD DATA	
Reduction	246 : 1
Absolute reduction	421824/1715
Max. motor shaft diameter	4 mm
Number of stages	4
Max. continuous torque	6 Nm
Max. intermittent torque	7.5 Nm
Direction of rotation, drive to output	=
Max. efficiency	60 %
Average backlash no load	1 °
Mass inertia	0.7 gcm²
Gearhead length (L1)	49.8 mm
Max. transmittable power (continuous)	20 W
Max. transmittable power (intermittent)	26 W
TECHNICAL DATA	
Radial play	max. 0.14 mm, 5 mm from flange
Axial play	max. 0.4 mm
Max. radial load	140 N, 10 mm from flange
Max. axial load (dynamic)	120 N
Max. force for press fits	120 N
Max. continuous input speed	8000 rpm
Max. intermittent input speed	8000 rpm
Recommended temperature range	-40...+100 °C
Number of autoclave cycles	0
PRODUCT	
Weight	160 g

Figure 89: Charecteristics of GP-32C

Data of selected gearhead 2 are shown in Fig.67.

	Stock program / Standard program / Special program (on request)		Part Numbers					
			166930	166933	166938	166939	166944	166949
	Gearhead Data							
1	Reduction		3.7 : 1	14 : 1	33 : 1	51 : 1	111 : 1	246 : 1
2	Absolute reduction		26/7	676/49	529/16	17576/343	13824/125	421824/1715
3	Max. motor shaft diameter	mm	6	6	3	6	4	4
	Part Numbers		166931	166934		166940	166945	166950
1	Reduction		4.8 : 1	18 : 1		66 : 1	123 : 1	295 : 1
2	Absolute reduction		24/5	624/35		16224/245	6877/56	101062/343
3	Max. motor shaft diameter	mm	4	4		4	3	3
	Part Numbers		166932	166935		166941	166946	166951
1	Reduction		5.8 : 1	21 : 1		79 : 1	132 : 1	318 : 1
2	Absolute reduction		23/4	299/14		3887/49	3312/25	389376/1225
3	Max. motor shaft diameter	mm	3	3		3	3	4
	Part Numbers			166936		166942	166947	166952
1	Reduction			23 : 1		86 : 1	159 : 1	411 : 1
2	Absolute reduction			576/25		14976/175	1587/10	359424/875
3	Max. motor shaft diameter	mm		4		4	3	4
	Part Numbers			166937		166943	166948	166953
1	Reduction			28 : 1		103 : 1	190 : 1	456 : 1
2	Absolute reduction			138/5		3588/35	12167/64	89401/196
3	Max. motor shaft diameter	mm		3		3	3	3
4	Number of stages		1	2	2	3	3	4
5	Max. continuous torque	Nm	1	3	3	6	6	6
6	Max. intermittent torque at gear output	Nm	1.25	3.75	3.75	7.5	7.5	7.5
7	Max. efficiency	%	80	75	75	70	70	60
8	Weight	g	118	162	162	194	194	226
9	Average backlash no load	°	0.7	0.8	0.8	1.0	1.0	1.0
10	Mass inertia	gcm^2	1.5	0.8	0.8	0.7	0.7	0.7
11	Gearhead length L1	mm	26.5	36.4	36.4	43.1	43.1	49.8

Figure 90: Gearhead 2 Data

Part number of our selected gearhead is 166949.

EC-flat 45 ∅42.9 mm, brushless, 30 Watt, with Hall sensors:

Part No: 339281

Model of selected motor 3 is shown in Fig.68.

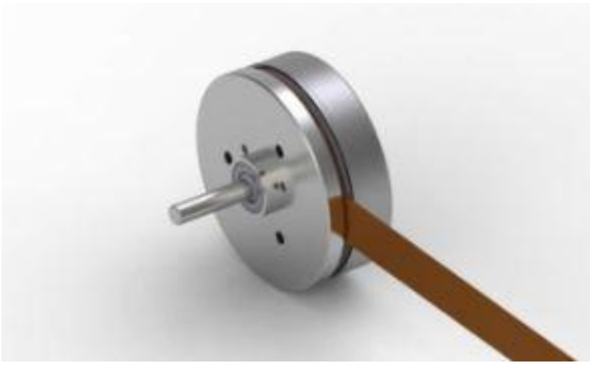

Figure 91: EC- 45 Flat

Technical drawing of selected motor 3 is shown in Fig.69.

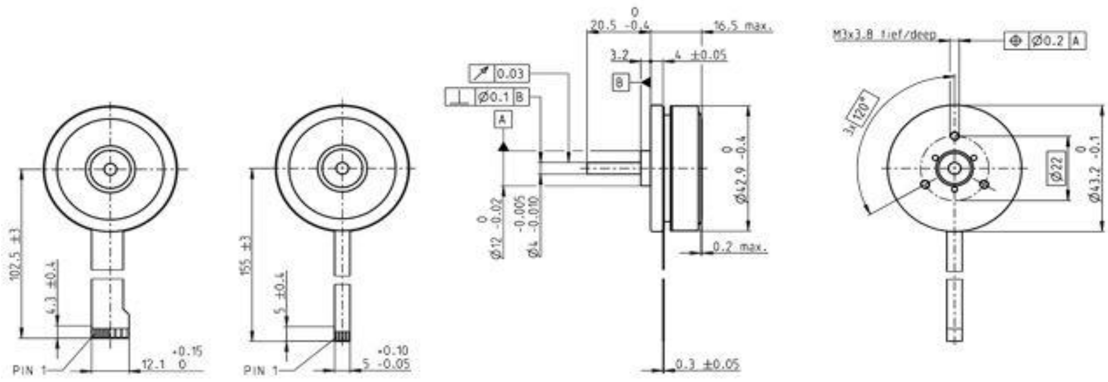

Figure 92: Drawing of EC-45 Flat

Important chracteristics of selected motor 3 is shown Fig.70.

VALUES AT NOMINAL VOLTAGE	
Nominal voltage	24 V
No load speed	4360 rpm
No load current	81.4 mA
Nominal speed	2930 rpm
Nominal torque (max. continuous torque)	54.7 mNm
Nominal current (max. continuous current)	1.01 A
Stall torque	251 mNm
Stall current	4.93 A
Max. efficiency	76 %

CHARACTERISTICS	
Terminal resistance	4.87 Ω
Terminal inductance	2.24 mH
Torque constant	51 mNm/A
Speed constant	187 rpm/V
Speed / torque gradient	17.9 rpm/mNm
Mechanical time constant	17.3 ms
Rotor inertia	92.5 gcm²

THERMAL DATA	
Thermal resistance housing-ambient	6.7 K/W
Thermal resistance winding-housing	3.92 K/W
Thermal time constant winding	11.5 s
Thermal time constant motor	295 s
Ambient temperature	-40...+100 °C
Max. winding temperature	+125 °C
MECHANICAL DATA	
Bearing type	ball bearings
Max. speed	10000 rpm
Axial play	0 - 0.14 mm
Max. axial load (dynamic)	4.8 N
Max. force for press fits (static)	53 N
(static, shaft supported)	1000 N
Max. radial load	18 N, 5 mm from flange
OTHER SPECIFICATIONS	
Number of pole pairs	8
Number of phases	3
Number of autoclave cycles	0
PRODUCT	
Weight	75 g

Figure 93: Charecteristics of EC-45 Flat

Data of selected motor 3 is shown in Fig.71.

Stock program
Standard program
Special program (on request)

Part Numbers							
A with Hall sensors		200142		339281		339282	
Option with Cable and Connector		387266		400527		400580	
B sensorless			200189		339283		339284
Motor Data							
Values at nominal voltage							
1 Nominal voltage	V	12	12	24	24	36	36
2 No load speed	rpm	4370	4350	4360	4380	4750	4760
3 No load current	mA	163	163	81.4	73	61.6	55.3
4 Nominal speed	rpm	2940	2800	2940	2900	3290	3270
5 Nominal torque (max. continuous torque)	mNm	55	54.7	54.8	55.2	66	66.6
6 Nominal current (max. continuous current)	A	2.02	2.02	1.01	1.01	0.847	0.849
7 Stall torque[1]	mNm	255	219	253	243	380	369
8 Stall current	A	10	8.58	4.97	4.77	5.38	5.22
9 Max. efficiency	%	76	75	76	77	80	81
Characteristics							
10 Terminal resistance phase to phase	Ω	1.2	1.4	4.83	5.03	6.69	6.89
11 Terminal inductance phase to phase	mH	0.56	0.56	2.24	2.24	4.29	4.29
12 Torque constant	mNm/A	25.5	25.5	51	51	70.6	70.6
13 Speed constant	rpm/V	374	374	187	187	135	135
14 Speed/torque gradient	rpm/mNm	17.6	20.5	17.7	18.5	12.8	13.2
15 Mechanical time constant	ms	17.1	19.9	17.2	17.9	12.4	12.8
16 Rotor inertia	gcm^2	92.5	92.5	92.5	92.5	92.5	92.5

Figure 94: Motor 3 Data

Part number of our selected EC-flat 45 motor is 339281.

Operating range of motor 3 is represented in Fig.72.

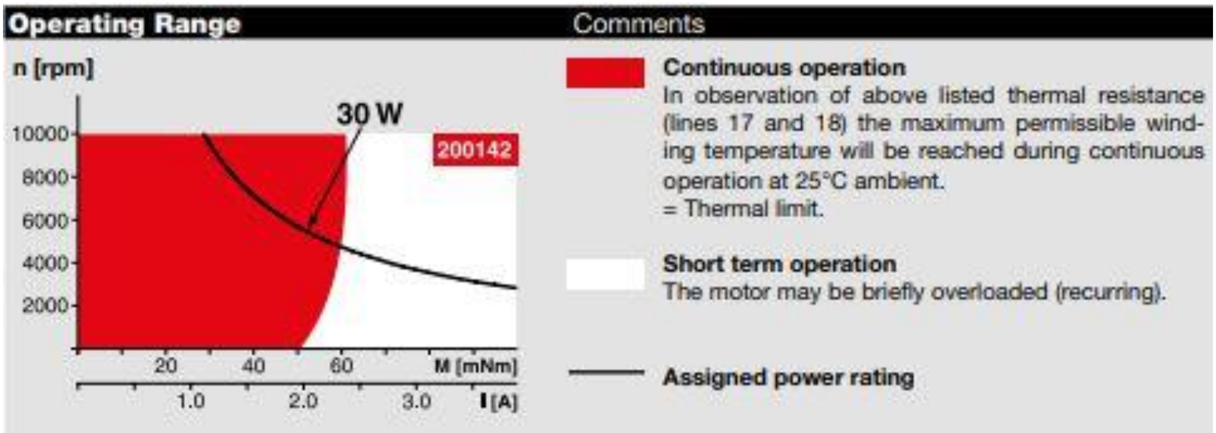

Figure 95: Operating Range of Motor 3

Suitable gearheads for motor 3 are shown in Fig.73.

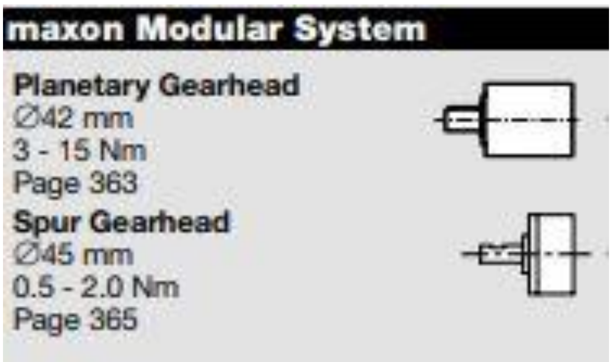

Figure 96: Suitable Gearhead for Motor 3

Planetary Gearhead GP-42 C Ø42 mm, 3 – 15 Nm, Ceramic Version:

Part No: 203127

Model of selected gearhead 3 is shown in Fig.74.

Figure 97: GP-42C Gearhead

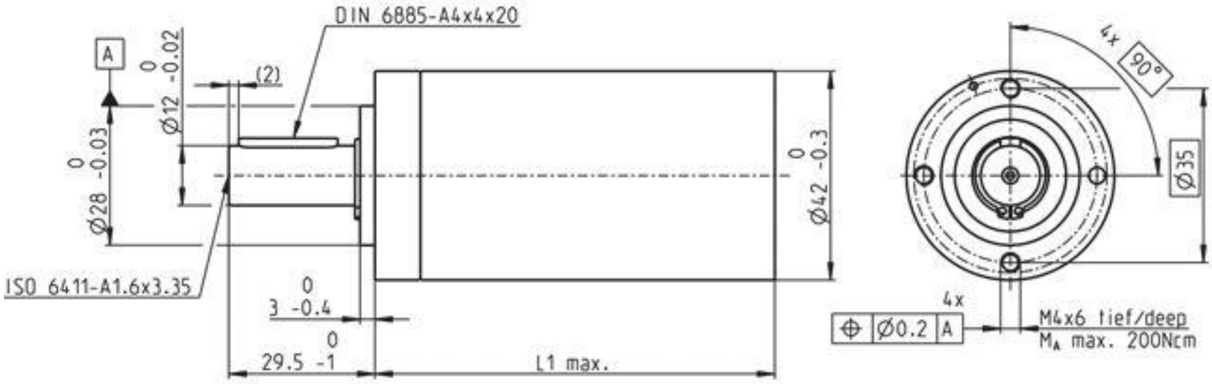

Figure 98: Drawing of GP-42C

Important characteristics of gearhead 3 are shown in Fig.76.

GENERAL INFORMATION	
Gearhead type	GP
Outer diameter	42 mm
Version	Ceramic version
GEARHEAD DATA	
Reduction	126 : 1
Absolute reduction	126/1
Max. motor shaft diameter	10 mm
Number of stages	3
Max. continuous torque	15 Nm
Max. intermittent torque	22 Nm
Direction of rotation, drive to output	=
Max. efficiency	72 %
Average backlash no load	1 °
Mass inertia	14 gcm²
Gearhead length (L1)	70 mm
Max. transmittable power (continuous)	100 W
Max. transmittable power (intermittent)	150 W

TECHNICAL DATA	
Radial play	max. 0.06 mm, 12 mm from flange
Axial play	max. 0.3 mm
Max. radial load	360 N, 12 mm from flange
Max. axial load (dynamic)	150 N
Max. force for press fits	300 N
Max. continuous input speed	8000 rpm
Max. intermittent input speed	8000 rpm
Recommended temperature range	-40...+100 °C
Number of autoclave cycles	0
PRODUCT	
Weight	460 g

Figure 99: Charecteristics of Gearhead 3

Data of selected gearhead 3 are shown in Fig.77.

Stock program
Standard program
Special program (on request)

			Part Numbers				
			203113	203115	203119	203120	203124
Gearhead Data							
1	Reduction		3.5:1	12:1	26:1	43:1	81:1
2	Absolute reduction		7/2	49/4	26	343/8	2197/27
10	Mass inertia	gcm²	14	15	9.1	15	9.4
3	Max. motor shaft diameter	mm	10	10	8	10	8
	Part Numbers		203114	203116	260552*	203121	203125
1	Reduction		4.3:1	15:1	36:1	53:1	91:1
2	Absolute reduction		13/3	91/6	36/1	637/12	91
10	Mass inertia	gcm²	9.1	15	5.0	15	15
3	Max. motor shaft diameter	mm	8	10	4	10	10
	Part Numbers		260551*	203117		203122	203126
1	Reduction		6:1	19:1		66:1	113:1
2	Absolute reduction		6/1	169/9		1183/18	338/3
10	Mass inertia	gcm²	4.9	9.4		15	9.4
3	Max. motor shaft diameter	mm	4	8		10	8
	Part Numbers			203118		203123	203127
1	Reduction			21:1		74:1	126:1
2	Absolute reduction			21		147/2	126
10	Mass inertia	gcm²		14		15	14
3	Max. motor shaft diameter	mm		10		10	10
4	Number of stages		1	2	2	3	3
5	Max. continuous torque	Nm	3.0	7.5	7.5	15.0	15.0
6	Max. intermittent torque at gear output	Nm	4.5	11.3	11.3	22.5	22.5
7	Max. efficiency	%	90	81	81	72	72
8	Weight	g	260	360	360	460	460
9	Average backlash no load	°	0.6	0.8	0.8	1.0	1.0
11	Gearhead length L1**	mm	41.0	55.5	55.5	70.0	70.0

Figure 100: Gearhead 3 Data

Part number of our selected GP-42 C is 203127.

APPENDIX B

Micro Load Cell CZL635:

ID No: 3134

Model of selected force sensor is shown in Fig.78.

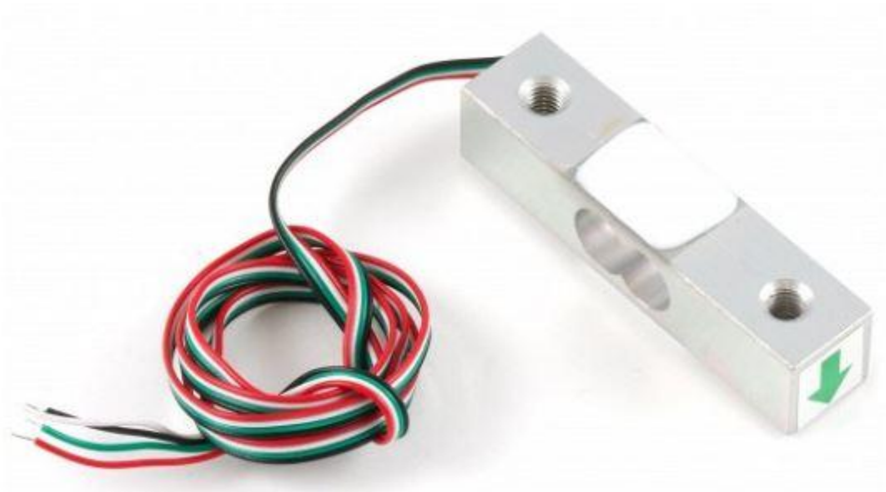

Figure 101: Micro Load Cell CZL635 [2]

Technical drawing of selected force sensor is shown in Fig.79

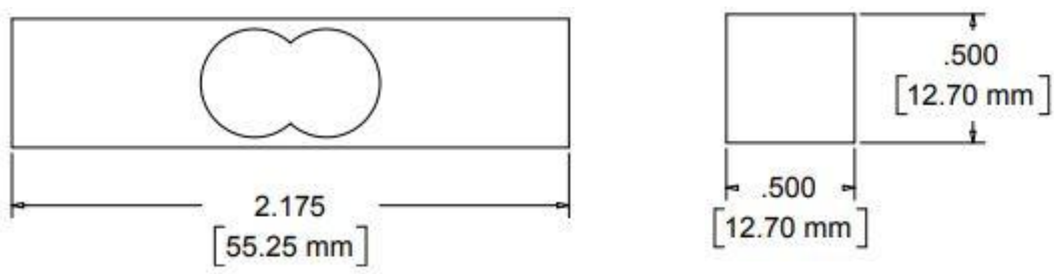

Figure 102: Drawing of Micro Load Cell CZL635

Specifications of selected force sensor are represented in Fig.80.

Product Specifications	
Mechanical	
Housing Material	Aluminum Alloy
Load Cell Type	Strain Gauge
Capacity	20kg
Dimensions	55.25x12.7x12.7mm
Mounting Holes	M5 (Screw Size)
Cable Length	550mm
Cable Size	30 AWG (0.2mm)
Cable - no. of leads	4
Electrical	
Precision	0.05%
Rated Output	1.0±0.15 mv/V
Non-Linearity	0.05% FS
Hysteresis	0.05% FS
Non-Repeatability	0.05% FS
Creep (per 30 minutes)	0.1% FS
Temperature Effect on Zero (per 10°C)	0.05% FS
Temperature Effect on Span (per 10°C)	0.05% FS
Zero Balance	±1.5% FS
Input Impedance	1130±10 Ohm
Output Impedance	1000±10 Ohm
Insulation Resistance (Under 50VDC)	≥5000 MOhm
Excitation Voltage	5 VDC
Compensated Temperature Range	-10 to ~+40°C
Operating Temperature Range	-20 to ~+55°C
Safe Overload	120% Capacity
Ultimate Overload	150% Capacity

Figure 103: Specifications of Micro Load Cell CZL365 [3]

Encoder MILE, 512 cpt, 2-channel, with line driver:

Part No: 651156

Model of selected encoder 1 is shown in Fig.81.

Figure 104: Encoder MILE 512 cpt

Technical drawing of selected encoder 1 is shown in Fig.82.

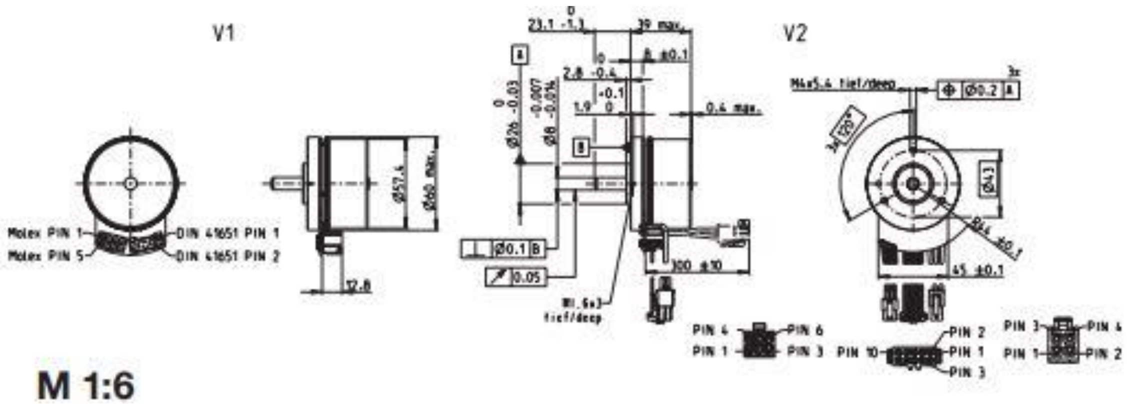

Figure 105: Drawing of Encoder 1

Data of selected encoder 1 are shown in Fig.83.

Stock program
Standard program
Special program (on request)

	Part Numbers			
V1 with connector	651156	651163	651166	651168
V2 with cable and connector	421985	421986	421987	421988
Type				
Counts per turn	512	1024	2048	4096
Number of channels	2	2	2	2
Max. operating frequency (kHz)	1000	1000	1000	1000
Max. speed (rpm)	6000	6000	6000	6000

Figure 106: Encoder 1 Data [5]

Important characteristics of selected encoder 1 are shown in Fig.84.

GENERAL INFORMATION	
Counts per turn	512
Number of channels	2
Line Driver	Yes
Max. electrical speed	112000 rpm
Max. mechanical speed	6000 rpm
TECHNICAL DATA	
Supply voltage V_{CC}	5.0V ± 10.0%
Output signal	Incremental
Driver used logic	Differential, CMOS
Output current per channel	-4...4 mA
Signal rise time	100 ns
Measurement condition for signal rise time	CL=25pF, RL=1kOhm
Signal fall time	100 ns
Measurement condition for signal fall time	CL=25pF, RL=1kOhm
Min. state duration	125 ns
Direction of rotation	A before B CW
Typical current draw at standstill	12 mA
Max. moment of inertia of code wheel	13 gcm²
Operating temperature	-40...+100 °C

Figure 107: Characteristics of Encoder 1

Channel A of encoder 1 is shown in Fig.85.

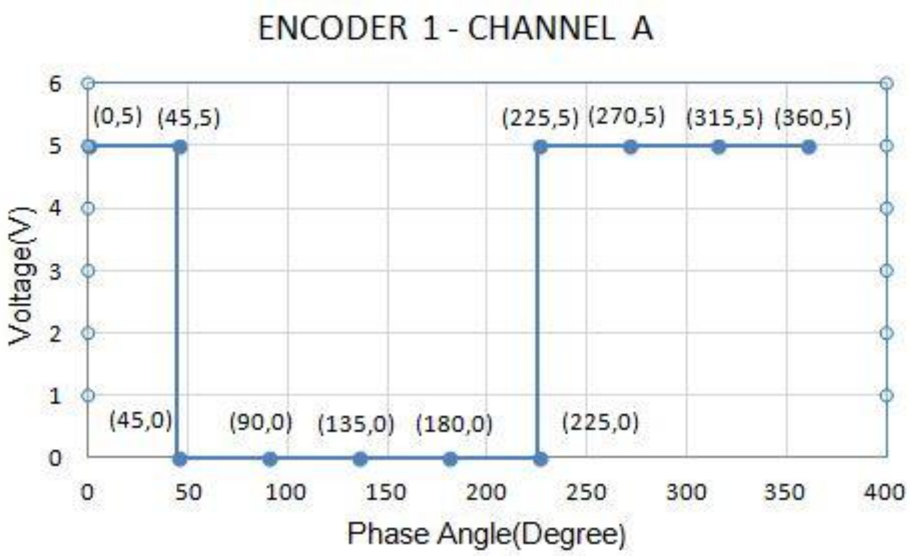

Figure 108 : Encoder 1 - Channel A

Channel B of encoder 1 is shown in Fig.86.

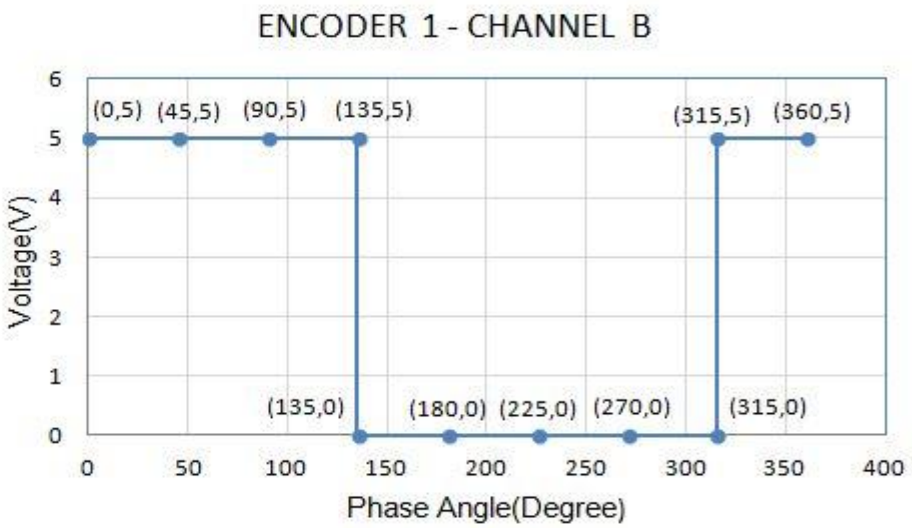

Figure 109 : Encoder 1 - Channel B

According to simulations which are shown in figure 99 and figure 100, the phase shift between channel A and channel B of encoder 1 is 90 degree. Furthermore, pulse of encoder 1 is 180 degree.

Encoder HEDL 5540, 500 CPT, 3 Channels, with Line Driver RS 422:

Part No: 110516

Model of selected encoder 2 is shown in Fig.87.

Figure 110 : Encoder HEDL 5540

Technical drawing of selected encoder 2 is shown in Fig.88.

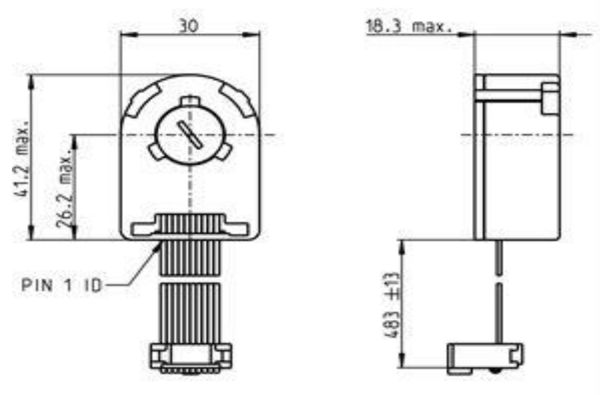

Figure 111 : Drawing of Encoder 2

Data of encoder 2 are shown in Fig.89.

Stock program / Standard program / Special program (on request)	Part Numbers		
	110512	110514	110516
Type			
Counts per turn	500	500	500
Number of channels	3	3	3
Max. operating frequency (kHz)	100	100	100
Max. speed (rpm)	12000	12000	12000
Shaft diameter (mm)	3	4	6

Figure 112 : Encoder 2 Data

Important characteristics of encoder 2 are represented in Fig.90.

GENERAL INFORMATION	
Counts per turn	500
Number of channels	3
Line Driver	DS26LS31
Max. mechanical speed	12000 rpm
Shaft diameter	6 mm
TECHNICAL DATA	
Supply voltage V_{CC}	5.0V ± 10.0%
Driver used logic	EIA RS 422
Max. angular acceleration	250000 rad / s²
Output current per channel	-20...20 mA
Signal rise time	180 ns
Measurement condition for signal rise time	CL=25pF, RL=2.7kOhm,
Signal fall time	40 ns
Measurement condition for signal fall time	CL=25pF, RL=2.7kOhm,
Phase shift	90 °e
Phase shift, inaccuracy	45 °e
Index synchronized to AB	Yes
Max. moment of inertia of code wheel	0.6 gcm²
Operating temperature	-40...+100 °C
Orientation of encoder output to motor flange	-1 °

Figure 113 : Characteristics of Encoder 2

Channel A of encoder 2 is shown in Fig.91.

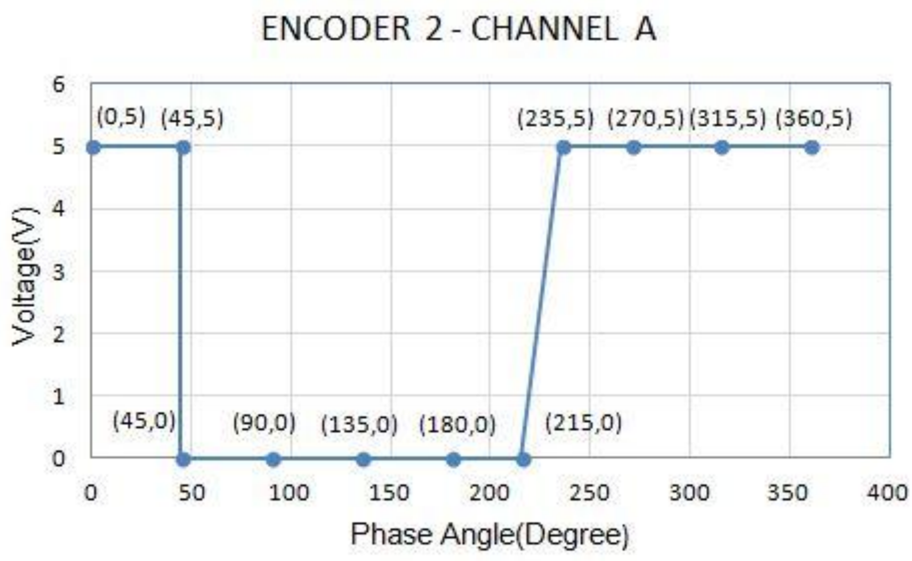

Figure 114 : Encoder 2 - Channel A

Channel B of encoder 2 is shown in Fig.92.

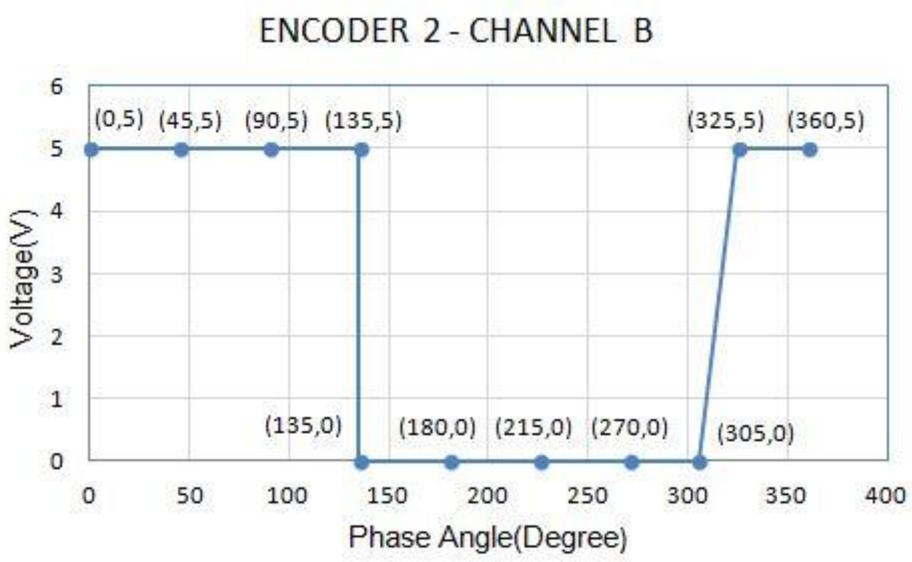

Figure 115 : Encoder 2 - Channel B

Channel 1 of encoder 2 is shown in Fig.93.

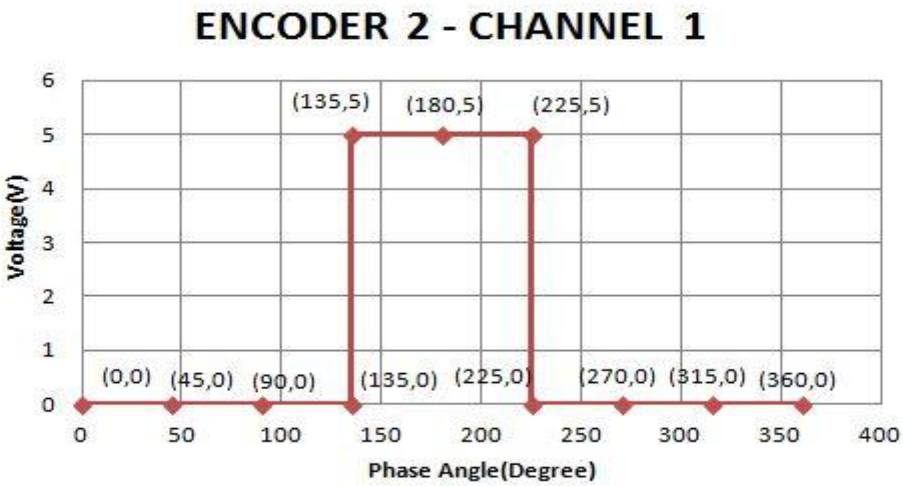

Figure 116 : Encoder 2 - Channel 1

According to simulations, the phase shift between channel A and channel B of encoder 2 is 90 degree. Moreover, pulse of encoder 2 is 180 degree.

Encoder MILE, 512 CPT, 2 Channels, with Line Driver:

Part No: 462003

Model of selected encoder 3 is shown in Fig.94.

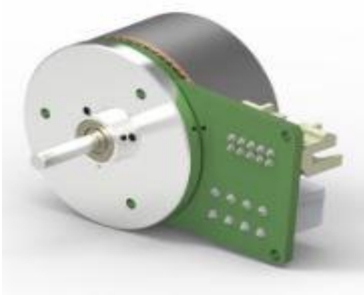

Figure 117: Encoder MILE 512 cpt

Technical drawing of selected encoder 3 is shown in Fig.95.

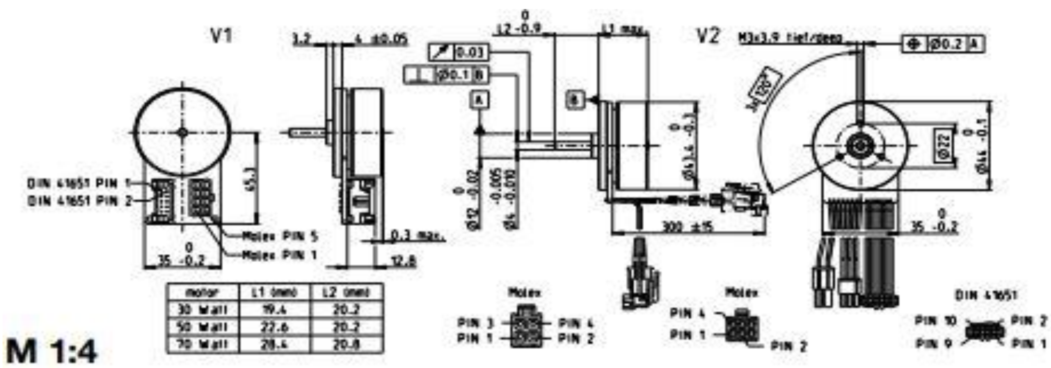

Figure 118: Drawing of Encoder 3

Data of encoder 3 are shown in Fig.96.

Stock program
Standard program
Special program (on request)

	Article Numbers		
V1 with connector	462002	462003	462004
V2 with cable and connector	613318	613319	613320
Type			
Counts per turn	256	512	1024
Number of channels	2	2	2
Max. operating frequency (kHz)	1000	1000	1000
Max. speed (rpm)	10000	10000	10000

Figure 119: Encoder 3 Data

Important characteristics of encoder 3 are shown in Fig.97.

GENERAL INFORMATION	
Counts per turn	512
Number of channels	2
Line Driver	Yes
Max. electrical speed	112000 rpm
Max. mechanical speed	10000 rpm
TECHNICAL DATA	
Supply voltage V_{CC}	5.0V ± 10.0%
Output signal	Incremental
Driver used logic	Differential, CMOS
Output current per channel	-4...4 mA
Signal rise time	100 ns
Measurement condition for signal rise time	CL=25pF, RL=1kOhm
Signal fall time	100 ns
Measurement condition for signal fall time	CL=25pF, RL=1kOhm
Min. state duration	125 ns
Direction of rotation	A before B CW
Typical current draw at standstill	15 mA
Max. moment of inertia of code wheel	3.5 gcm²
Operating temperature	-40...+100 °C
PRODUCT	
Weight	10 g

Figure 120: Characteristics of Encoder 3

Channel A of encoder 3 is shown in Fig.98.

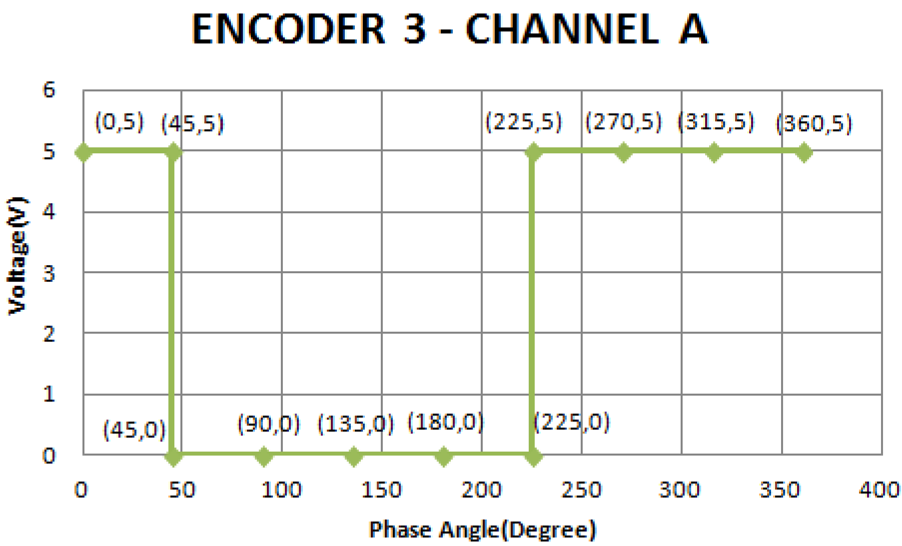

Figure 121: Encoder 3 - Channel A

Channel B of encoder 3 is shown in Fig.99.

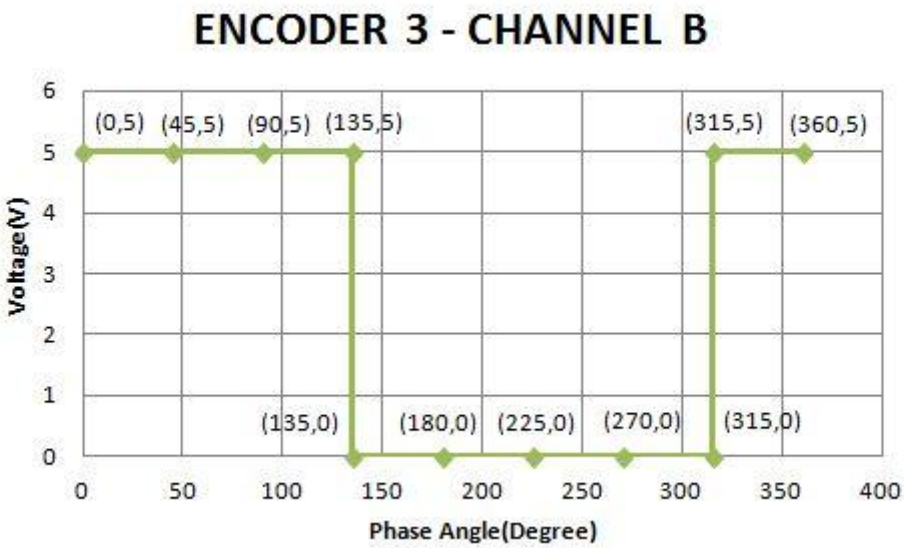

Figure 122: Encoder 3 - Channel B

According to simulations, the phase shift between channel A and channel B of encoder 3 is 90 degree. Additionally, pulse of encoder 3 is 180 degree.